AN ABSTRACT OF THE DISSERTATION OF

Nathaniel L. Osborne for the degree of Doctor of Philosophy in Sustainable Forest Management

presented on August 26, 2015

Title: Simulating Wood Properties in the Context of a Growth and Yield Model for Planted Douglas-fir

Abstract approved: _____

Douglas A. Maguire

Forest growth and yield models are critical to supporting decision making in forestry, but often lack considerations for wood properties. The feasibility of simulating wood properties in the context of a Douglas-fir individual tree growth and yield model was evaluated. This assessment explored the effect of predicted sapwood width, stem taper, branch size and juvenile wood proportion on recovery of utility poles and sawn lumber. Results from the assessment indicated wood properties can be simulated in the context of growth and yield modeling systems with biologically reasonable results. The same assessment indicated recovery of wood products may be overestimated in the absence of penalties for stem defects. Two critical Douglas-fir wood attributes, knot geometry and wood density, were targeted for modeling after the feasibility analysis. A model for Douglas-fir knot pith curvature was developed based on predicted branch angle and growth ring position over time. Based on the predicted knot pith curvature, knot geometry could be implied from branch radius predicted at the stem surface. Medical computed tomography was identified as one way to rapidly and efficiently estimate Douglas-fir wood

density from the proxy of X-ray attenuation. In support of deploying this technology, the effect of wood moisture content and other scanner settings on the relationship of X-ray attenuation and wood density was modeled. Results indicated that X-ray attenuation explains most of the variation in predicting wood density, but moisture content and other scanner settings have a small but significant effect. A number of knowledge gaps should be resolved to sufficiently and robustly simulate wood properties in the context of Douglas-fir growth and yield simulation. Models for sawing simulation and for addressing deficits in existing wood properties models should be an important focus for future research in this field.

Simulating Wood Properties in the Context of a Growth and Yield Model for Planted Douglas-fir

by

Nathaniel L. Osborne

A DISSERTATION

submitted to

Oregon State University

in partial fulfillment of

the requirements for the

degree of

Doctor of Philosophy

Presented August 26, 2015

Commencement June 2016

Doctor of Philosophy dissertation of Nathaniel L. Osborne presented on August 26, 2015

APPROVED:

_____

Major Professor, representing Sustainable Forest Management

_____

Head of the Department of Forest Engineering, Resources and Management

_____

Dean of the Graduate School

I understand that my dissertation will become part of the permanent collection of Oregon State University libraries. My signature below authorizes the release of my dissertation to any reader upon request.

_____

Nathaniel L. Osborne, Author

ACKNOWLEDGMENTS

This research was made possible through the contributions of my colleagues, friends and family. Doug Maguire was always there, with just the right advice and plenty of patience. I wore a groove down the hall to Doug Mainwaring's office. Mainwaring helped me understand biometrics while keeping me entertained with his unique antics. David Hann was essential to the development of the *cipsr* software, even when 'chaos reigned'. Olav Høibø brought new energy and enthusiasm to the end of my Ph.D. program, while teaching me about Norway and wood science. Francis Colin and François de Coligny were excellent hosts during my time in France and provided me new perspectives on science and taught me how to have a good dinner. Special thanks are extended to my colleagues in the basement of Peavy Hall, who refined my research through extensive discussion and debate. I could not have made through this Ph.D. without the support of my wife Catherine Osborne, who has travelled the world for me.

CONTRIBUTIONS OF AUTHORS

Dr. Doug Maguire provided extensive comments, guidance and financial support, which contributed to development of all chapters. Dr. Aaron Weiskittel (University of Maine) provided extensive edits to Chapter seven. Dr. Olav Høibø (Norges miljø- og biovitenskapelige universitet) provided extensive edits and assisted with the sampling described in Chapter five. Derek Gourley (Oregon State University) assisted with collecting the wood samples described in Chapter five. Dr. Peter Gould (Washington Department of Natural Resources), Dr. David Marshall (Weyerhaeuser Company) and Dr. David Hann (Oregon State University) provided examples of calling dynamic link libraries in R, which was critical to the software development described in Chapters two, three and six.

TABLE OF CONTENTS

TABLE OF CONTENTS (Continued)

Page

TABLE OF CONTENTS (Continued)

Page

TABLE OF CONTENTS (Continued)

Page

TABLE OF CONTENTS (Continued)

Page

LIST OF FIGURES

Page

LIST OF FIGURES (Continued)

Page

LIST OF FIGURES (Continued)

Page

LIST OF FIGURES (Continued)

Page

LIST OF TABLES

Page

LIST OF TABLES (Continued)

Page

LIST OF TABLES (Continued)

Page

Chapter 1: Introduction

Nathaniel OSBORNE

Wood properties and their importance to wood end use

Wood properties are a set of anatomical features in a tree which individually or as an aggregate, influence wood end use. Some of the most important wood macro-anatomic features are knots, sapwood and heartwood delineation, juvenile wood and mature wood zones, and shape of the tree stem. Knots are living or dead branches encapsulated in xylem of the tree bole. Knots are directly related to the chronology of the branch angle and stem radial growth over time. Around knots, discontinuities and change in orientation of wood fibers reduce strength of wood (Buksnowitz et al. 2010). In Douglas-fir the wood formed under knots is of higher density but is also more brittle, modifying wood strength even further (Kollmann and Côte 1968). All wood formed in trees is initially sapwood that aids in water conductivity (Spicer and Gartner 2001) and supports the transpirational stream to foliage (Assman 1970). Over time sapwood transitions to heartwood, a collection of non-living cells impregnated with extractives (Bamber 1976). The death of cells and deposition of extractives that marks the transition to heartwood is a continuous process, with only about 2% of the tree xylem containing living cells (Franklin et al. 1987). The geometry of sapwood and heartwood plays a role in determining their relative contribution to some solid wood products. Heartwood is sometimes desirable for aesthetic reasons, due to differences in wood coloration, but also is prized for a higher durability. Sapwood is preferred if the wood will be treated with chemical preservatives because sapwood cells are more conductive and therefore amenable to pressure treatment for penetration of preservatives. As cambial age increases (Di Lucca 1989) or distance from the tree crown increases (Maguire et al. 1991), wood transforms from juvenile wood to mature wood. While the juvenile wood

core is generally characterized as a discrete zone of the bole xylem, it is actually characterized by change in many wood properties parameters (Cahill and Briggs 1992). As cambial age increases fibril angle, longitudinal shrinkage, moisture content, and incidence of spiral grain decreases. Other properties like specific gravity, longitudinal cell length, cell wall thickness, transverse shrinkage and percentage of latewood increases with cambial age. The combined change in these wood properties influences many variables like wood strength (Evans and Ilic 2001; Lachenbruch et al. 2010) and deformation of sawn products (Leonardon et al. 2010; Ormarsson et al. 2000).

Modeling wood properties in the context of growth and yield simulation

Various influences of silviculture on Douglas-fir wood properties has been known for a considerable time (McArdle and Meyer 1930; Paul 1947; Larson 1969), so it is possible to design silvicultural regimes that have a qualitatively predictable effect, without rigorous modeling of wood properties or tree growth and yield. The primary silvicultural tools for controlling wood properties in intensively managed Douglas-fir plantations are the initial spacing of a trees (Maguire et al. 1991), thinning and fertilization (Jozsa and Brix 1989), irrigation (Brix 1972) and pruning (Barbour et al. 2003). The latter two treatments are not commercially viable in the management of most plantations but the former are extensively applied. Other silvicultural treatments may have an effect on wood properties, but are either not tested or documented. Integrative modeling of individual tree growth, yield and wood properties allows for a general quantitative refinement of silvicultural regimes that would be difficult under a more qualitative approach. Modeling wood properties also allows exploration of several complex

relations of tree growth and recovery of specific wood products. Issues receiving much public attention, for example the effect of changing climate on carbon storage (e.g., through effects on wood density), can be assessed using forest growth, yield and wood properties simulation. The same simulation software can be used to estimate product recovery under different environmental and silvicultural conditions. Using a relatively coarse resolution of information on log attributes, the potential recovery of different grades of lumber can be predicted (Fahey et al. 1991). Increasing the scope and resolution of wood properties information may permit more sophisticated analysis like simulated sawing of virtual logs (Mäkelä et al. 2010). "Within this context, one of the main challenges for the current forest-wood research is to bring together the knowledge on how wood properties are developed and can be controlled in forests and the performance required for traditional and emerging end-use wood products" (Colin et al. 2015).

Research objective

The objective of this dissertation was to explore and develop methods to simulate wood properties in the context of a Douglas-fir growth and yield model, ORGANON. ORGANON (ORegon Growth ANalysis and projectiON) is an individual tree growth and yield model for managed Douglas-fir stands in the Pacific Northwestern United States (Hann 2011). The dissertation objective was addressed in four steps. The first step was to assess the feasibility of simulating wood properties and estimating forest product recovery using forest growth models (Chapters 2 and 3). Chapter two predicted the recovery of lumber from trees and logs produced under different silvicultural regimes,

mediated by effects on branch size and juvenile wood core percentage (Osborne et al. 2014). Chapter three predicted utility pole recovery under widely varying silvicultural regimes designed to modify tree taper and sapwood width (Osborne and Maguire 2015*a*). As feasibility studies, these two sets of simulations identified several knowledge gaps that were then addressed in Chapters 4 and 5. Although Chapter two demonstrated that lumber recovery could be predicted reasonably well by simulating branch size and juvenile wood core, strong evidence from other species suggested that lumber recovery could be predicted at an even higher resolution using sawing simulation. Sawing simulation would require three-dimensional characterization of knots within a virtual log and projection of knots onto virtual lumber sawn from this log. A publically available model for Douglas-fir knot geometry could not be found during an extensive literature search, so Chapter four (Osborne and Maguire 2015*b*) sought to fill that knowledge gap by developing a knot model.

Spatial variation in wood density is another wood attribute that has direct relevance to the products that can be manufactured from different regions of the tree stem or its constituent logs. Modeling density of bole-wood in Douglas-fir has been a key area of research in the Pacific Northwest, but more work needs to be done on characterizing complete density profiles and the effects of silviculture and site on these profiles. Obtaining a large sample size has been difficult due to time and financial cost of sample collection, preparation, and estimation of fine-scale wood density. Most analysis has been achieved by means of X-ray densitometry. Medical computed tomography (CT) has been shown to be one alternative for rapidly estimating wood density in other tree species

(Steffenrem et al. 2014). Application of CT scanning to characterize fine-scale patterns in Douglas-fir wood density seemed promising, but several questions needed to be resolved. Chapter five (Osborne et al. 2015) followed the work of Freyburger et al. (2009) by examining the effect of moisture content and other CT scanner settings on estimating wood density from X-ray attenuation.

One of most important outcomes of this dissertation was development of simulation software, *cipsr*, for Douglas-fir growth, yield and wood properties. A brief introduction to *cipsr* is provided in Chapter six.

The final step in the dissertation research was to describe the current status of research for simulating Douglas-fir growth, yield and wood properties in a way that proposes future direction for this research (Chapter 7). The work described in this dissertation is broad and only partially addresses the motivating statements of Colin et al. (2015). More work is needed to adequately simulate individual tree growth, yield and wood properties, but this dissertation contributed some significant results and provided an analytical framework for this topic of forestry research.

Literature Cited

Assman, E. 1970. The principles of forest yield study. Pergamon, Oxford, New York. 506 p.

Bamber, R. K. 1976. Heartwood, its function and formation. Wood Science and Technology, 10(1):1-8.

Barbour, R. J., Marshall, D.D., Lowell, E.C. 2003. Managing for wood quality. In Compatible forest management. Springer Netherlands. Pp. 299-336.

Buksnowitz, C., Hackspiel, C., Hofstetter, K., Müller, U., Gindl, W., Teischinger, A., Konnerth, J. 2010. Knots in trees: strain distribution in a naturally optimised structure. Wood science and technology, 44(3): 389-398.

Brix, H. 1972. Nitrogen fertilization and water effects on photosynthesis and earlywood-latewood production in Douglas-fir. Canadian Journal of Forest Research, 2(4): 467-478.

Cahill, B., Briggs, D. 1992. Effects of Fertilization on Wood Quality and Tree Value Proc. Forest Fertilization Pp. 145-161 in H.N. Chappell, G.F. Weetman, and R.E. Miller (eds). Forest Fertilization: Sustaining and improving nutrition and growth of western forests. Institute of Forest Resources, University of Washington, Seattle, WA, USA. Contribution Number 73.

Colin, F., Laborie, M.P., Fortin, M. 2015. Wood properties: future needs, measurement and modelling. Annals of Forest Science 72(6): 665-670.

Di Lucca, C.M. 1989. Juvenile - Mature Wood Transition. Pp. 23-38 in R.M. Kellog (ed). Second growth Douglas-fir: Its management and conversion for value. Forintek Canada, Vancouver, BC, Canada. Spec. Publ. No. SP-32.

Evans, R., Ilic, J. 2001. Rapid prediction of wood stiffness from microfibril angle and density. Forest products journal, 51(3): 53.

Fahey, T. D., Cahill, J. M., Snellgrove, T. A., Heath, L. S. 1991. Lumber and veneer recovery from intensively managed young-growth Douglas-fir. Res. Pap. PNW-RP-437. Portland, OR: US Department of Agriculture, Forest Service, Pacific Northwest Research Station.

Franklin, J. F., Shugart, H. H., Harmon, M. E. 1987. Tree death as an ecological process. BioScience, 37(8): 550-556.

Freyburger, C., Longuetaud, F., Mothe, F., Constant, T., Leban, J. 2009. Measuring wood density by means of X-ray computer tomography. Annals of Forest Science. 66(8): 804.

Hann, D.W. 2011. ORGANON User's Manual, Edition 9.1. College of Forestry, Oregon State University, Corvallis, OR, USA.

Jozsa, L.A., Brix, H. 1989. The effects of fertilization and thinning on wood quality of a 24-year-old Douglas-fir stand. Canadian journal of forest research, 19(9): 1137-1145.

Kollmann, F.F., Côte Jr, W.A. 1968. Principles of Wood Science and Technology: in Chapter 2 "Chemical Composition of Wood". Springer-Verlag.

Lachenbruch, B., Johnson, G. R., Downes, G. M., Evans, R. 2010. Relationships of density, microfibril angle, and sound velocity with stiffness and strength in mature wood of Douglas-fir. Canadian Journal of Forest Research, 40(1): 55-64.

Larson, P. R. 1969. Wood formation and the concept of wood quality. Yale Univ. School Forestry, Bull, (74): 1-54.

Leonardon, M., Altaner, C.M., Vihermaa, L., Jarvis, M.C. 2010. Wood shrinkage: influence of anatomy, cell wall architecture, chemical composition and cambial age. European Journal of Wood and Wood Products, 68(1): 87-94.

Maguire, D.A., Kershaw, J.A., Hann, D.W. 1991. Predicting the effects of silvicultural regime on branch size and crown wood core in Douglas-fir. Forest Science, 37(5): 1409-1428.

Mäkelä, A., Grace, J., Deckmyn, G., Kint, A.K.V. 2010. Simulating wood quality in forest management models. Forest Systems 19(S1): 48-68.

McArdle, R.E., Meyer, W.H. 1930. The yield of Douglas-fir in the Pacific Northwest. US Dept. Agr. Tech. Bul, 201, G4.

Ormarsson, S., Dahlblom, O., Petersson, H. 2000. A numerical study of the shape stability of sawn timber subjected to moisture variation. Wood Science and Technology, 34(3): 207-219.

Osborne, N., Maguire, D., Hann, D. 2014. Simulating Douglas-fir Tree and Stand Development Under Varying Initial Spacings with ORGANON: Knot Size and Juvenile Wood Core Effects on Grade Recovery of Lumber. Center for Intensive Planted-forest Silviculture, 2013 Annual Report, Pp. 22-28.

Osborne, N., Maguire, D. 2015*a*. Implications of Stand Density Regime for Meeting Douglas-fir Pole Specifications. Center for Intensive Planted-forest Silviculture, 2014 Annual Report, Pp. 24-27.

Osborne, N., Maguire, D. 2015*b*. Modeling knot geometry from branch angles in Douglas-fir (Pseudotsuga menziesii), Canadian Journal of Forest Research. *under review*.

Osborne, N., Høibø, O., Maguire, D., Gourley, D. 2015. Estimating the density of coast Douglas-fir wood samples at different moisture contents using medical X-ray computed tomography. Computers and Electronics in Agriculture. *in preparation*.

Paul, B.H. 1947. Knots in second-growth Douglas-fir. US Department of Agriculture Forest Service, Forest Products Laboratory, Madison Wisconsin. No. R1690.

Spicer, R., Gartner, B.L. 2001. The effects of cambial age and position within the stem on specific conductivity in Douglas-fir (Pseudotsuga menziesii) sapwood. Trees, 15(4): 222-229.

Steffenrem, A., Kvaalen, H., Dalen, K., Høibø, O. 2014. A high-throughput X-ray-based method for measurements of relative wood density from unprepared increment cores from Picea abies. Scandinavian Journal of Forest Research. 29(5):506-514.

Chapter 2: Simulating Douglas-fir Tree and Stand Development Under Varying Initial Spacings with ORGANON: Knot Size and Juvenile Wood Core Effects on Grade Recovery of Lumber.

Nathaniel OSBORNE

Douglas MAGUIRE

David HANN

Published in:

2014. Center for Intensive Planted-forest Silviculture, 2013 Annual Report, Pp. 22-28.

Abstract

Many wood properties determine the quality of lumber that may be extracted from Douglas-fir logs. Two of the most important log attributes identified by product recovery studies are the maximum size of branches (knots) and percent juvenile wood by volume. Our aim was to quantify the influence of stand density management on size of the juvenile wood core, maximum whorl branch size, and corresponding effects on grade distribution of recovered lumber. Stand growth and yield was simulated with the ORGANON growth model under a variety of initial planting densities and thinning treatments. Initial spacing influenced the grade distribution of recoverable lumber after fifty years of simulated growth. Thinning did not have a substantial influence on lumber grade recovery. Tighter initial spacing produced smaller branches with moderate levels of juvenile wood and large proportions of high quality lumber. Thinning imposed when the crown base height was above or near the top of the bottom log had no effect on branch size and grade recovery in that log. Planting at high densities, and thinning when crown base attains a target height is one way to produce high quality lumber while maximizing yield in intensively-managed Douglas-fir forests.

Introduction

Lumber value recovery in planted Douglas-fir forests has been linked to the size and abundance of branches on individual trees as well as the proportion of juvenile wood within the stem (Fahey et al. 1991). Generally, higher-value forest products can be recovered from trees with fewer branches of smaller diameter and a narrow juvenile

wood core. The biological controls on the rate of transition from juvenile wood to mature wood are still subject to debate (e.g., Gartner et al. 2002 versus DiLucca 1989), and the transition depends in part on the attribute applied in its definition (e.g. wood density, microfibril angle, tracheid length; Cown 1992). The growth model TASS forms part of a comprehensive evaluation system, SYLVER, and has been designed to estimate the transition between juvenile and mature wood as a function of distance below live crown base (DiLucca 1989). This approach adheres to the working hypothesis that juvenile wood and crown wood are closely related if not equivalent. An opposing working hypothesis assumes that the transition is genetically predetermined to occur at a specific cambial age that varies by species and perhaps by provenance or silvicultural regime with a species (Larson 1969; Megraw 1985).

ORGANON is an individual-tree, distance-independent growth model developed for various species and sub-regions within the Pacific Northwest region of the United States (PNW). Simulation of stand dynamics in ORGANON is linked closely with crown and canopy structure and their dynamic change over the course of stand development. As a result, the pattern in predicted crown recession lends itself well to estimation of maximum branch diameter (Maguire et al. 1999) and crown wood core (Josza et al. 1989) under differing silvicultural regimes. The interaction of stand density, crown size, maximum branch size, and the proportion of juvenile wood have therefore all been incorporated into the wood quality module of the ORGANON growth model (Maguire et al. 1991; Briggs and Fight 1992; Maguire et al. 1999; Barbour et al. 1997). As an alternative to assuming the equivalence of crown wood and juvenile wood, ORGANON

allows the user to define the juvenile-mature wood transition by cambial age (Hann 2011). In short, ORGANON can be used to explore how a variety of stand density management regimes affect Douglas-fir branch characteristics, proportion of juvenile wood and wood product grade recovery when linked to product recovery equations (Fahey et al. 1991).

Pruning is not financially feasible under current or foreseeable market conditions for Douglas-fir lumber and veneer. Therefore, promoting earlier crown recession and maintaining minimal branch size in the lower bole where most of the recoverable value accumulates (Lowell et al. 2012) is best achieved by tighter initial spacing. Once the lower branches have died from suppression, growth can be accelerated through subsequent thinning to yield optimal value recovery. In short, initial planting density affects crown morphology by controlling the timing of crown closure and rate of crown recession, with close spacing promoting earlier crown closure and shorter branch longevity. Because closer spacing also reduces growing space available to individual trees, thinning is essential to relieve competition between residual trees and to allow them to experience enhanced growth through crown expansion and increased net photosynthesis. An optimal silvicultural regime is one which balances potential wood quality and quantity in a way that maximizes the potential value of wood products while reducing silvicultural costs.

The objective of this analysis was to explore the implications of initial spacing and subsequent thinning on the yield of Douglas-fir lumber grades under alternative rotation

ages. The analysis was performed by simulating growth responses to an arbitrary but wide range of stand density management regimes with ORGANON, and applying product recovery equations developed for intensively-managed Douglas-fir.

Materials and Methods

The simulations were initiated with measurements from one of numerous spacing trials (Type III installations) established by the Stand Management Cooperative (SMC), hosted at the University of Washington (Maguire et al. 1991). The Lewisburg Saddle replication (SMC Type III Installation 914) was installed on the McDonald-Dunn Forest, a teaching, demonstration, and research forest owned and operated by the Oregon State University College of Forestry. Lewisburg Saddle is located on the eastern edge of the Oregon Coast Ranges near the central Willamette Valley (approximately 44°38' N latitude and 123°17' W longitude). Like all other SMC Type III installations, this trial consists of six blocks with different initial spacings that targeted 250, 500, 740, 1075, 1680, or 2990 trees per hectare. Stand age and site productivity were generally uniform among the six spacing blocks at Lewisburg Saddle, with site index averaging 37.5 m at 50 years (Bruce 1981). The site was clearcut and planted in early 1989 with 1:1 Douglas-fir seedlings. Chemical release treatments were applied in 1989 and 1990 to reduce competing vegetation. Simulations were initiated with data collected at plantation age 15-years. For each level of initial planting density, a scenario with and without thinning was considered across a wide range of rotation ages between 20 and 115-years. The single thinning was applied at age fifteen to stands planted at initial densities of 2990 and 1680 trees per

hectare. Trees were removed from below until the residual relative density (Curtis 1982) was 30% of maximum carrying capacity.

Bucking rules were adopted that placed first priority on 5-meter saw logs with a minimum scaling diameter of 16.5 centimeters (Table 2.1). If a 5-meter saw log could not be cut from the tree, a 5-meter pulp log with a minimum scaling diameter of 7.5 centimeters was produced. Portions of the tree which could not yield a saw or pulp log were considered non-merchantable and excluded from analysis. For each tree, log trim of 20 centimeters and a stump height of 15 centimeters were assumed.

The logs resulting from each of the simulations were characterized by their largest branch diameter and the percent of juvenile wood by cubic volume. Equations for managed Douglas-fir were applied to estimate the percentage of the total log volume contributed by lumber in each of the six lumber grades (Table 2.2; Fahey et al. 1991). Specifically, estimates of both branch size and juvenile wood core allowed prediction of lumber grade recovery by machine stress rating (MSR) standards; however, boards unable to meet one of the MSR grades were relegated to a visual grade, and remaining volume was accumulated as pulpwood (Table 2.2). Total volume of each lumber grade for a given log was estimated as the product of the percentage grade recovery and total log volume, the latter by numerical integration of a Douglas-fir taper equation (Walters and Hann 1986). Treatment effects on the distribution of volume recovered in the six grades (MSR 2100f, MSR 1600f, MSR 1450f, No. 3, economy, and pulpwood) was tested by multivariate

analysis of variance (R Core Team 2013; manova; $\alpha = 0.05$). Treatments included both initial spacing and the rotation length (15 to 115 years).

Results

Simulated responses of crown morphology were consistent with numerous field trials on initial spacing, thinning, or a combination of the two. Height to crown base generally increased as initial stand density increased (Figure 2.1); however, heights to crown base are inconsistently low in the nominal stand density of 1075 trees per hectare, primarily because the plot established in this stand density contained a wet area that reduced Douglas-fir survival, causing it to behave more like a stand of lower initial density. In contrast to crown base height, crown length increased with increasing spacing, causing the number of live branch whorls and hence branch longevity to increase (Figure 2.2A), consistent with documented results from field trials (e.g., Marshall and Curtis 2002; Brix 1981). In contrast, as initial spacing increased, the proportion of juvenile wood increased only slightly (Figure 2.2B). Thinning caused some increase in the largest branch diameter and juvenile wood at and above crown base at time of thinning, so the increase in juvenile wood percentage apparently occurred in the upper logs of the trees. In the five widest spacings, crown bases were within the basal log at time of thinning, so if thinning had also been implemented in the four widest spacings at the same time, it most likely would have increased the proportion of juvenile wood even more than in the two closest spacings. Generally, plantings with high initial density yielded trees with small branch diameters and moderate proportions of juvenile wood, with only a slight peak in

percentage of juvenile wood at moderate spacings (4 m). Planting at low initial density yielded trees with large branch diameters and moderate proportions of juvenile wood.

The multivariate analysis of covariance provided evidence that initial spacing significantly affected lumber and volume grade distribution (R Core Team 2013; manova). Initial spacing had an effect on the relative distribution of recovered lumber grades, although total volumes were more ambiguous due to the differing cubic yields among initial spacings and rotation ages. Recoverable lumber distributions differed significantly by initial planting density both with and without thinning ($p < 0.001$). Stands with tighter initial spacing yielded a higher percentage of high quality lumber than stands with wider initial spacing (Figure 2.3). The number and size distribution (by scaling diameter) of harvested logs also differed substantially by initial spacing (Figure 2.4). As initial stand density increased, the range in scaling diameter decreased, as did the mode and mean. Total yields were relatively similar among the different initial spacings with and without thinning, especially at longer rotation lengths. At a rotation length of 50 years all but the widest initial spacings produced between 600 and 700 cubic meters per hectare of lumber (Figure 2.5). Saw logs constituted approximately 90% of the total yield, with the remaining volume in pulp logs (Figure 2.5). Thinning was shown to have little effect on yield in either stands planted at an initial density of 2990 and 1680 trees per hectare (Figure 2.5).

Discussion

The highest initial density (2990 trees per hectare) produced the largest volume of highest quality lumber relative to other levels of initial density. Planting at a closer spacing increased the crown base height, minimized average branch diameter, and maintained a moderate absolute size of the juvenile wood core. The latter was a direct result of suppressed diameter growth up to cambial age 20 years in the tight spacing. Conversely, trees at the widest spacing attained the largest diameters at cambial ages of 20 years. Total yields at rotations lengths of 50 years or longer were only slightly different. Hence, given that the proportion of tree and log volume composed of mature wood was highest at the 740 trees per hectare, its absolute yield of mature wood was also highest, and producing high quality lumber in the densest stand came with only a modest sacrifice in total yield due to the smaller tree size and greater loss to mortality. Two thinning prescriptions were applied to evaluate if diameter growth rates could be maintained in the two densest stands after crown recession had already proceeded further, and in the case of the closest spacing past the top of the basal log, thereby creating stand conditions conducive to establishment of small branch size and more rapid formation of mature wood with superior mechanical properties in the high-value basal log.

As indicated above, the behavior of the stand with nominal initial density of 1075 trees per hectare was somewhat unusual because the plot in this stand density contained a wet area that reduced Douglas-fir survival. It therefore behaved more like a stand of lower initial density. Like height to crown base (Figure 2.1), the trends for branch diameter and juvenile wood proportion were more consistent with the lower initial stand densities than

would have been the case if high survival maintained the plot at 1075 trees per hectare (Figure 4.2A, Figure 2.2B).

In the stands examined, thinning was found to reduce the yield of high quality lumber by slightly increasing branch size and the size of the juvenile wood core in the section of the stem that was above crown base at time of thinning. Consistent with results from the plethora of thinning trials in a variety of species, thinning also resulted in some reduction in total yield. Thinning was arbitrarily based on the stand age, rather than other tree or stand conditions that might be targeted more precisely to yield specific types of logs or yield specific lumber grades. To devise an optimal thinning scenario, the timing and intensity should be weighed against trends in tree diameter growth and height to crown base at time of thinning. The optimal thinning prescription will therefore differ by site quality and initial spacing. A silvicultural prescription that minimizes branch diameter could be considered at the expense of increases in juvenile wood core, although the two will probably be correlated if a functional relationship exists between distance below crown and the juvenile-mature wood transition. In these simulations, lumber recovery was shown to be very sensitive to branch size, but relatively insensitive to size of the juvenile wood core (Figure 2.5).

Biological responses to initial stand density and thinning were discussed in this paper. To more fully address optimal initial spacing and thinning for producing high quality lumber, economic analyses must be performed. Any economic analysis requires assumptions about future financial conditions, costs of planting and harvesting, and the

value of harvested logs and/or manufactured products. These assumptions are likely to vary widely by region and the landowners objectives.

Conclusions

The quality of lumber produced from Douglas-fir stands can be influenced substantially by the stand density regime under which it is managed. Product recovery studies are logistically complex and expensive to implement for a wide range of stand conditions, and results will vary by the configuration technology of a certain sawmill. Forest models provide a useful tool for simulating the effects of alternative silvicultural regimes on tree and log attributes that have direct effect on the grades of lumber that can be recovered. In this paper, we assessed the wood quality output from the ORGANON growth model to estimate grades of lumber recovered under an array of silvicultural regimes, based on grade distribution equations developed from a large product recovery study at one mill. Forest model output that includes estimates of wood product quality allows for financial forecasting at a higher resolution than that of financial analysis performed on log quality without recognizing associated differences in wood product quality. In many cases, financial decisions in forestry are based on log volume and weight, and de-emphasize lumber grade potential. This simulation analysis demonstrated how wood quality output from a forest model can be used to analyze, and potentially leveraged into, a larger economic analysis to identify optimal silvicultural prescriptions and forest management strategies. Due to the limitations of the product recovery equations applied to logs with varying average knot size and juvenile wood core, work is currently under way to develop “glass log” models that include internal knot geometry and gradients in wood

density and other attributes that influence product quality. These log models can then serve as input to sawing simulators (e.g., Todoroki et al. 2005), with the ultimate goal of providing the capacity to explore product and value recovery under a range of product and milling specifications.

Literature Cited

Barbour, R. J., Johnston, S., Hayes, J. P., Tucker, G. F. 1997. Simulated stand characteristics and wood product yields from Douglas-fir plantations managed for ecosystem objectives. Forest Ecology and Management, 91(2):205-219.

Briggs, D. G., Fight, R. D. 1992. Assessing the effects of silvicultural practices on product quality and value of coast Douglas-fir trees. Forest products journal, 42(1):40-46.

Brix, H. 1981. Effects of thinning and nitrogen fertilization on branch and foliage production in Douglas-fir. Canadian Journal of Forest Research, 11(3):502-511.

Bruce, D. 1981. Consistent height-growth and growth-rate estimates for remeasured plots. Forest Science, 27(4):711-725.

Cown, D. J. 1992. Corewood (juvenile wood) in Pinus radiata–should we be concerned. New Zealand Journal of Forestry Science, 22(1):87-95.

Curtis, R. O. 1982. A simple index of stand density for Douglas-fir. Forest Science, 28(1):92-94.

Di Lucca, C.M. 1989. Juvenile - Mature Wood Transition. Pp. 23-38 in R.M. Kellog (ed). Second growth Douglas-fir: Its management and conversion for value. Forintek Canada, Vancouver, BC, Canada. Spec. Publ. No. SP-32.

Fahey, T. D., Cahill, J. M., Snellgrove, T. A., Heath, L. S. 1991. Lumber and veneer recovery from intensively managed young-growth Douglas-fir. Res. Pap. PNW-RP-437. Portland, OR: US Department of Agriculture, Forest Service, Pacific Northwest Research Station.

Gartner, B. L., North, E. M., Johnson, G. R., Singleton, R. 2002. Effects of live crown on vertical patterns of wood density and growth in Douglas-fir. Canadian Journal of Forest Research, 32(3):439-447.

Hann, D.W. 2011. ORGANON User's Manual, Edition 9.1. College of Forestry, Oregon State University, Corvallis, OR, USA.

Josza L.A., Richards J., Johnson S.G. 1989. Relative density. Pp. 5-19 in R.M. Kellogg (ed). Second growth Douglas-fir: Its management and conversion for value. Forintek Canada, Vancouver, BC, Canada. Spec. Publ. No. SP-32.

Larson P.R. 1969. Wood formation and the concept of wood quality. School of Forestry, Yale University, New Haven, CT, USA. Bulletin 74. 54 p.

Lowell, E. C., Dykstra, D. P., Monserud, R. A. 2012. Evaluating effects of thinning on Wood Quality in Southeast Alaska. Western Journal of Applied Forestry, 27(2):72-83.

Maguire, D. A., Bennett, W. S., Kershaw, J. A., Gonyea, R., Chappell, H. N. 1991. Establishment report: Stand Management Cooperative silviculture project field installations. College of Forestry, University of Washington, Seattle, WA, 42.

Maguire, D. A., Johnston, S. R., Cahill, J. 1999. Predicting branch diameters on second-growth Douglas-fir from tree-level descriptors. Canadian Journal of Forest Research, 29(12):1829-1840.

Marshall, D.D., Curtis R.O. 2002. Levels-of-Growing-Stock Cooperative Study in Douglas-fir: Report No. 15–Hoskins: 1963–1998. USDA-FS Pacific Northwest Research Station, Portland, OR, USA. Research Paper PNW-RP-537.

Megraw, R. A. 1985. Wood quality factors in loblolly pine: the influence of tree age, position in tree, and cultural practices on wood specific gravity, fiber length, and fibril angle. Atlanta, GA: TAPPI Press.

R Development Core Team. 2013. R: A language and environment for statistical computing. R Foundation for Statistical Computing, Vienna, Austria.

Todoroki, C. L., Monserud, R. A., Parry, D. L. 2005. Predicting internal lumber grade from log surface knots: Actual and simulated results. Forest products journal, 55(6):38-47.

Walters, D. K., Hann, D. W. 1986. Taper equations for six conifer species in southwest Oregon. Oregon State University, School of Forestry, Forest Research Laboratory.

Tables:

Table 2.1 Tree merchandizing specifications used in the bucking of simulated trees

Stump Height	15 cm	Trim Allowance	20 cm
Minimum Saw Log Scaling Diameter	16.5 cm	Log Length	5 m
Minimum Pulp Log Scaling Diameter	7.5 cm		

Table 2.2 Equations for predicting MSR and visual grade recovery percentages (Fahey et al. 1991)

Lumber Grade	Model Equation and Coefficients*
MSR 2100f 1.8E	$18.69 \cdot \exp(1.166 \cdot LLAD + 0.25 \cdot JWPC - 0.4585 \cdot LLAD^2 - 0.000783 \cdot JWPC^2)$
MSR 1650f 1.5E	$38.1 \times \exp(0.311 \times LLAD^2 - 0.000105 \times JWPC^2)$
MSR 1450f 1.3E	Obtained by subtraction
Visual No. 3	$0.93 \times \exp(1.344 \times LLAD - 0.118 \times LLAD^2) + 0.003 \times JWPC^2$
Visual Economy	$2.93 \times \exp(0.435 \times LLAD - 0.0106 \times JWPC)$

Figure Captions:

Figure 2.1. ORGANON simulation results: Lorey's top height and crown base height at plantation age fifteen and fifty in relation to height of the bottom five-meter log.

Figure 2.2. ORGANON simulation results: (A) largest limb average diameter in the bottom log of a given tree by initial planting density; and (B) percent of recovered saw log volume as juvenile wood by initial planting density.

Figure 2.3. ORGANON predictions of percent total log volume contributed by different lumber grades in the stands planted to 250, 740, 1680, and 2960 TPH with no subsequent thinning.

Figure 2.4. ORGANON simulation results: the number of recovered five-meter logs per hectare for three levels of initial planting density by their scaling diameter.

Figure 2.5. ORGANON simulation results: total lumber and pulp yield at a plantation age fifteen years in relation to volume of juvenile wood harvested as saw timber, the average largest branch in the bottom log, for stands with and without thinning.

Figure 2.1 ORGANON simulation results: Lorey's top height and crown base height at plantation age fifteen and fifty in relation to height of the bottom five-meter log.

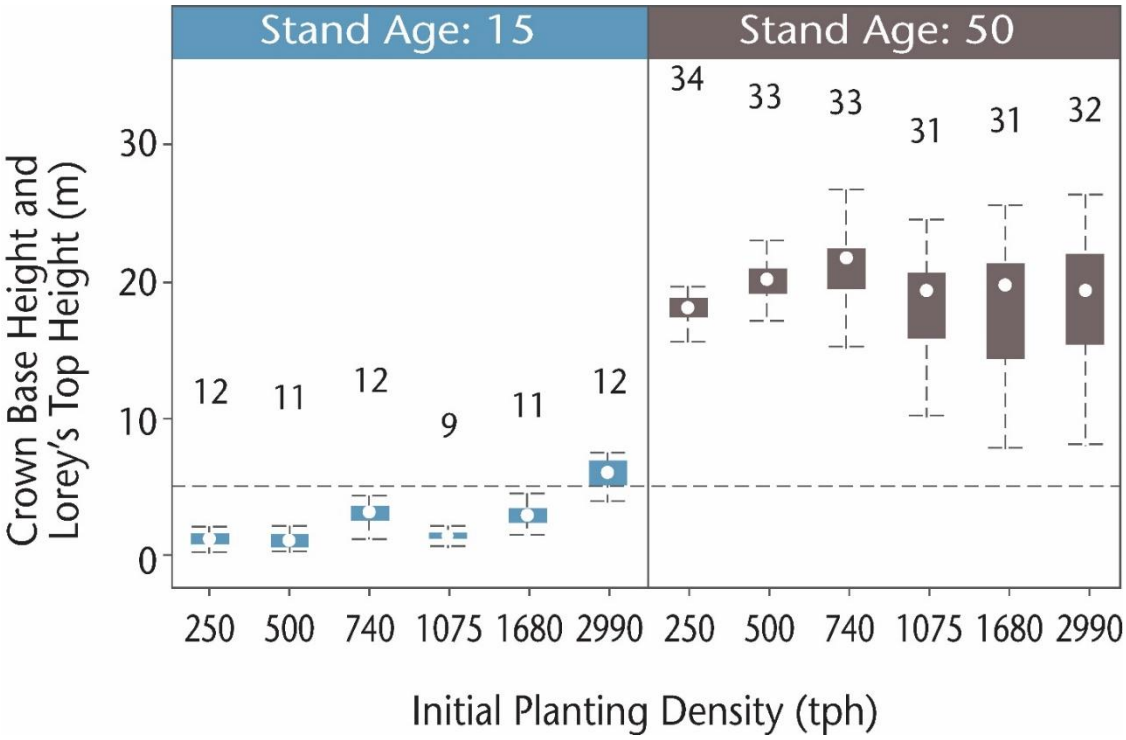

Figure 2.2 ORGANON simulation results: (A) largest limb average diameter in the bottom log of a given tree by initial planting density; and (B) percent of recovered saw log volume as juvenile wood by initial planting density.

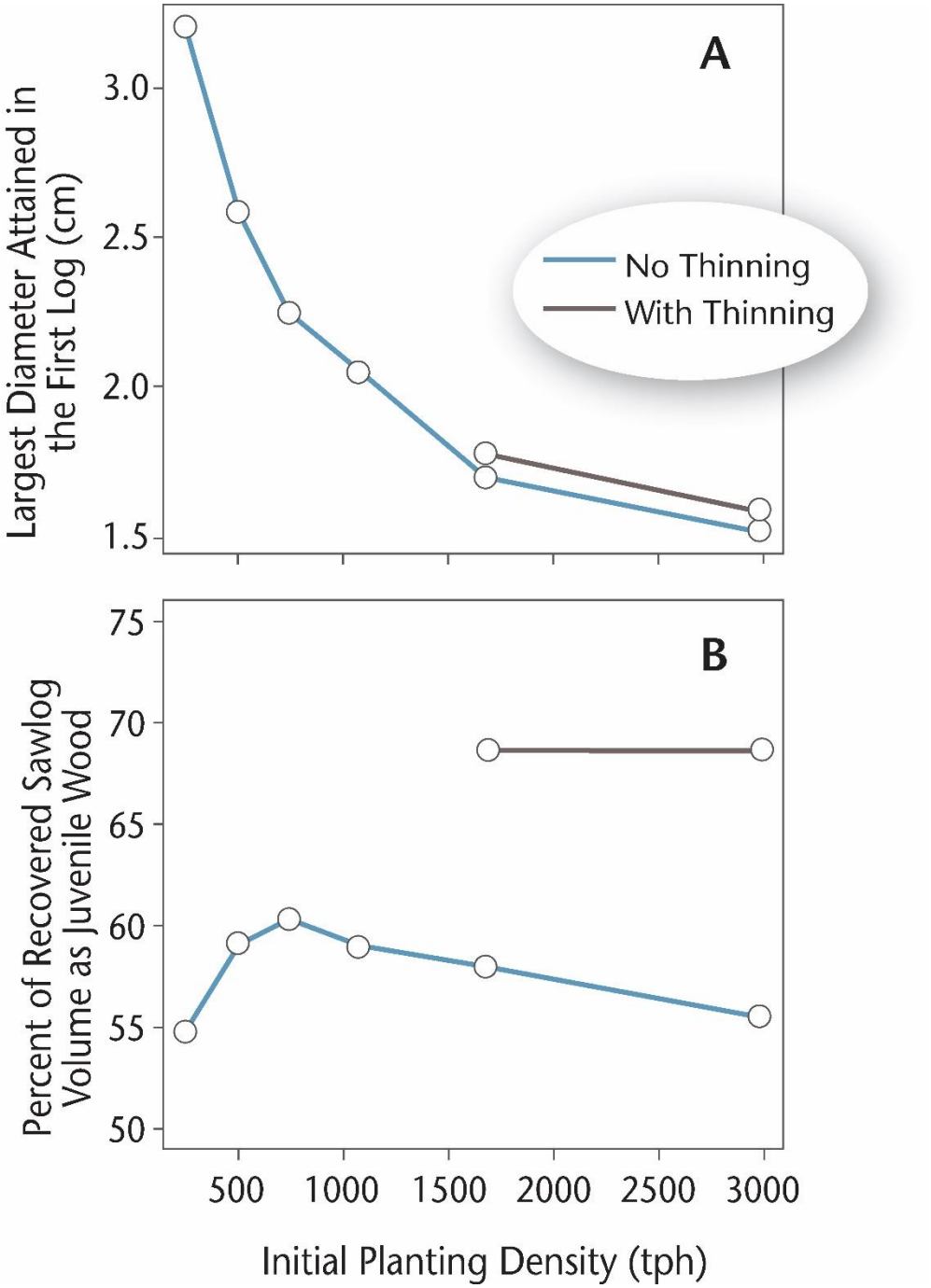

Figure 2.3 ORGANON predictions of percent total log volume contributed by different lumber grades in the stands planted to 250, 740, 1680, and 2960 TPH with no subsequent thinning.

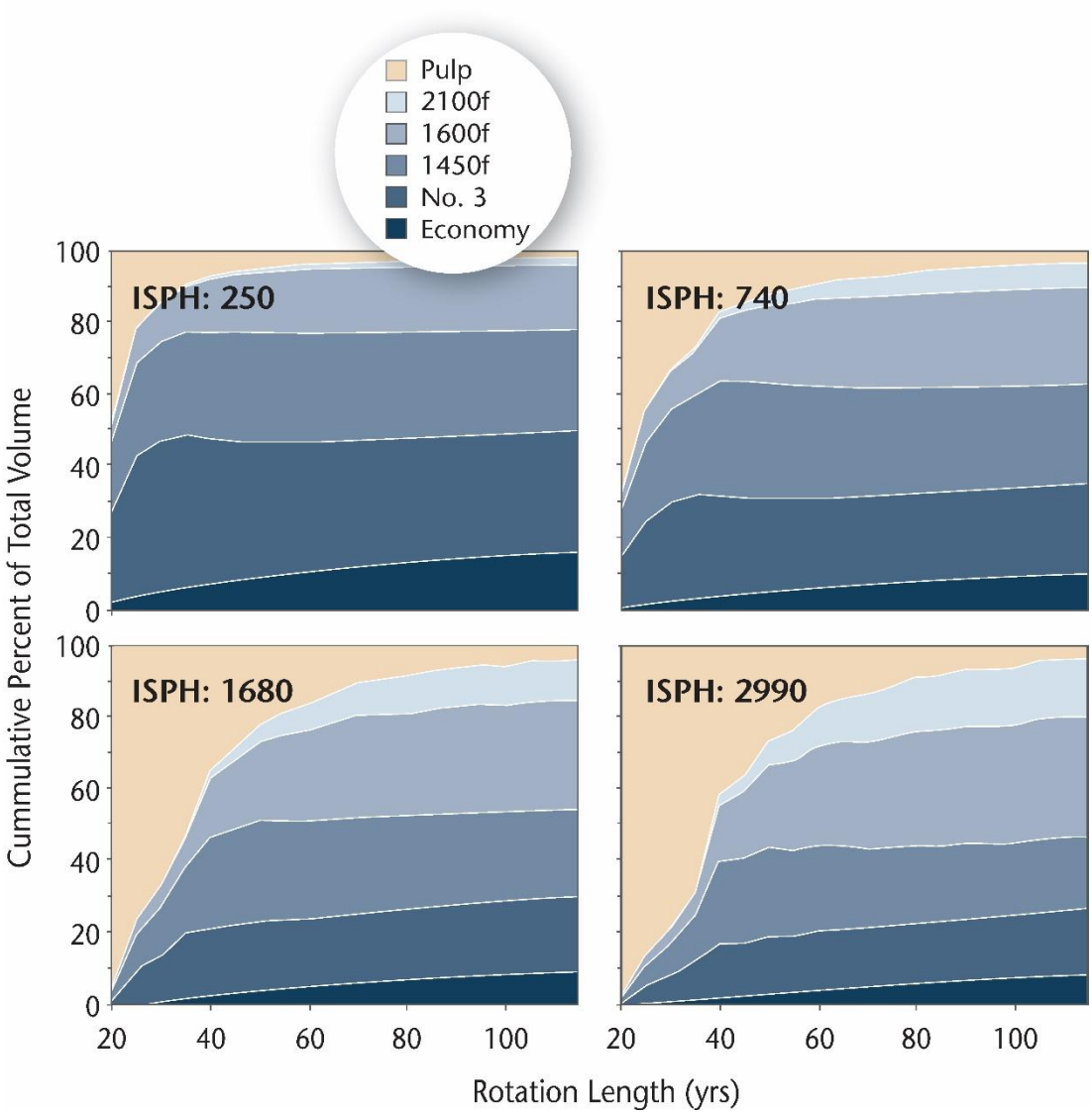

Figure 2.4 ORGANON simulation results: the number of recovered five-meter logs per hectare for three levels of initial planting density by their scaling diameter.

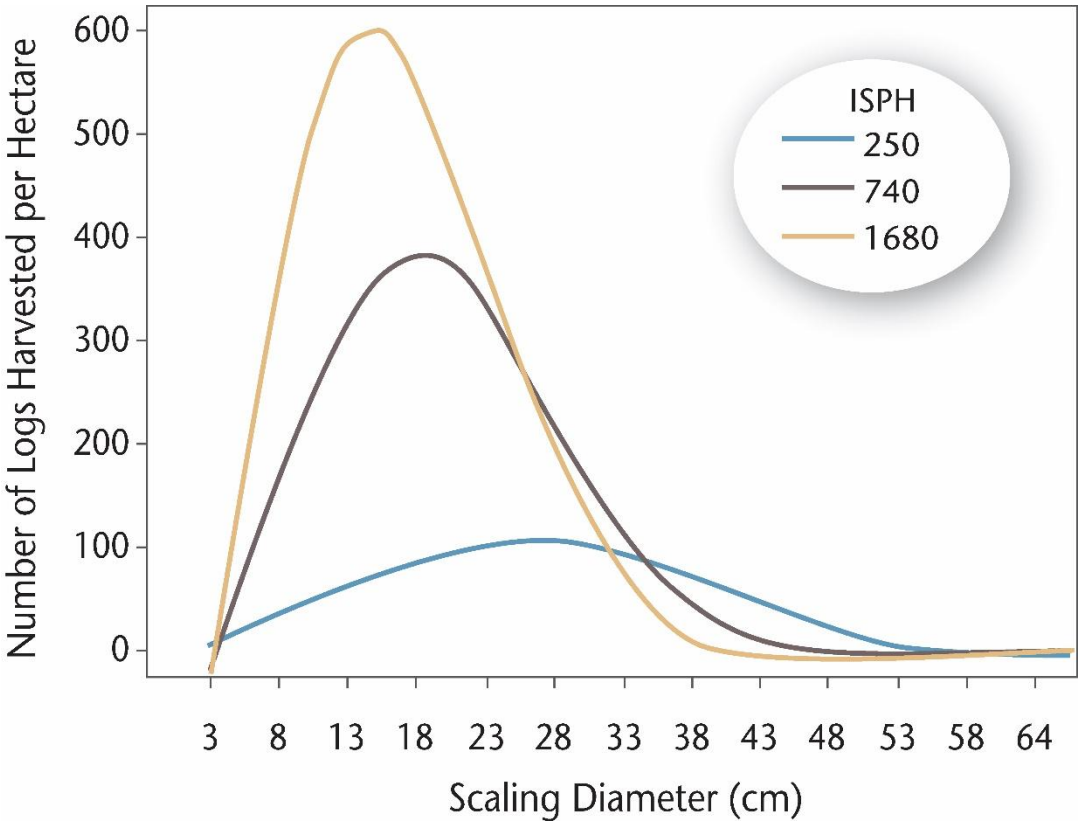

Figure 2.5 ORGANON simulation results: total lumber and pulp yield at a plantation age fifteen years in relation to volume of juvenile wood harvested as saw timber, the average largest branch in the bottom log, for stands with and without thinning.

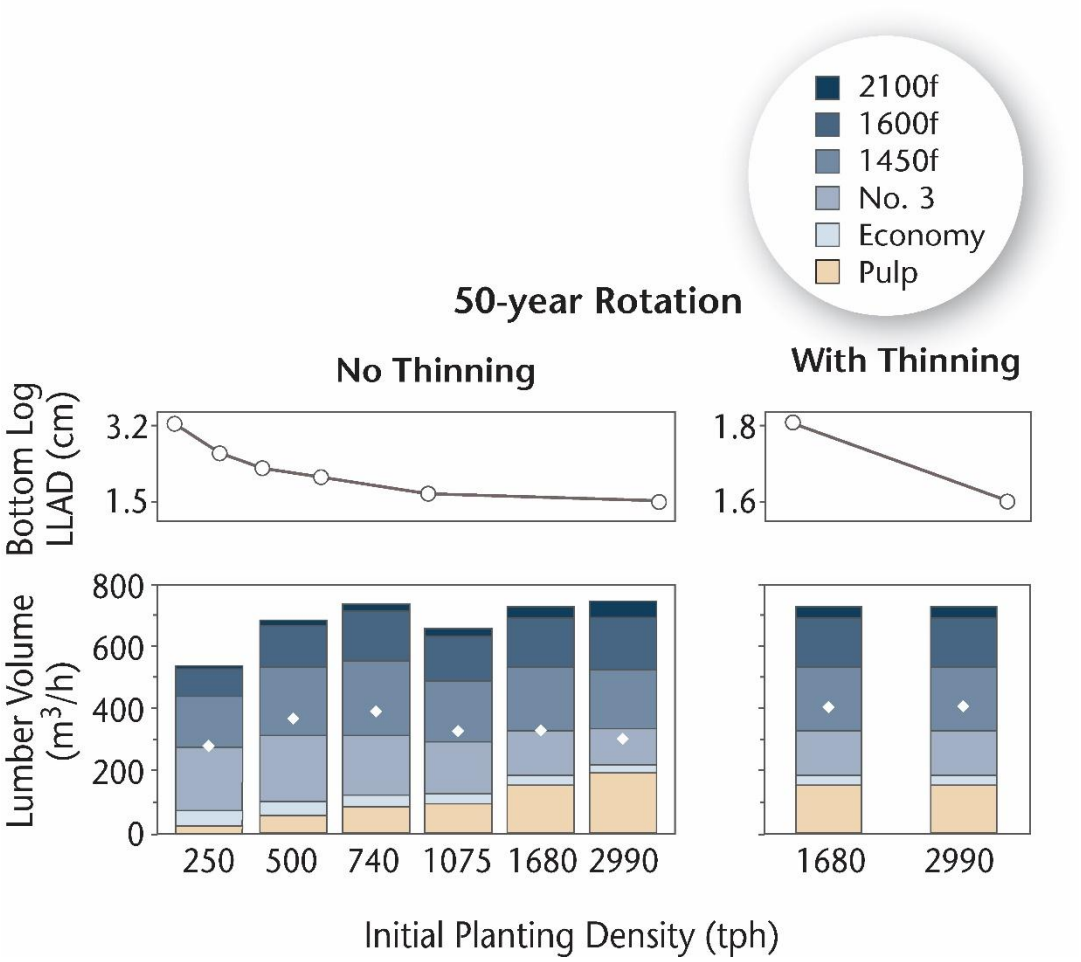

Chapter 3: Implications of Stand Density Regime for Meeting Douglas-fir Pole Specifications.

Nathaniel OSBORNE

Douglas MAGUIRE

Published in modified form in:

2015. Center for Intensive Planted-forest Silviculture, 2014 Annual Report, Pp. 24-27.

Abstract

Sapwood area is an important surrogate for total leaf area, an indicator of tree vigor and a predictor in ecophysiological tree growth models. For this reason, models have been developed to predict the area of sapwood for individual trees in intensively managed Douglas-fir plantations. However, models for sapwood area can be extended to other applications. The sapwood rind and heartwood core are important in the manufacturing of many wood products. One of the most valuable products that depend on a minimum sapwood width is utility poles. These poles have strict requirements for taper, sapwood thickness at the pole base, and appearance of the pole surface. Using young stand growth equations, and a forest growth and yield simulator, the development of 216 theoretical stands were simulated. Trees from each stand were bucked into virtual logs and utility poles. Results from the analysis provided insights to biologically optimal silvicultural regimes to produce utility poles. More importantly, the analysis highlighted knowledge gaps in wood properties models for intensively managed Douglas-fir plantations. Without penalties for surface and stem form defects along individual trees, the yield and recovery of high value forest products can be seriously overestimated. Despite the pitfalls of this analysis, there appears to be a budding potential to utilize linked forest growth, yield and wood properties models to support identification of optimal silvicultural regimes.

Introduction

Sapwood and heartwood are important features of the tree bole, related to the physiological function of living wood and the material behavior of forest products. The

physiological role of sapwood is to transport nutrients and water from the root system to the foliage during active transpiration, as well as to store these materials at different times of the year (Kramer and Kozlowski 1979). As a consequence there is a strong relationship between sapwood cross-sectional area, crown length (CL) and recession and foliage mass (Shinozaki et al. 1964). The sapwood area of any tree is proportional to the total foliage mass it services (Assman 1970), so it can be considered an indicator of photosynthetic capacity, tree vigor and physiological development. Heartwood formation is also a growth-regulated process, which is proportional to an optimal sapwood area (Bamber 1976). The formation of heartwood is characterized by death of parenchyma cells and the successive impregnation of cell lumens with decay resisting extractives. Area of sapwood and heartwood also affect mechanical properties along the living tree bole (Long et al. 1981). The inactive heartwood is relatively less conductive and stiff, while the sapwood rind is permeable and flexible, owing to higher moisture content. Mechanical properties in the living tree bole do not necessarily transfer to the material behavior of forest products. After removing the effect of moisture content, heartwood and sapwood do not differ in strength properties (Forest Products Lab, 1966). The principle difference between heartwood and sapwood is suitability for wood preservation treatment and decay resistance (Sung-Mo and Morrell 2000; Islam et al. 2008; Vikram et al. 2011).

A primary mechanism controlling sapwood area in Douglas-fir is soil moisture availability over the growing season. As soil moisture decreases, the sapwood area decreases (Beedlow et al. 2007; Brix and Mitchell 1985). Stand density management

influences soil moisture availability and sapwood area (Brix and Mitchell 1983; Aussenac and Granier 1988) through the rate of tree and stand evapotranspiration. The initial spacing of a stand, thinning and fertilization all have the possibility to modify the trajectory of a stands density over time (Drew and Flewelling 1979). Stand density dynamics and relations to sapwood area along the tree bole can be modeled at an individual tree level (Maguire and Hann 1987; Maguire and Batista 1996). Models for the sapwood rind and heartwood core have various applications to forest modeling and decision support. Predicting the delineation of sapwood and heartwood informs wood use in manufacturing, elemental composition for nutrient budgeting and support for predicting individual tree and stand leaf area index for ecophysiological forest growth models.

Linked forest growth, yield and wood properties models (GYWP) is a larger concept, which includes models for sapwood and heartwood delineation (Mäkelä et al. 2010). The focus of GYWP system has been to predict wood material properties resulting from alternative silvicultural regimes to support decision making. We describe the application of a new model for sapwood and heartwood taper (Maguire 2014) in a GYWP software package. The modeling software is used to predict potential yield of utility poles under several silvicultural regimes across a wide range of site conditions. Utility poles are one of the highest value forest products from Douglas-fir forests (Landgren et al. 1994). These poles are usually large, mostly defect free tree boles with little taper but requiring a minimum thickness of sapwood. A minimum requirement for sapwood area ensures effective penetration of wood preservatives under pressure treatment (Colley 1942).

Heartwood, while decay resistant, is less permeable and unsuitable for preservation treatment.

Methods

Models for the heartwood core and sapwood rind

Three equations to delineate heartwood and sapwood were developed by Maguire (2014): height of the heartwood core; heartwood at breast height; and taper of the heartwood core (Table 3.1). Height of the heartwood core is modeled as a proportion of total height of the tree using model forms similar to those used for modeling crown ratio or bole ratio:

[1] $$HT_{HWD} = \frac{HT}{1+exp\left[2.3615+1.9650\cdot\ln(CR)-1.3129\cdot\ln(CL)+1.1380\cdot\left(\frac{HT}{DBH}\right)\right]}$$

The heartwood at breast height is modeled using a power function:

[2] $$HWD_{BH} = 0.6368 \cdot DBH^{[-0.0112\cdot HT-0.4137\ln(CR)+0.3964\cdot\ln(CL)]}$$

The heartwood profile is modeled with a segmented quadratic-quadratic equation with equal predictions and equal first derivatives at the join point (Max and Burkhart 1976; Walters and Hann 1986):

[3] $$HWD_h = HWD_{BH}\left[1 - X + Y_1 + \left(-0.11664 \cdot exp\left(\frac{DBH}{HT}\right)\right)Y_2 + \left(-0.66487 \cdot \right.\right.$$ *expHTDBHY3*

where,

Y_1 = $I_2[X + I_1(W(1+Z)-1)] - (X-1)(X - I_2 \cdot X)$

$$Y_2 = I_2[X + I_1(W \cdot (X + K \cdot Z) - X) - (X - 1) \cdot (X - I_2 \cdot X)]$$

$$Y_3 = I_2[X^2 + I_1(K \cdot W(2 \cdot X - K + K \cdot Z) - X^2)]$$

$$Z = \frac{K - X}{K - 1}$$

$$W = \frac{X - 1}{K - 1}$$

$$X = \frac{(h - 1.37)}{(HT_{HWD} - 1.37)}$$

$$K = \frac{(0.5\,HCB - 1.37)}{(HT_{HWD} - 1.37)}$$

$$\text{CR} = \frac{1}{\left[1 + exp(-1.15127 + 0.9693 \cdot \ln(DBH) - 1.6713 \cdot \left(\frac{DBH}{HT}\right)\right]}$$

$$\text{HCB} = HT - (CR \cdot HT)$$

$$I_1 = \begin{cases} K \leq 0 \; or \\ K > 0 \; and \; X \leq K, & 0 \\ K > 0 \; and \; X > K, & 1 \end{cases}$$

$$I_2 = \begin{cases} K \leq 0, & 0 \\ K > 0, & 1 \end{cases}$$

Simulating yield of utility poles under various silvicultural regimes

Equations [1-3] allowed estimation of the profile of heartwood core and implied sapwood rind. These models were incorporated in the *cipsr* GYWP software (Osborne et al. 2015). The *cipsr* GYWP software is an interface to the ORGANON and CIPSANON (Weiskittel et al. 2011) forest growth and yield (GY) models, which can be linked to several wood properties (WP) models. Using the *cipsr* software and young stand growth equations, 216 silvicultural regimes and their effect of pole yield were simulated.

Silvicultural regimes represented different combinations of initial spacing, rotation length, site-productivity (SI) and commercial thinning intensity (Table 3.2). Commercial thinning was implemented as thinning from below to a target residual relative density (Curtis 1970), contingent upon reaching a designated maximum relative density as the thinning trigger for the stand.

Young stand growth and diameter distribution for the first ten years were estimated from the set of initial planting densities and SI values using a modified cumulative Weibull distribution function described by Knowe et al. (2005):

[4] $$F(D) = 1 - exp\left\{-\left(\frac{D-a}{b}\right)^{c}\right\}$$

where D was the diameter at breast height at stand age ten (cm) and a, b and c were parameters for the function location, scale and shape, conditional upon a series of other D-distribution recovery equations. Complete control of hardwood basal area was assumed for all simulations. The continuous Weibull distribution was segregated into discrete diameter classes based on 1-cm intervals (Figure 3.2). The implied empirical diameter distribution that included only tree DBH records was passed to *cipsr*. Using the CIPSANON model, missing tree heights and crown ratios were imputed, and the development of each stand was simulated to the desired rotation age.

Simulated bucking of virtual trees

Some silvicultural regimes with scheduled thinnings were removed from analysis because the required relative density targets were never reached in simulation. After removing

these simulations from the analysis, virtual trees from each simulation were bucked into poles and logs using the *process* algorithm in *cipsr*. The process algorithm is applied at the individual tree scale, until the sum of x_1 - x_3 equals zero (Figure 3.3). If a product is successfully harvested during the bucking simulation, the value of h_0 is updated based on the harvested product length and kerf and another harvest is attempted on the virtual tree. If the indicator x_2 is set equal one, a more detailed optimization procedure follows. In that procedure, branch profile is estimated using equations by Weiskittel et al. (2007). Using the branch profile and a numerically integrated estimate of the log volume (Walters and Hann 1986), the volume of lumber recovery from a given log is estimated (Fahey et al. 1991). Otherwise, if the indicators x_1 or x_3 are set equal one, then the length of product is maximized to ensure the best possible recovery of product from a given tree. For this analysis, poles were required to have a minimum top diameter (PTD) of 23.36-cm and minimum pole log length (PLL) of 15.24-m. These harvesting constraints restricted poles to the most profitable classes, $H_1 – H_6$ (Table 3.2).

Results and Discussion

Simulation results and interpretation

Stand density management generally had an effect on pole yield which became more pronounced with time (Figure 3.4). The surfaces in Figures 3.4 – 3.5 were generated using the Albrecht Gebhardt aspline and smoothing algorithm (Petzoldt and Maechler 2013). Care should be taken when interpreting individual values of proportional yield from the smoothed surfaces (i.e. these are not empirical values). As rotation length increased, the yield of utility poles increased, with the greatest proportion of yield from

densely stocked stands. Tightly spaced stands yielded more utility poles than widely spaced stands because closer spacing led to reduced tree taper. If a tightly spaced stand is allowed to mature (60–70 years), self-thin, and increase in diameter along the bole, the proportional yield of poles is implied to be substantial. Site fertility also had an apparent effect on the proportional yield of poles (Figure 3.5). As site fertility increased, the yield of poles also increased. The homogeneity in yield, however, appeared to decrease with increased site fertility. The increased variability in pole yield, conditional on site quality, was a function of the rate of self-thinning (Drew and Flewelling 1977). As site quality increases, stands move along a self-thinning trajectory more rapidly, accelerating the size differentiation of constituent trees.

Preliminary results suggest that relationships between product yield and stand density regimes met expectations based on known stand dynamics. Yields also matched expectations about tree physiological development and, more generally, product recovery. However, a more complete assessment of the wood properties and forest growth and yield system is necessary. That assessment should include comparison to pole recovery in operational stands, and comparisons of both to existing tree bucking simulators (Leary 1997).

Future research and development

Pole recovery estimated with the *process* function is contingent on product length, diameter (e.g. PBD, PTD) and a requirement for sapwood width. Grade recovery of poles is maximized when the trees are large, with little taper and with a thick rind of

sapwood at the pole base. Currently the abundance and distribution of defects is not estimated in the *process* function. Estimating the width of growth rings, knot clusters, spur knots, resin pockets, sinuosity and other stem defects will be important to avoid over-estimating product recovery and biasing subsequent financial analyses. In the *processControl* function, a default of 2.54-cm of sapwood is required at the base of any pole. The area of sapwood is based on estimation of sapwood at breast height, heartwood taper, and implied sapwood profile (Maguire 2014). In the *process* function, the stem is assumed to be a symmetric frustum of a cone with sapwood uniformly distributed around the circumference of the tree bole. However, the tree bole is rarely perfectly round and sapwood is therefore not always of uniform thickness around the bole. Assumptions about the cross-sectional shape of the tree bole and sapwood area could also lead to overestimation of potential pole yield. At this time, it is not recommended to use the *process* function in *cipsr* for financial analyses until the algorithm can be refined to better account for surface defects, stem form and the cross-sectional distribution of sapwood, all of which usually require field assessment.

Research efforts are required to modify stem bucking algorithms to accurately and efficiently estimate product recovery. The most challenging and pressing issue to resolve is predicting the expected frequency and severity of common defects like forking, ramicorns, knot clusters, resin pockets, and knot types. Simulated bucking of virtual stems can also require substantial computing resources. Memory and processing requirements could be minimized by developing more efficient programs, or calling compiled code (DLL), instead of relying on object oriented languages like R. However,

an argument can be made to sacrifice some program efficiency for decreasing the chance of software obsolescence. Forestry software programmed in compiled languages has a history of obsolescence that can only been avoided through strong institutional efforts to maintain code.

This analysis demonstrated one way to assess the complex dynamics of individual tree growth, form, and stem wood attributes on product yield. The information generated in this type of analysis could be used to support high resolution financial analyses and choose among competing silvicultural regimes, but is also subject to the vagaries of high-value markets. To become a reliable tool for estimating product recovery, the *process* function must estimate the distribution and nature of various defects in trees from managed Douglas-fir forests, highlighting a key need for improvements in the *process* function of *cipsr*.

Literature Cited

Aussenac, G., Granier, A. 1988. Effects of thinning on water stress and growth in Douglas-fir. Canadian Journal of Forest Research, 18(1):100-105.

Assman, E. 1970. The principles of forest yield study. Pergamon, Oxford, New York. 506 p.

Bamber, R. K. 1976. Heartwood, its function and formation. Wood Science and Technology, 10(1):1-8.

Beedlow, P.A., Tingey, D. T., Lee, E. H., Phillips, D. L., Andersen, C. P., Waschmann, R. S., Johnson, M. G. 2007. Sapwood moisture in Douglas-fir boles and seasonal changes in soil water. Canadian Journal of Forest Research, 37(7):1263–1271.

Brix, H., Mitchell, A. K. 1983. Thinning and nitrogen fertilization effects on sapwood development and relationships of foliage quantity to sapwood area and basal area in Douglas-fir. Canadian Journal of Forest Research, 13(3):384-389.

Brix, H., Mitchell, A. K. 1985. Effects of disrupting stem sapwood water conduction on the water status in Douglas-fir crowns. Canadian Journal of Forest Research, 15(5):982-985.

Curtis, Robert O. 1970. Stand density measures: an interpretation. Forest Science. 16(4):403-414.

Drew, T.J., J.W. Flewelling. 1977. Some recent Japanese theories of yield-density relationships and their application to Monterey pine plantation. Forest Science 23:517-534.

Fahey, T.D., J.M. Cahill, T.A. Snell- grove, L.S. Heath. 1991. Lumber and veneer recovery from intensively managed young-growth Douglas-fir. USDA-Forest Service Pacific Northwest Research Station, Portland, OR, USA. Research Paper PNW-RP-437.

Islam, M. N., Ando, K., Yamauchi, H., Kobayashi, Y., Hattori, N. 2008. Comparative study between full cell and passive impregnation method of wood preservation for laser incised Douglas fir lumber. Wood Science and Technology. 42(4):343-350.

Knowe, S. A., Radosevich, S. R., & Shula, R. G. 2005. Basal area and diameter distribution prediction equations for young Douglas-fir plantations with hardwood competition: Coast Ranges. Western Journal of Applied Forestry, 20(2):77-93.

Kramer, P.J., Kozlowski, T.T. 1979. Physiology of woody plants. Academic press. New York.

Landgren, C. G., Bondi, M. C., & Emmingham, W. H. 1983. Growing and harvesting Douglas-fir poles. Corvallis, Oregon: Extension Service, Oregon State University.

Leary, R. A. 1997. Testing models of unthinned red pine plantation dynamics using a modified Bakuzis matrix of stand properties. Ecological Modelling, 98(1):35-46.

Long, J. N., Smith, F. W., & Scott, D. R. 1981. The role of Douglas-fir stem sapwood and heartwood in the mechanical and physiological support of crowns and development of stem form. Canadian Journal of Forest Research, 11(3):459-464.

Maguire, D. A., Hann, D. W. 1987. Equations for predicting sapwood area at crown base in southwestern Oregon Douglas-fir. Canadian Journal of Forest Research, 17(3):236-241.

Maguire, D. A., Batista, J. L. 1996. Sapwood taper models and implied sapwood volume and foliage profiles for coastal Douglas-fir. Canadian Journal of Forest Research, 26(5):849-863.

Maguire, D. A., Kanaskie, A. 2002. The ratio of live crown length to sapwood area as a measure of crown sparseness. Forest science, 48(1):93-100.

Maguire, D. Models for the height and shape of the heartwood core in Douglas-fir. 2014. Pp. 37-41 in D.A. Maguire and D.B. Mainwaring (eds). CIPS 2013 Annual Report. Center for Intensive Planted-forest Silviculture, College of Forestry, Oregon State University, Corvallis, OR, USA.

Mäkelä, A., Grace, J., Deckmyn, G., Kantola, A., Kint, V. 2010. Simulating wood quality in forest management models. Forest systems, 3(4):48-68.

Max, T.A., Burkhart, H.E. 1976. Segmented polynomial regression applied to taper equations. Forest Sci. 22:283-289.

Osborne, N., Maguire, D., Hann, D. 2015. cipsr: An R interface to the ORGANON and CIPSANON models. R package version 2.2.2.

Petzoldt, T., Maechler, M. 2013. akima: Interpolation of irregularly spaced data. Package version 0.5.11.

Shinozaki, K., K. Yoda, K. Hozumi, and T. Kira. 1964. A quantitative analysis of plant form – the pipe model theory. I. Basic analyses. Japanese Journal of Ecology 14:97-105.

Sung-Mo, K., Morrell, J. 2000. Fungal colonization of Douglas-fir sapwood lumber. Mycologia. 609-615.

Vikram, V., Cherry, M. L., Briggs, D., Cress, D. W., Evans, R., Howe, G. T. 2011. Stiffness of Douglas-fir lumber: effects of wood properties and genetics. Canadian Journal of Forest Research. 41(6):1160-1173.

Walters, D. K., Hann, D. W. 1986. Taper equations for six conifer species in southwest Oregon. Oregon State University, School of Forestry, Forest Research Laboratory.

Weiskittel, A. R., Maguire, D. A., Monserud, R. A. 2007. Modeling crown structural responses to competing vegetation control, thinning, fertilization, and Swiss needle cast in coastal Douglas-fir of the Pacific Northwest, USA. Forest ecology and management, 245(1):96-109.

Weiskittel, A. R., Hann, D. W., Kershaw Jr, J. A., Vanclay, J. K. 2011. Forest growth and yield modeling. John Wiley & Sons.

Tables:

Table 3.1 Definition of terms and their associated units

Term	Definition	Units
HT_{HWD}	Estimated height of the heartwood core	m
HT	Total tree height	m
DBH	Diameter at breast height	cm
CL	Crown length	m
CR	Crown ratio (CL/HT)	ratio
HWD_{BH}	Estimated heartwood at breast height	cm
h	Height on stem	m
HWD_h	Estimated heartwood diameter at height h	cm
DIB	Diameter inside bark using Walter and Hann (1987)	cm
PLL	Maximum pole length	m
SLL	Maximum saw log length	m
CLL	Maximum chip log length	m
h_0	Cutting height	m
PBD	Pole diameter limit at 15.24 cm above pole base	cm
PTD	Top diameter limit for the pole	cm
SBD	Saw log bottom diameter limit	cm
STD	Saw log top diameter limit	cm
h_1	Maximum cutting height determined by product class (*e.x.* $h_0 + PLL$ for a utility pole)	m
x_1 - x_3	Indicators parameters for if a product has been harvested.	factor

Table 3.2 Site and silvicultural conditions considered in the set of simulations.

Treatment		Level of Treatment
Initial Planting Density (trees/hectare)	=	{494, 1,976, 3,459, 4,942}
Rotation Length (years)	=	{40, 60, 80}
50-year Site Index (meters)	=	{24, 30, 36}
Thinning trigger (relative density percent)	=	{50, 60}
Thinning residual (relative density percent)	=	{30, 40}

Table 3.3 Merchandising specifications required for Douglas-fir pole by class.

Pole Class	PTD (cm)	PBD_{min} (cm)	PBD_{max} (cm)	Pole Length (m)
H_1	23.36	49.27	54.35	15.24 – 38.1
H_2	25.14	52.07	57.40	
H_3	26.67	54.35	60.45	
H_4	28.19	57.40	63.24	
H_5	29.97	60.19	66.80	
H_6	31.49	62.48	69.59	

Figure captions:

Figure 3.1. Schematic for the *cipsr* forest growth, yield and wood properties (GYWP) system.

Figure 3.2. Continuous and implied discrete diameter distribution for a simulated stand at after ten years of growth, planted to an initial density of 1112 trees per hectare.

Figure 3.3. Procedure for selecting utility poles, saw logs and chip logs for harvest using the *process* function in the *cipsr* (Osborne et al. 2015) software.

Figure 3.4. Effect of initial planting density and rotation length on the proportion of total stand volume yield as utility poles (e.g classes $H_1 – H_6$; shaded region and contour lines).

Figure 3.5. Effect of initial planting density and final plant density and site index (24, 30 and 36 meters) on the proportion of total stand volume yield as utility poles (e.g classes $H_1 – H_6$; shaded region and contour lines) under a 50-year rotation age.

Figure 3.1 Schematic for the cipsr forest growth, yield and wood properties (GYWP) system.

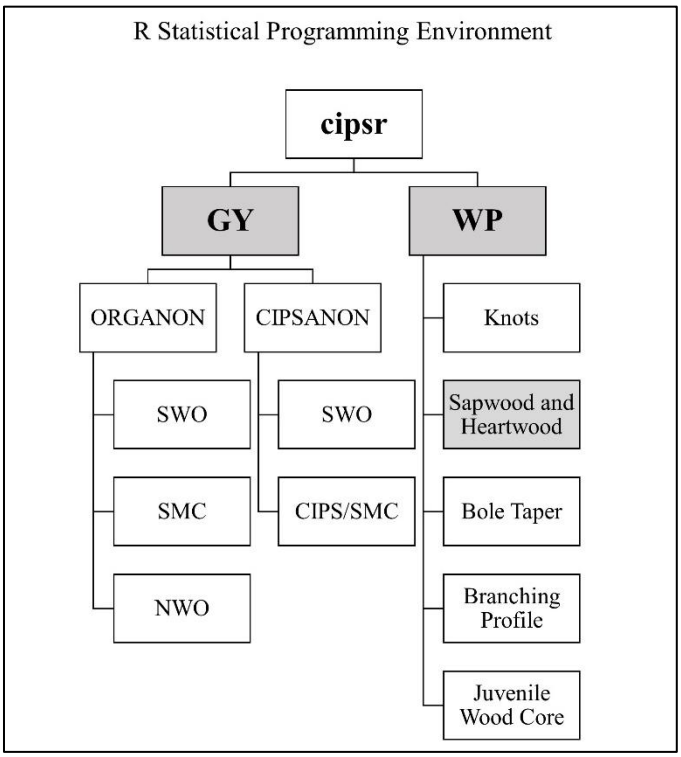

Figure 3.2 Continuous and implied discrete diameter (DBH) distribution for a simulated stand at after ten years of growth, planted at an initial density of 1112 trees per hectare.

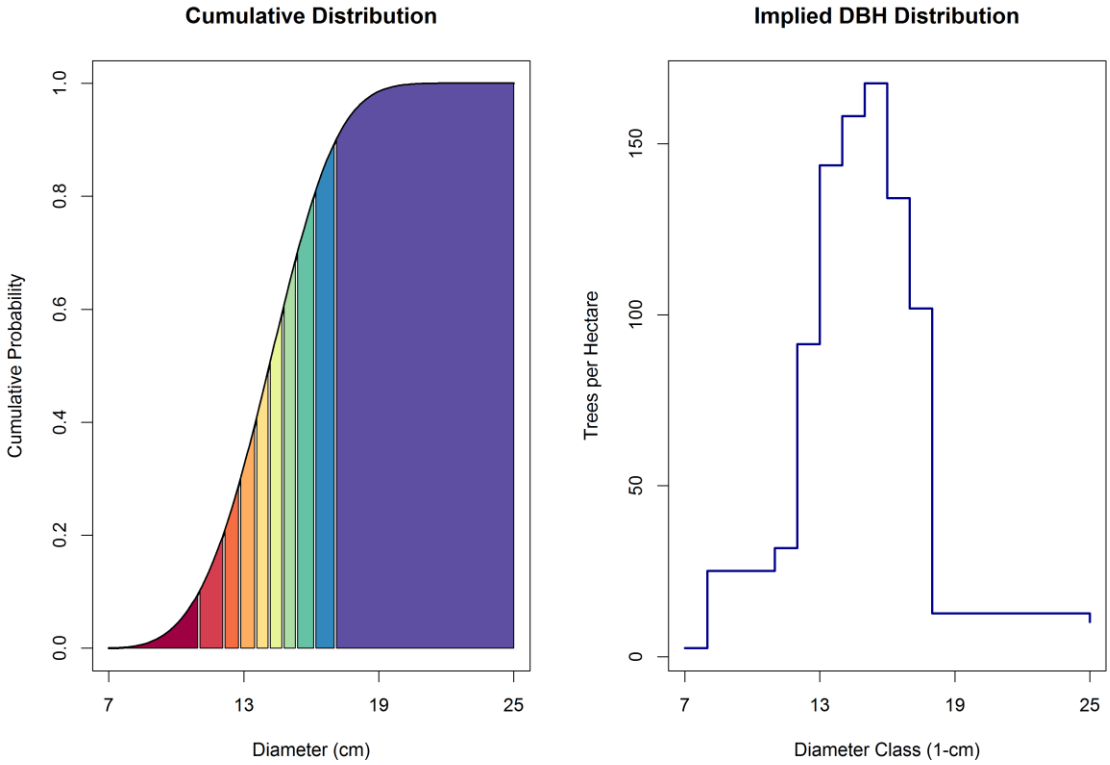

Figure 3.3 Procedure for selecting utility poles, saw logs and chip logs for harvest using the process function in the *cipsr* (Osborne et al. 2015) software.

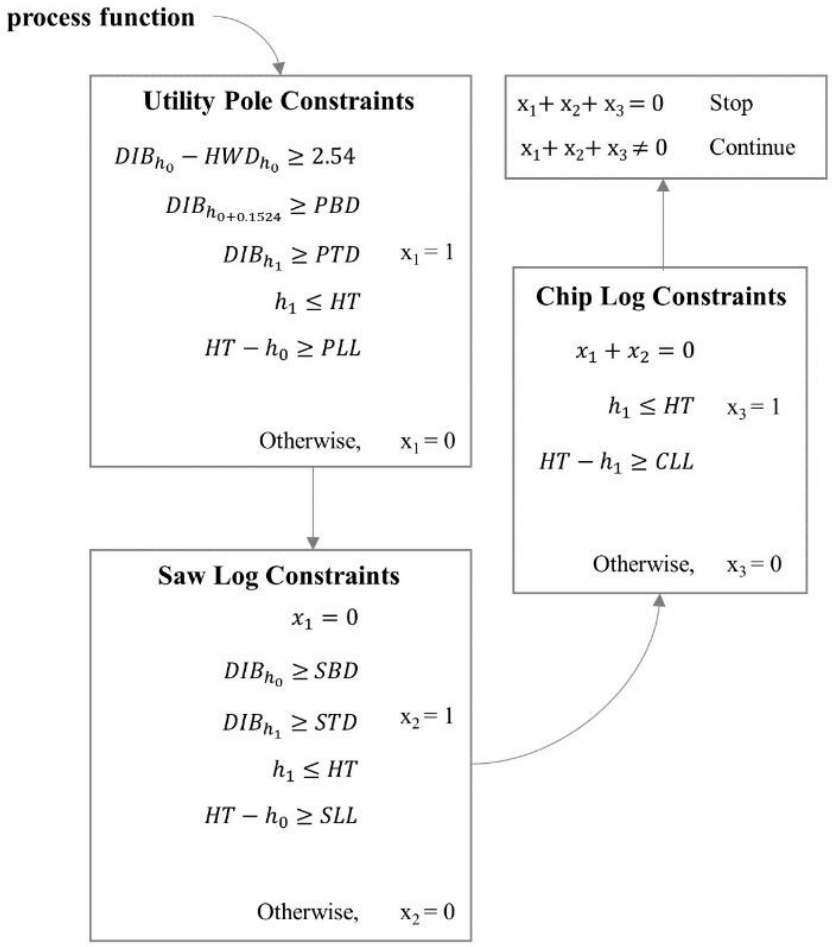

Figure 3.4 Effect of initial planting density and rotation length on the proportion of total stand volume yield as utility poles (e.g classes H_1 – H_6; shaded region and contour lines).

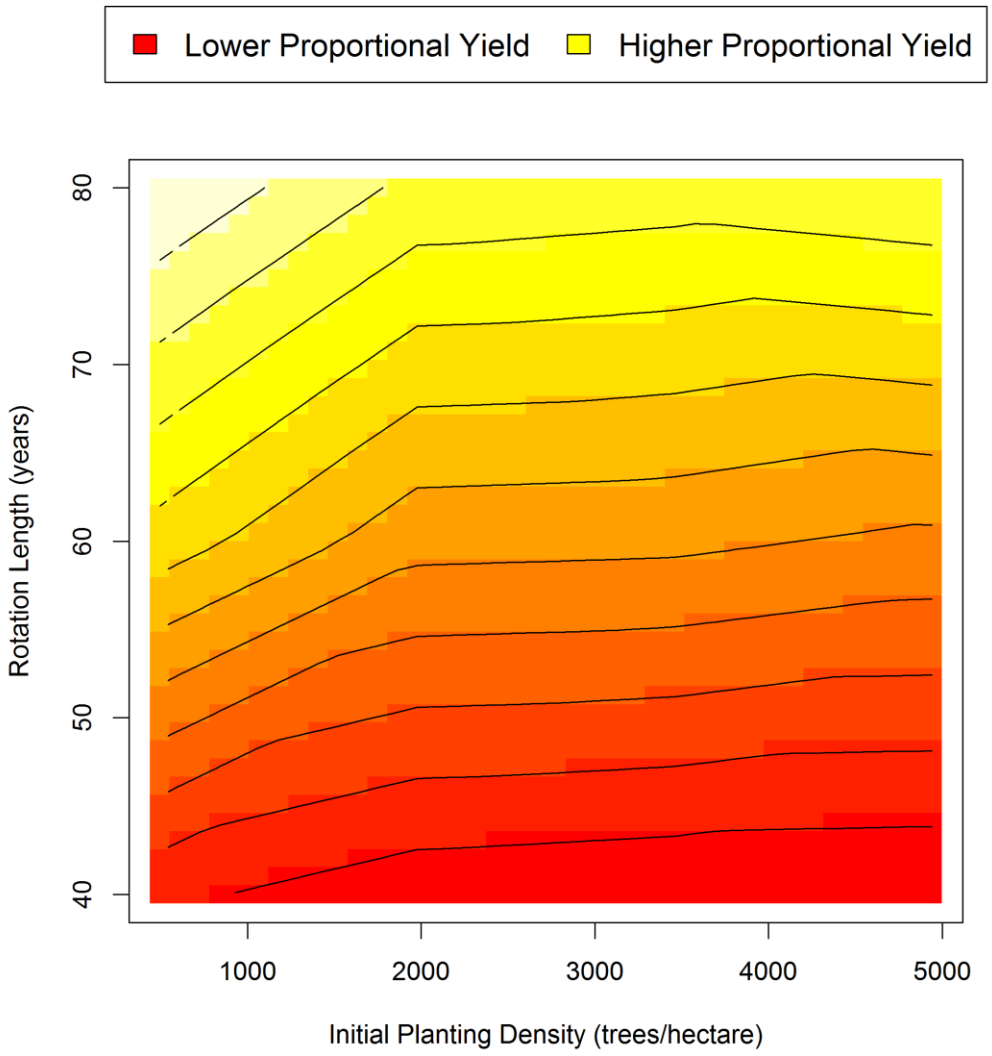

Figure 3.5 Effect of initial planting density and final plant density and site index (24, 30 and 36 meters) on the proportion of total stand volume yield as utility poles (e.g classes H_1 – H_6; shaded region and contour lines) under a 50-year rotation age.

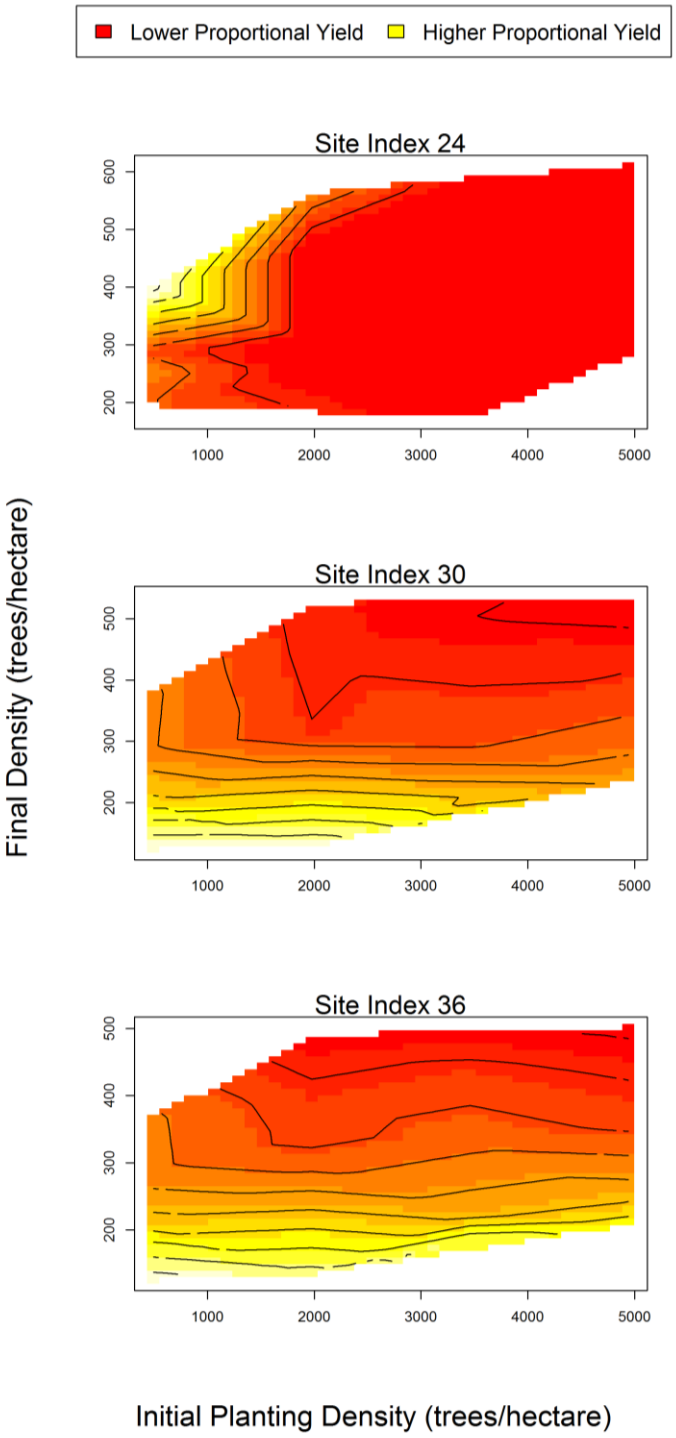

Chapter 4: Modeling knot geometry from branch angles in Douglas-fir (*Pseudotsuga menziesii*)

Nathaniel OSBORNE

Douglas MAGUIRE

Manuscript under review in:

Canadian Journal of Forest Research

Abstract

Lumber and veneer recovery from Douglas-fir (*Pseudotsuga menziesii*) trees depends on the size and distribution of knots. Two approaches have been used to simulate the effect of knots on recovery of these products: (1) prediction of recovery based on mill studies; and (2) simulated milling of virtual trees. A benefit of the latter approach, is that different milling configurations may be tested. Attributes of virtual logs are usually based on data from X-ray scanning, but knot geometry can also be modeled from a time series or chronosequence of branch angle and diameter measurements. Branch angle was modeled from a database of 17,953 branch measurements on 412 trees sampled in 16 Douglas-fir plantations. Dimensions of these sample trees, and a series of published models, were used to reconstruct annual growth rings. A dataset for knot pith curvature was then generated by imposing a time-series of branch angles across reconstructed annual growth rings of individual trees. Knot pith curvature was modeled as a first degree inverse polynomial, conditioned upon tree size and position within the tree bole. Knot pith was predicted to follow a linear path near the tree tip, becoming curvilinear with increasing age and depth into the crown.

Key Words

Knot geometry; Branch angle; Douglas-fir; Wood properties; Pith curvature

Introduction

Knots are one of the most important wood anatomical features affecting product and value recovery from Douglas-fir (*Pseudotsuga menziesii*) trees. A knot is formed as a

branch grows concurrently with, but generally perpendicular to the tree stem. The wood formed by knots creates discontinuities in longitudinal fibers of the tree bole, reducing wood strength (modulus of rupture), stiffness (modulus of elasticity) and visual appearance (Barbour and Parry 2001). A combination of these wood properties influences product recovery and value (Gartner 2005).

Over the last twenty years, numerous product recovery studies have been carried out in the Pacific Northwest (Fahey et al. 1991). These studies have generated product recovery equations that account for the effect of internal knots through surrogate variables like average branch size on the surface of the log. The possibility to link outputs from forest growth models to product recovery equations is well demonstrated (Briggs and Fight 1992; Houllier et al. 1995; Weiskittel et al. 2006). Simulation of tree growth, using a system of forest growth and product recovery equations, facilitates fine-tuning of silvicultural regime to maximize product recovery, and associated forest land value.

Product recovery equations developed from mill studies depend on mill configuration and on the target products. As a result, these equations provide limited options for exploring alternative products and sawing patterns. A greater versatility for estimating product recovery can be achieved through simulated sawing of virtual logs (Mäkelä et al. 2010). In this approach, products are sawn from three-dimensional virtual logs produced from a forest model or X-ray scanning image, and knot size and location is then evaluated along with other features to grade the product and assign a value. Numerous sawing simulators have been developed that vary widely with regard to computational sophistication and

required input: SAWSIM (Halco 1970), BOF (Lewis 1985), AutoSaw (Todoroki 1990), RadSawSim (Ištvanić et al. 2010), Grasp (Occeña and Schmoldt 1995), LogCast (Occeña et al. 2000), TopSaw (Yun et al. 2008), Optitek (FPInnovations 2014), WoodCim (Usenius 2000) and Cutlog (Turcan 2005). Analyses have demonstrated that simulated sawing can provide reliable estimates of product recovery (Todoroki et al. 2005).

A critical step in developing virtual Douglas-fir logs that can be passed from growth models into sawing simulators involves modeling the geometry of knots. The curvature in knot pith between stem pith and stem surface must be modeled accurately to represent the internal knot geometry within the bole and within sawn or peeled wood products (Figure 4.1). One of the first mathematical models for describing knot shape was developed for *Pinus sylvestris* based on assumptions about cross-sectional shape and fixed angles (Samson 1993). Models allowing knot curvature were developed later from data collected on dissected knots in *Pinus taeda* (Trincado and Burkhart 2008), and *Picea abies* (Lemieux et al. 1997). Dissection techniques have increasingly been replaced by X-ray computed tomography (CT). This technique has been used to model knot geometry of *Pinus sylvestris* (Moberg 2006), *Picea mariana*, *Pinus banksiana* (Duchateau et al. 2013), *Picea abies* (Andreu and Rinnhofer 2003; Oja 2000; Moberg 2001) and *Picea glauca* (Tong et al. 2013).

Curvature of the knot pith results from a gradual increase in branch angle (*VBA*) toward a horizontal position (branch angle throughout this analysis refers to angle of origin or angle at point of attachment to the main stem, measured relative to vertical). The angle of

a branch formed at the tree tip defines the initial angle of the knot that eventually results from that branch. Curvature in the knot pith between the bole pith and stem surface (Figure 4.1) therefore reflects the change in branch angle over time. This time-series of branch angles can be observed in the chronosequence of branch angles from the tree tip to the crown base. As depth into crown increases, branch age and angle increase, causing a gradual curvature in the pith of a given knot. Representation of a true time-series of branch angles by the chronosequence of branches with increasing age and depth into crown offers a non-destructive sampling approach to construct a database for modeling knot pith curvature.

The goal of this research was to produce a three-dimensional model of a knot within a tree stem so that knot size and location can be predicted on virtual boards created during sawing simulation. The specific objective of this analysis was to model the curvature of knot pith so that knots in virtual boards have an accurate shape and implied grain distortion relative to the angle at which the sawing simulator cuts through the log and branch. An assessment of mechanisms controlling knot formation, identification of analytical gaps, and future research needs are also discussed.

Methods

Construction of a database for modeling knot pith curvature requires two precursor models: 1) a model accounting for the change in branch angle with depth into crown; and 2) a model for estimating diameter inside bark (*dib*) at any height on the tree bole. Several models for branch angle (*VBA*) have been presented in the forestry literature

(Table 4.1). The first model was developed for young *Picea sitchensis* as a linear function of whorl order (Cochrane and Ford 1978). Later curvilinear models for branch angle were produced for *Picea abies* (Colin and Houllier 1992), Douglas-fir (Roeh and Maguire 1997; Weiskittel et al. 2007*a*) and *Pinus sylvestris* (Mäkinen and Colin 1998). Segmented polynomial taper models are available for estimation of *dib* at any height on a Douglas-fir stem (Walters and Hann 1986). Equipped with these models, a suitable database for modeling knot pith curvature can be assembled as a time-series of Cartesian coordinates (*x*-*y*) representing the succession of points where the knot pith emerged from the cambial surface at the end of each growing season (Figure 4.2). The *x*-coordinates correspond to the horizontal distance to the bole pith (*rib*) and the *y*-coordinates correspond to the height of knot pith at cambial emergence (h_1).

Models for Douglas-fir branch angle

Two models were developed to predict the insertion angle of live branches from the top to bottom of individual Douglas-fir crowns. All-subsets regression (*regsubsets*; Lumley 2009) in the R statistical programming language (R Core Team 2015) was used to screen several linearized candidate models and associated explanatory variables. The proposed models have a form similar to existing equations (Roeh and Maguire 1997; Weiskittel et al. 2007*a*), but the equations are better constrained by an empirically derived minimum value (w_0).

The data used to fit the models for branch angle were first described by Roeh and Maguire (1997) and involved climbing the sample tree and placing a clinometer at the

base of whorl branches and reading the angle to the nearest degree from the external scale. The database included 17,953 branch measurements (Table 4.2) taken from 412 trees (Table 4.3) across 16 Stand Management Cooperative (SMC) Type I and Type II installations (Maguire et al. 1991). The SMC installations are a network of experimental research plots in managed Douglas-fir forests, covering different levels of initial planting density, site class, and silvicultural treatments that include respacing, thinning, and fertilization. The first model describing branch angle took the following form:

[1] $$VBA = (\omega_0 + \omega_{11}CR) + \omega_{12}\left[1 - e^{\left(\beta_{11}DINCR + \beta_{12}CL + \beta_{13}\frac{DBH}{HT}\right)}\right] + \varepsilon_1$$

where *VBA* was branch angle (insertion angle measured from vertical in degrees), w_0 was an empirical minimum value calculated as the upper limit of the 25th percentile of minimum *VBA* observations for each tree in the modeling database, ω_{11} - ω_{12} and β_{11} - β_{13} were parameters to be estimated from the data, *DINCR* is relative depth into crown (*DINC*/*CL*), *DINC* was depth into crown from the tree top (m), *CL* was live crown length (m), *DBH* was tree diameter at breast height (cm), *HT* was total tree height (m), *CR* was the crown ratio (CL/HT), and ε_1 was the error term with $\varepsilon_1 \sim N(0,\sigma_{\varepsilon 1}^2)$.

The second model for predicting branch angle allowed a more gradual increase in branch angle with increasing *DINCR* by including an effect of branch diameter (*BD*):

[2] $$VBA = (\omega_0 + \omega_{21}CR) + \omega_{22}\left[1 - e^{(\beta_{21}DINCR + \beta_{22}CL + \beta_{23}DBH + \beta_{24}BD)}\right] + \varepsilon_2$$

where ω_{21} - ω_{22} and β_{21} - β_{24} were parameters to be estimated from the data, *BD* was the measured branch diameter (mm), ε_2 was the error term with $\varepsilon_2 \sim N(0,\sigma_{\varepsilon 2}^2)$, and all other variables were defined above.

Validation of branch angle models

Prior to fitting Equation [1] and Equation [2], a validation dataset was constructed. The validation dataset consisted of 3,281 branch measurements from 14 randomly selected SMC plots. The validation dataset represented about 16% of the entire dataset available for modeling, and both SMC Type I and II installations were represented. Statistics used in the validation of models for branch angle were as follows:

D = deviation = observed *VBA* – predicted *VBA*

AD = absolute deviation = |deviation|

D^2 = squared deviation = deviation^2

Construction of a dataset for modeling knot pith curvature

No attempt was made in this analysis to account for the azimuth of the branch around the circumference of the stem. Until evidence accumulates to the contrary, branch distribution will be assumed to follow a uniform distribution around the stem, as has been found in intensively managed *Pinus taeda* plantations (Doruska and Burkhart 1994). The spatial position of the knot pith for each past year was therefore described only by *x*-*y* Cartesian coordinates where, as described above, *x* represented the radial distance from the center of the bole pith (*rib*) and *y* represented the height of the knot pith from its point

of origin at the bole pith (H_{rib}). These annual *x-y* coordinates were estimated for an average branch at each whorl of each tree sampled to construct the modeling dataset. This process required the following three steps: (1) reconstruction of the stem *dib* profile for each year of past tree growth; (2) prediction of branch angle for each year the branch was alive (Equation 1); and (3) numerical solution of these equations to find the *x-y* coordinates of the intersection of stem *dib* profile and knot pith, corresponding to the point of knot pith emergence from the cambium (Figure 4.2).

The past *dib* of each tree was estimated from a segmented polynomial taper equation (Walters and Hann 1986). Estimation of past-annual *dib* profiles from the taper equation required reconstruction of past-annual *DBH*, *HT*, and *CL*. The past-annual *DBH* and *HT* were estimated using a scaling factor, which was the ratio of the current diameter and height to maximum potential diameter and height, for each year of reconstruction. Curves representing cumulative potential diameter growth were estimated using an annualized Douglas-fir *DBH* growth equation (Weiskittel et al. 2007*b*) that depended on only initial *DBH* and site quality (*SI*). Potential cumulative height growth curves were similarly estimated from a top-height growth equation (King 1966), and rescaled to individual sample trees using the ratio of current tree height to potential top-height for the respective site quality (*SI*) and tree age. These adjustments of the cumulative *HT* and *DBH* growth curves assumed past *DBH* and *HT* growth of any given tree had maintained the same proportion of maximum throughout the life of the sample tree.

A static allometric equation was developed to estimate height to crown base (*HCB*) for any year of backdating based on site quality and estimates of that year's *DBH* and *HT*. This estimate of HCB was used in the taper equation to estimate past *dib* profile, but also to identify the year of branch mortality. The *HCB* model was fit by combining eight different datasets from studies with consistent definitions of *HCB* (i.e., consistent with "compacted crown ratio" *sensu* Monleon et al. (2004)). Three of the datasets were from experimental studies of young plantations at five separate locations in western Oregon and Washington, and included tree height and crown base height measurement from time of planting up to ten years of age (Maguire et al. 2009). Three of the datasets included SMC Type I, II, and III plots with measurements from more than 66 locations extending from southern Oregon to northern Vancouver Island, and with ages ranging from 4 - 58 years (Maguire et al. 1991). The final two datasets were from long-term studies at five different locations in Oregon and Washington, and included trees ranging in age from 37 - 92 years (Ares et al. 2007; Curtis et al. 1997). After testing several candidate models, the following equation was selected:

[3] $$HCB = \frac{HT}{1+\exp\left[\alpha_0+\alpha_1 HT+\alpha_2\left(\frac{HT}{DBH}\right)+\alpha_3 SI\right]} + \varepsilon_3$$

where, *HCB* was height to crown base (m), α_0 - α_3 were parameters to be estimated from the data, *SI* was King's (1966) site index (m at 50-year breast height age), ε_3 was the error term with $\varepsilon_3 \sim N(0,\sigma_{\varepsilon 3}^2)$, and all variables were defined above.

For each whorl on each tree, a time-series of branch angles (*VBA*) was predicted starting at the initial whorl height indicated by predicted cumulative tree height growth. After the

crown base receded past a given whorl (implying branch mortality), the branch angles in the subsequent part of the time-series for that branch were fixed at the last angle predicted while the branch was still alive.

Models for knot pith curvature

Two models for estimating knot pith curvature were fit using the database of *x-y* coordinates of annual knot pith locations. These models were formulated based upon two potential applications requiring a slightly different set of predictor variables. The first and presumably dominant application was to estimate knot pith curvature during simulation of individual tree growth. In this application, tree level predictors such as *DBH*, *HT*, *CL* and whorl height (height of knot pith origin, h_0) would be available. Several model forms were tested, including a modified Weibull form (Duchateau et al. 2013) and a non-linear form that was a ratio of polynomials of radial distance (Lemieux et al. 1997). The final model was the following first-degree inverse polynomial, selected on the basis of model residual pattern (homogeneity of variance and lack of bias) and expected biological behavior:

$$[4] \qquad H_{rib} = \frac{rib}{\left(\gamma_{10}+\gamma_{11}CL+\gamma_{12}\left(\frac{DBH}{HT}\right)\right)+rib\left(\gamma_{13}+\gamma_{14}rib_0+\gamma_{15}\left(\frac{h_0}{HT}\right)\right)} + \varepsilon_4$$

where H_{rib} was the height of the knot pith above its estimated point of origin at the bole pith (cm), h_0 was the simulated whorl height where knot pith was defined to emerge from the bole pith (m), rib_0 was the radius inside bark at height h_0 (cm), *rib* was the radius

inside bark at H_{rib} (cm), $\gamma_{10} - \gamma_{15}$ were parameters to be estimated from the data, ε_4 was the error term with $\varepsilon_4 \sim N(0,\sigma_{\varepsilon 4}^2)$, and all other variables were defined above.

The second model was developed for instances where only exterior features of the tree, including the height of branch attachment (h_1, BR_{ht}) are available. The final model for this application was the following first-degree inverse polynomial:

$$[5] \qquad H_{rib} = \frac{rib}{\left(\gamma_{20}+\gamma_{21}CL+\gamma_{22}\left(\frac{DBH}{HT}\right)\right)+rib\left(\gamma_{23}+\gamma_{24}rib_1+\gamma_{25}\left(\frac{h_1}{HT}\right)\right)} + \varepsilon_5$$

where H_{rib} was the height of the knot pith above its estimated point of origin at the bole pith, h_1 was the height of knot pith at emergence from the cambium, rib_1 was the radius inside bark at h_1, $\gamma_{20} - \gamma_{25}$ were parameters to be estimated from the data, ε_5 was the error term with $\varepsilon_5 \sim N(0,\sigma_{\varepsilon 5}^2)$, and all other variables were defined above.

The use of the pith curvature models was demonstrated by constructing some three-dimensional knots of the type that would be contained in a virtual tree or log for sawing simulation. Equation [5] was first applied to a tree typical of the Roeh and Maguire (1997) dataset (*DBH* = 26 cm, *HT* = 16 m, *CL* = 14 m) to predict the pith or central axis of several branches at different heights within the live crown. The knot diameter at the point of branch insertion was assumed circular and symmetric around the knot pith and equal to the predicted maximum branch diameter (BD_{max}) at a specific depth into crown (Weiskittel et al. 2007*a*). The diameter of the knot was assumed to decrease non-linearly as radial distance (*rib*) approached zero in a manner described by the following equation:

[6] $$RAD = \frac{BD_{max}}{2}\left[1 - e^{(-\delta \cdot rib)} \Big/ 1 - e^{(-\delta \cdot rib_{max})}\right]$$

where *RAD* was the knot radius at *rib* (cm), BD_{max} was the predicted maximum branch diameter at the point of insertion (cm), δ was a subjectively estimated shape parameter, and *rib* was radial distance from the tree bole pith (cm).

Results

Equations [1] and [2] explained 16.6% and 21.5%, of the residual variation (R^2) in branch angles, respectively (Table 4.4). The residuals for both equations indicated constant variance across the range of predicted branch angles and depth into crown (Figure 4.3). Predictions from Equations [1] and [2] indicated that branch angle increased consistently with depth into crown for branches on individual Douglas-fir trees (Figure 4.4). The trend in branch angle varied by the combination of *DBH*, *HT*, and *CL* among individual trees. Large trees and those in a superior social position tended to have a greater initial branch angle, but converged toward the same maximum branch angle at crown base as smaller trees (Figure 4.5). Equation [2] produced a behavior very similar to Equation [1], but caused the branch angle to change at a slower rate with increasing *DINC*. Instabilities in Equation [2] were exposed when the model was extrapolated beyond the scope of the modeling dataset. Validation of Equations [1] and [2] suggested reasonable model behavior, although a separate and truly independent database of branch angles is needed for more rigorous validation (Table 4.5).

The model for HCB was required for backdating tree dimensions because, consistent with wide recognition of a functional link between stem profile and crown length (Larson 1963), the taper equations included live crown length as a predictor (Walters and Hann 1986). The HCB model (Equation [3]) explained 92.9% of the variation in height to crown base (Table 4.6), and behaved well by providing consistent declines in HCB as tree dimensions were back-predicted.

Models predicting knot pith curvature (Equations [4] and [5]) produced estimates consistent with observations on longitudinal-radial sections through knots (Figures 1 and 6). At the tree tip, knot pith curvature is predicted to be nearly linear. As depth into crown increases (decreasing h_0 or h_1), the knot pith becomes more curved towards a horizontal asymptote. Residuals for Equations [4] and [5] indicated homogeneity of variance and no or little bias. Because Equation [1] smoothed away much of the inherent variation in angles within and among branches, and was then used in constructing the modeling database, both Equations [4] and [5] explained nearly all of the variation in the resulting knot pith curvature patterns (Table 4.7). Predicting H_{rib} from h_0 versus h_1 did not change the goodness of fit or residual behavior of Equation [4] or [5].

The simulated knots resembled curved cones, except that the rate of increase in knot diameter decreased with increasing distance from the bole pith (Figure 4.7). Knots near the tip of the tree (Figure 4.7D) are oriented more vertically and increase in diameter rapidly throughout their length, whereas knots near the base of the crown (Figure 4.7A)

become more horizontal and almost cylindrical in shape due to their slow growth rate deep in the crown.

Discussion

Mechanisms controlling branch angle and knot pith curvature

Models for describing or predicting patterns in branch angle typically explain only a small portion of the total variation in this attribute (Roeh and Maguire 1997; Weiskittel et al. 2007*a*). Branch angle is partly controlled by genetics (St. Clair 1994), but must also influenced by interactions with other branches within the whorl, within adjacent whorls, and within crowns of surrounding trees, all of which otherwise appear as random variation (Colin and Houllier 1992; Vestøl et al. 1999). These interactions probably include mutual shading and shifts in light quality, causing differentiation in growth rates sink strength for water, nutrients, and plant growth regulators. The Douglas-fir data in our analysis exhibited a large amount of variation in branch angle within a given whorl on the same tree. Most forest growth and yield experiments do not take into account the genotype or family of subject trees, unless the field trials are progeny tests designed specifically for tree breeding purposes (Howe et al. 2006), realized gain trials designed to test different mixes of families (e.g., St. Clair et al. 2004), or clonal tests to identify the best performing genotypes (Li et al. 2015). St. Clair (1994) found that individual tree heritability (h^2) of Douglas fir branch angle was only 0.06 in one progeny test in the Oregon Coast Range, with angles ranging from 32-78° among individual trees and from 51-59° for averages among different families. However, others have found heritability as high as 0.49 (Birot and Christophe 1983) and 0.73 (King et al. 1992). St. Clair's (1994)

results suggest that within a site much of the variation in branch angle is environmentally controlled, likely in response to gradients in light intensity and quality imposed by adjacent branches and trees, by depth of the branch in the tree crown, and by the structure of the stand canopy. These responses are also reflected in crown width and may have been selected for to maximize light interception, individual branch growth, and ultimately reproductive success of the tree (Chmura et al. 2007). Although some genetic gain may be possible if more horizontal or more vertical branches were deemed desirable from either a growth or wood quality perspective, the low to moderate heritability of branch angle and apparent strong influence of the light environment suggest that tree improvement efforts might be better focused on wood properties that have been shown to be more strongly heritable (Howe et al. 2006).

Additional variation might be explained by measuring promising environmental factors associated with site-to-site variation (Hein et al. 2007) after controlling for genetic effects on branch angle. Elevation has been shown to explain some variability in wood properties of Scots pine (Høibø and Vestøl 2010) and Norway spruce (Moberg 2006), and these results could possibly apply to Douglas-fir. Other authors have found a significant effect of site index (SI) on branch angle, but the effects have been uniformly weak (Roeh and Maguire, 1997; Weiskittel et al., 2007*a*). Both elevation and site index probably exert some selective pressure on optimal branch angles by achieving a balance between minimization of shear stress/breakage and optimization of light interception. However, to thoroughly assess hypotheses about adaptive values of varying branch angle that might

be naturally selected for, common garden experiments would be needed to separate genetic and site effects.

Models for knot pith curvature described in this paper predict only the average trend for a given whorl. Given the variation in branch angles within a whorl of given age, the time series of those angles would impose corresponding variation in knot pith curves. Future analysis should consider how to translate the within whorl variation in branch angles into a corresponding set of stochastic knot pith curves, for example, by introducing variation into the equation parameters. This approach could reproduce the natural variability in knot geometry observed within a whorl, such that knot attributes of products generated from simulated sawing would be very realistic even though the mechanisms generating the variability may not be explicitly represented.

Applications and limitations

Predicting knot pith curvature from a predicted or measured time-series of branch angles and reconstructed *dib* profiles is a non-destructive sampling approach that is applicable to monitoring permanent plots, but becomes logistically more difficult and more expensive as trees become taller. Predicted angle of branches described in Equations [1] and [2] apply only to primary branches formed in annual whorls of Douglas-fir. Insertion angle of interwhorl and epicormic branches can be measured and curvature of resulting knots can be estimated on these types of branches in the same way as on whorl branches. Although these types of branches have been shown to carry a significant amount of

foliage in Douglas-fir and therefore may be important for tree growth (Jensen and Long 1983), they have relatively little influence on wood quality and product recovery.

A key assumption in reconstructing knot pith curves was that the growth rate in diameter and height maintained the same proportion of the maximum cumulative growth curves over time. This assumption would hold best for trees in even-aged stands with no silvicultural intervention. The sampled plots were from Douglas-fir plantations with some respacing, and little to no thinning. The initial respacings were done prior to crown closure, so these treatments would have virtually no release effect on tree growth. None of the 37 SMC Type I plots received any thinning before the branch angles in the modeling or validation datasets had been measured, and only 7 had been fertilized. Growth responses to fertilization were variable, and depended on the level of respacing (Sucre et al. 2008). Of the 12 plots on the SMC Type II installations, 5 had received one thinning before branch measurement. In short, some departure from the assumption of constant growth proportion may have been imposed by silvicultural treatments on a small minority of the plots, and some additional but less systematic departure was almost certainly imposed by annual weather fluctuations. These departures could have caused some short-term bias in the estimated knot pith curves, but only within approximately four years prior to the branch measurements.

Of greater significance is that fact that the measured trees on these long-term silvicultural field trials were subsequently subjected to much more complex silvicultural regimes. Under this scenario, repeated measurements of branch angles and diameters would be

required to correctly infer internal knot geometry from branch measurements, because it is quite likely that the crown responses to thinning and to fertilization (assuming a growth response) would include abrupt shifts in diameter growth and quite possibly branch angle of insertion. However, from a silvicultural viewpoint, more insight into the biological response mechanisms of knot geometry can be learned by understanding the dynamic response of branches relative to the timing of silvicultural treatments of known intensity.

The approach applied in this analysis also can facilitate distinction of the live or tight knot zone from the dead or loose knot zone. Repeated application of the height to crown base model allows prediction of the year of whorl branch mortality. By estimating the spatial location of the branch pith, specifically by tracking estimated H_{rib} and *rib*, the growth ring corresponding to the year of crown recession past a given branch whorl would mark the beginning of the dead knot zone at that height in the stem.

The dataset used in this analysis came from relative young, planted Douglas-fir trees (Table 4.2). To better understand the change in branch angles on planted Douglas-fir over time, additional data should be collected from larger trees, across additional explanatory variables, and over time on individual branches. Because it is likely that average branch angle near the tip of the tree (at a given depth into crown) will change as trees age, grow in height, and experience lower water potentials near the top, it would be highly desirable to measure angle on some branches closer to the tree tip than can be accessed by climbing (Table 4.3). Measurements on these youngest branches should facilitate more dependable estimation of the lower asymptote to branch angle as depth

into crown approaches zero (Equations [1] and [2]). More vertical branches increase the effective knot size in wood products sawn parallel to the bole pith. However, branches with the lowest angle of insertion are also the youngest, so their influence is most pronounced within the low-quality juvenile wood core rather than in high-quality mature wood. Micro- and macro-anatomical attributes other than knot size and geometry may be more important determinants of wood quality and value in the juvenile wood core, obviating the importance of branch angle measurements in the very top portion of the tree.

Conclusions

Our procedure for constructing a modeling dataset required only three analysis steps: (1) reconstruction of the stem *dib* profile for each year of past tree growth; (2) prediction of branch angle for each year of branch growth (Equation 1); and (3) numerical solution to find the *x*-*y* Cartesian coordinates for the intersection of stem *dib* profile and the branch or knot pith in that year. Using this approach it was possible to model the arc formed by the knot pith at various heights on a Douglas-fir tree. With an assumption of knot size based on modeled trends in BD_{max} it was possible to generate a three-dimensional knot. Sawing simulation involves projecting such a knot onto a virtual board produced from the virtual log, as well as classifying it as a live or dead knot (e.g., Duchateau et al. 2015). The next step in developing this approach should be validation of models describing knot geometry. This validation can be achieved by X-ray tomography of whorl sections taken across a wide range of tree size and growing conditions, covering at least the range used for model development (Tables 2.2 and 2.3). The knot mapping software, “Gourmands”,

described by Tong et al. (2013) and developed at the Institut National de la Recherche Agronomique (INRA), demonstrates the potential of X-ray tomography for validation.

Acknowledgements

Data used in this analysis were made available by the Stand Management Cooperative at the University of Washington. We gratefully acknowledge Doug Mainwaring, David Hann, and Henry Rodman for many helpful suggestions during modeling and manuscript preparation.

Literature Cited

Andreu, J.P., Rinnhofer, A. 2003. Modeling knot geometry in Norway spruce from industrial CT Images, in: SCIA 2003, pp. 786-791.

Ares, A., Terry, T., Harrington, C., Devine, W. 2007. Biomass removal, soil compaction, and vegetation control effects on five-year growth of Douglas-fir in coastal Washington. Forest Science. 53(5): 600–611.

Barbour, R.J., Parry, D.L. 2001. Log and lumber grades as indicators of wood quality in 20- to 100-year old Douglas-fir trees from thinned and unthinned stands. USDA Forest Service Pacific Northwest Research Station, Portland, Oregon. Gen. Tech. Rep. PNW-GTR-510. 22 p.

Birot, Y., Christophe, C. 1983. Genetic structures and expected genetic gains from multitrait selection in wild populations of Douglas-fir and sitka spruce. Silvae Genetica 32(5/6): 141-151.

Briggs, D.G., Fight, R.D. 1992. Assessing the effects of silvicultural practices on product quality and value of coast Douglas-fir trees. Forest Products Journal 42(1): 40-46.

Chmura, D.J., Rahman, M.S., Tjoelker, M.G. 2007. Crown structure and biomass allocation patterns modulate aboveground productivity in young loblolly pine and slash pine. Forest Ecology and Management 243(2): 219-230.

Cochrane, L., Ford, E.D. 1978. Growth of a Sitka spruce plantation: analysis and stochastic description of the development of branching structure. Journal of Applied Ecology 15: 227-244.

Colin. F., Houllier, F. 1992. Branchiness of Norway spruce in north-eastern France: predicting the main crown characteristics from usual tree measurements. Annals of Forest Science 49(5): 51l-538.

Curtis, R., Marshall, D., Bell, J. 1997. LOGS: a pioneering example of silvicultural research in coast Douglas-fir. Journal of Forestry (USA) 95(7): 19–25.

Doruska, P.F., Burkhart, H.E. 1994. Modeling the diameter and locational distribution of branches within the crowns of loblolly pine trees in unthinned plantations. Canadian Journal of Forest Research 24: 2362-2376.

Duchateau, E., Longuetaud, F., Mothe, F., Ung, C., Auty, D., Achim, A. 2013. Modelling knot morphology as a function of external tree and branch attributes. Canadian Journal of Forest Research, 43(3): 266-277.

Duchateau, E., Auty, D., Mothe, F., Longuetaud, F., Ung, C.H., Achim, A. 2015. Models of knot and stem development in black spruce trees indicate a shift in allocation priority to branches when growth is limited. PeerJ, 3:e873.

Fahey, T.D., Cahill, J.M., Snellgrove, T.A., Heath, L.S. 1991. Lumber and veneer recovery from intensively managed young-growth Douglas-fir. Res. Pap. PNW-RP-437. Portland, OR: U.S. Department of Agriculture, Forest Service, Pacific Northwest Research Station. 25 p.

FPInnovations. 2014. Optitek 10: user's manual. FPInnovations, Quebec, Canada.

Gartner, B.L. 2005. Assessing wood characteristics and wood quality in intensively managed plantations. Journal of Forestry 103(2): 75–77.

Halco Inc. 1970. SAWSIM: Sawmill Simulation Program, Carroll-Hatch, Vancouver, Canada.

Hein, S., Mäkinen, H., Yue, C., Kohnle, U. 2007. Modelling branch characteristics of Norway spruce from wide spacings in Germany. Forest Ecology and Management 242(2): 155–164.

Høibø, O., Vestøl, G.I. 2010. Modelling the variation in modulus of elasticity and modulus of rupture of Scots pine round timber. Canadian Journal of Forest Research 40(4): 668–678.

Houllier, F., Leban, J., Colin, F. 1995. Linking growth modelling to timber quality assessment for Norway spruce. Forest Ecology and Management 74(1): 91–102.

Howe, G.T., Jayawickrama, K.M., Cherry, Johnson, G. R., Wheeler, N. C. 2006. Breeding Douglas-fir. Plant Breeding Review 27: 245-353.

Ištvanić, J., Piljak, K., Antonović, A., Luˇić, R. B., Jambreković, V., Pervan, S. 2010. The Theory and Mathematical Model Underlying the Radial Sawing Simulator—RadSawSim. Forest Products Journal 60(1): 48–56.

Jensen, E.C., Long, J.N. 1983. Crown structure of a co-dominant Douglas-fir. Canadian Journal of Forest Research 13:264-269.

King, J.E. 1966. Site index curves for Douglas-fir in the Pacific Northwest. Weyerhaeuser For. Pap. 8. Weyerhaeuser Research Technology Center, Federal Way, WA. 49 p.

King, J.N., Yeh, F.C., Heaman, J.C., Dancik, B.P. 1992. Selection of crown form traits in controlled crosses of coastal Douglas-fir. Silvae Genetica 41: 362-370.

Larson, P.R. 1963. Stem form development of forest trees. Forest Science Monograph 5. 42 p.

Lemieux, H., Samson, M., Usenius, A. 1997. Shape and distribution of knots in a sample of *Picea abies* logs. Scandinavian Journal of Forest Research 12(1): 50-56.

Lewis, D. 1985. Sawmill simulation and the best opening face system: a user's guide. USDA Forest Service, Forest Products Laboratory FPL-48. Madison, WI. 29 p.

Li, Y., Xue, J., Clinton, P.W., Dungey, H.S. 2015. Genetic parameters and clone by environment interactions for growth and foliar nutrient concentrations in radiata pine on 14 widely diverse New Zealand sites. Tree Genetics and Genomes 10(11): 1-16.

Lumley T. 2009. leaps: Regression Subset Selection. R package version 2.9.

Maguire, D., Bennett, W.S., Kershaw, J. 1991. Establishment report: Stand Management Cooperative silviculture project field installations. College of Forest Resources, University of Washington, Seattle WA. 42 p.

Maguire, D.A., Mainwaring, D.B., Rose, R., Garber, S.M., Dinger, E.J. 2009. Response of coastal Douglas-fir and competing vegetation to repeated and delayed weed control treatments during early plantation development. Canadian Journal of Forest Research 39: 1208-1219.

Mäkelä, A., Grace, J., Deckmyn, G., Kantola, A., Kint, V. 2010. Simulating wood quality in forest management models. Forest systems 19: 48-68.

Mäkinen, H., Colin, F. 1998. Predicting branch angle and branch diameter of Scots pine from usual tree measurements and stand structural information. Canadian Journal of Forest Research 28(11): 1686–1696.

Moberg, L. 2001. Models of internal knot properties for *Picea abies*. Forest Ecology and Management 147(2): 123–138.

Moberg, L. 2006. Predicting knot properties of *Picea abies* and *Pinus sylvestris* from generic tree descriptors. Scandinavian Journal of Forest Research 21(S7): 49–62.

Monleon, V.J., Azuma, D., Gedney, D. 2004. Equations for predicting uncompacted crown ratio based on compacted crown ratio and tree attributes. Western Journal of Applied Forestry 19(4): 260-267

Occeña, L.G., Schmoldt, D. L. 1995. GRASP - A Prototype Interactive GRAphical Sawing Program. MU-IE Technical Report, Pp. 1–17.

Occeña, L.G., Santitrakul E., Schmoldt. D.L. 2000. Hardwood sawyer trainer. Pp. 43-47 in Proc. 28th Annual Hardwood Symposium – West Virginia Now – The Future for the Hardwood Industry, Davis, WV. National Hardwood Lumber Assoc., Memphis, TN.

Oja, J. 2000. Evaluation of knot parameters measured automatically in CT-images of Norway spruce (Picea abies (L.) Karst.). European Journal of Wood and Wood Products, 58(5): 375-379.

R Development Core Team. 2015. R: A language and environment for statistical computing. R Foundation for Statistical Computing, Vienna, Austria.

Roeh, R.L., Maguire, D.A. 1997. Crown profile models based on branch attributes in coastal Douglas-fir. Forest Ecology and Management 96(1): 77–100.

Samson, M. 1993. Modeling of Knots in Logs. Wood Science and Technology 27(6): 429–437.

St. Clair, J.B. 1994. Genetic variation in tree structure and its relation to size in Douglas-fir. II. Crown form, branch characteristics, and foliage characters. Canadian Journal of Forest Research 24(6): 1236-1247.

St. Clair, J.B., Mandel, N.L., Jayawickrama, K.J.S. 2004. Early realized genetic gains for coastal Douglas-fir in the northern Oregon Cascades. Western Journal of Applied Forestry 19(3): 195-201.

Sucre, E.B., Harrison, R.B., Turnblom, E.C., Briggs, D.B. 2008. The use of various soil and site variables for estimating growth response of Douglas-fir to multiple applications of urea and determining potential long-term effects on soil properties. Canadian Journal of Forest Research 38: 1458-1469.

Todoroki, C.L. 1990. AUTOSAW system for sawing simulation. New Zealand Journal of Forestry Science 20(3): 332-348.

Todoroki, C.L., Monserud, R.A., Parry, D.L. 2005. Predicting internal lumber grade from log surface knots: Actual and simulated results. Forest products journal, 55(6): 38-47.

Tong, Q., Duchesne, I., Belley, D., Beaudoin, M., Swift, E. 2013. Characterization of knots in plantation white spruce. Wood Fiber Sci. 45: 84-97.

Trincado, G., Burkhart, H. 2008. A model of knot shape and volume in loblolly pine trees. Wood and Fiber Science 40(4): 634-646.

Turcan, P. 2005. CutLog: Optimum sawing solution software, Tekl STUDIO. Detva, Slovakia.

Usenius, A. 2000. WoodCim – Integrated planning and optimizing system for sawmilling industry. VTTs Building Technology. Internal Report. 8 p.

Vestøl, G.I., Colin, F., Loubère, M. 1999. Influence of progeny and initial stand density on the relationship between diameter at breast height and knot diameter of *Picea abies*. Scandinavian Journal of Forest Research 14(5): 470–480.

Walters, D., Hann, D. 1986. Taper equations for six conifer species in southwest Oregon. Forest Research Lab, Oregon State University, Corvallis, OR. Research Bulletin 56.

Weiskittel, A., Maguire, D. 2006. Intensive management influence on Douglas fir stem form, branch characteristics, and simulated product recovery. New Zealand Journal of Forestry Science 36(2/3): 293–312.

Weiskittel, A.R., Maguire, D.A., Monserud, R.A. 2007*a*. Modeling crown structural responses to competing vegetation control, thinning, fertilization, and Swiss needle cast in coastal Douglas-fir of the Pacific Northwest, USA. Forest Ecology and Management 245(1): 96–109.

Weiskittel, A.R., Garber, S.M., Johnson, G.P., Maguire, D.A., Monserud, R. A. 2007*b*. Annualized diameter and height growth equations for Pacific Northwest plantation-grown Douglas-fir, western hemlock, and red alder. Forest Ecology and Management 250(3): 266–278.

Weiskittel, A.R., Maguire, D.A., Monserud, R.A. 2007*c*. Response of branch growth and mortality to silvicultural treatments in coastal Douglas-fir plantations: Implications for predicting tree growth. Forest Ecology and Management 251(3): 182-194.

Yun, Z., Chang, S., Lei, Z., Gabrielle, A., and Ashwin, B. 2008. Grid-enabled Sawing Optimization: from scanning images to cutting solution. Proceedings of the 15th ACM Mardi Gras Conference, Baton Rouge, LA. Pp. 1-8.

Tables:

Table 4.1 Definitions and units of variables used in modeling Douglas-fir branch angle and knot pith curvature.

Variable	Definition	Units
VBA	Branch angle from vertical	^{o}
CL	Crown length	m
HT	Total tree height	m
HCB	Height to the crown base	m
DBH	Diameter at breast height	cm
BR_{ht}	Branch height at insertion	m
HT_{rel}	Branch height at insertion relative to HT (1 at tree tip to 0 at tree base)	-
BD	Branch diameter at the point of insertion	mm
SI	Site index at a base of 50-years	m
DINC	Depth into crown	m
DINCR	Relative depth into crown (1 at HCB to 0 at HT)	-
H_{rib}	Increase in knot pith height from height where knot pith intersects tree bole pith	cm
rib	Radial distance from the tree bole pith	cm
rib_1	Radius inside bark of the tree at height of knot pith emergence from cambium	cm
rib_0	Radius inside bark of the tree at height of intersection of knot pith and tree bole pith	cm
h_1	Height of knot pith at emergence from the cambium	m
h_0	Height of knot pith at intersection of knot pith and tree bole pith	m

Table 4.2 Attributes of Douglas-fir plots and installations on which sample trees were measured for branch angle and diameter. Trees were sampled from 38 plots on 10 Stand Management Cooperative Type I installations and 16 plots on 6 Type II installations.

Attribute	Mean	Standard Deviation	Minimum	Maximum
Type I:				
Total basal area (m^2 ha^{-1})	10.4	7.6	0.8	26.1
Relative density (%)	18.8	12.8	2.1	45.1
Trees per hectare	703	447	188	2,085
Breast height age	9	3	3	14
Elevation (m)	368	224.5	167.6	822.9
Site index (m)	36.5	3.6	27.4	42.6
Type II:				
Total basal area (m^2 ha^{-1})	32.2	7.1	19.9	41.5
Relative density (%)	44.8	9.6	29.7	62.2
Trees per hectare	680	226	420	1,384
Breast height age	21	4	16	27
Elevation (m)	406.5	226.8	104.8	731.5
Site index (m)	36.5	3.3	32	41.1

Table 4.3 Attributes of Douglas-fir trees measured for branch angle and diameter. Angles of origin were measured on 15,662 branches from 287 trees on 10 Stand Management Cooperative Type I installations and from 2,291 branches from 125 trees on 6 Type II installations.

Attribute	Mean	Standard Deviation	Minimum	Maximum
Type I:				
DBH (cm)	14.5	5	3.3	26.6
HT (m)	10	3.1	3.8	22.5
CL (m)	9	3	2.7	20.9
VBA (^{o})	67.9	12.7	0	160
BD (mm)	20.9	6.9	1	75
HT_{rel}	0.3	0.1	0	0.8
Type II:				
DBH (cm)	28.3	6.7	14.8	46.2
HT (cm)	22.1	4.7	14.3	34.6
CL (m)	19.4	5.1	11.3	32.9
VBA (^{o})	74.6	10.9	3	138
BD (mm)	22.9	6.7	5	64
HT_{rel}	0.2	0.09	0	0.5

Table 4.4 Parameter estimates and fit statistics for the models describing the vertical trend in branch angle (Equation [1] and Equation [2]). All p-values of estimated parameters were less than 0.001.

Parameter	Variable	Estimated value	Standard Error
Equation [1]			
ω_0	-	37	-
ω_{11}	*CR*	10.7130	1.5767
ω_{12}	-	35.1457	1.5161
β_{11}	*DINCR*	-1.1599	0.0719
β_{12}	*CL*	-0.0623	0.0057
β_{13}	*DBH/HT*	0.3026	0.0363
		RMSE: 11.43	R^2: 17.6%
Equation [2]			
ω_0	-	37	-
ω_{21}	*CR*	8.3492	1.2202
ω_{22}	-	38.1013	1.0207
β_{21}	*DINCR*	-1.2481	0.0637
β_{22}	*CL*	-0.0265	0.0051
β_{23}	*DBH*	-0.0432	0.0039
β_{24}	*BD*	0.03755	0.0025
		RMSE: 11.16	R^2: 21.5%

Table 4.5 Mean fit and validation statistics for Equation [1] and Equation [2]. Validation data consisted of 3,281 branch angle measurements from 14 plots and 9 installations in the Roeh and Maguire (1997) dataset.

Equation	**Dataset**	**Mean *D***	**Mean *AD* (^{o})**	**Mean D^2**
Equation [1]	Modeling data	-0.03	8.59	130.61
	Validation data	-0.14	8.70	143.99
Equation [2]	Modeling data	-0.05	8.38	124.39
	Validation data	-0.32	8.23	130.58

Table 4.6 Parameter estimates for modeling height to crown base using Equation [3]. All p-values of estimated parameters were less than 0.001.

Parameter	Variable	Estimated value	Standard Error
α_0	-	2.5857	0.0138
α_1	*HT*	-0.0847	0.0002
α_2	*HT/DBH*	-1.7064	0.0085
α_3	*SI*	-0.0133	0.0003
		RMSE: 2.58	R^2: 92.9%

Table 4.7 Parameter estimates for Equation [4] and Equation [5] describing knot pith curvature in Douglas-fir trees. All p-values of estimated parameters were less than 0.001.

Parameter	Variable	Estimated value	Standard Error
Equation [4]			
γ_{10}	-	1.4817	0.0072
γ_{11}	*CL*	-0.0043	0.0001
γ_{12}	*DBH/HT*	-0.1187	0.0035
γ_{13}	-	0.1501	0.0008
γ_{14}	rib_0	-0.0052	0.0000
γ_{15}	h_0/HT	-0.0867	0.0009
		RMSE: 0.18	R^2: 99%
Equation [5]			
γ_{20}	-	1.4803	0.0072
γ_{21}	*CL*	-0.0043	0.0001
γ_{22}	*DBH/HT*	-0.1182	0.0034
γ_{23}	-	0.1506	0.0008
γ_{24}	rib_1	-0.0052	0.0000
γ_{25}	h_1/HT	-0.0869	0.0009
		RMSE: 0.18	R^2: 99%

Figure captions:

Figure 4.1. Longitudinal-radial section of a Douglas-fir stem exposing the bole and knot pith.

Figure 4.2. One segment of a tree with annual stem growth layers reconstructed using a *dib* taper model (Walters and Hann 1986) and a superimposed time-series of branch angles. Points identify the numerical solution for the intersection of (*dib/*2) and knot pith for each year. A photograph of a similarly sized tree section is provided for reference.

Figure 4.3. Residuals from Equation [1] for describing the trend in vertical branch angle plotted against predicted branch angle and relative depth into crown.

Figure 4.4. Observed branch angle (from vertical) over relative depth into crown by quantile of crown length (m) from the Roeh and Maguire (1997) dataset, with trend in branch angle for the median tree of each quantile predicted using Equation [1].

Figure 4.5. Vertical trend in branch angle predicted by Equation [1] and Equation [2] for three trees covering the size range of the Roeh and Maguire (1997) dataset.

Figure 4.6. Knot pith curvature predicted using Equation [5] for branches at several heights (h_1) on a large tree from the Roeh and Maguire (1997) dataset (*DBH* = 46, *HT* = 31, *CL* = 29). The left panel depicts knot curvature on a relative scale in the stem profile and the right pane depicts knot curvature on an absolute scale.

Figure 4.7. Knot geometry for a typical tree in the Roeh and Maguire (1997) dataset (*DBH* = 26, *HT* = 16, *CL* = 14), predicted using Equation [5], Equation [6] and a branch diameter model (Weiskittel et al. 2007*a*) at several heights along the stem (h_1): (A) 4 m, (B) 10 m, (C) 12 m and (D) 14 m.

Figure 4.1 Longitudinal-radial section of a Douglas-fir stem exposing the bole and knot pith

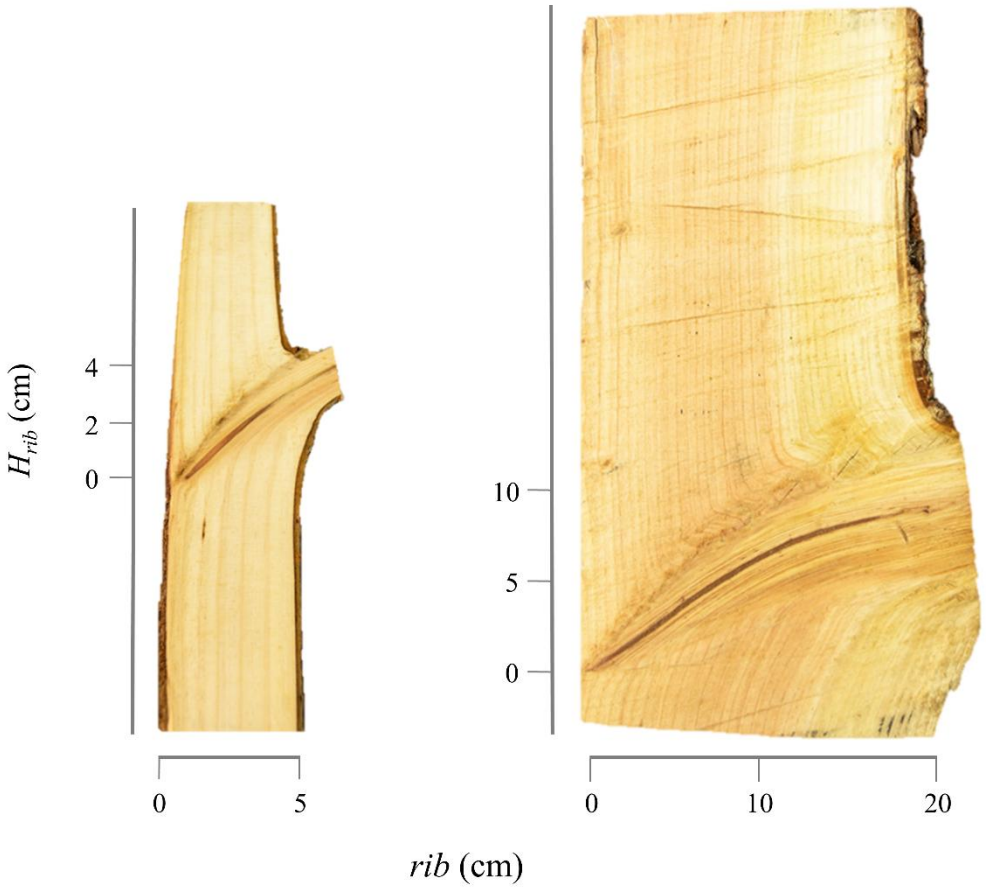

Figure 4.2 One segment of a tree with annual stem growth layers reconstructed using a dib taper model (Walters and Hann 1986) and a superimposed time-series of branch angles. Points identify the numerical solution for the intersection of (dib/2) and knot pith for each year. A photograph of a similarly sized tree section is provided for reference.

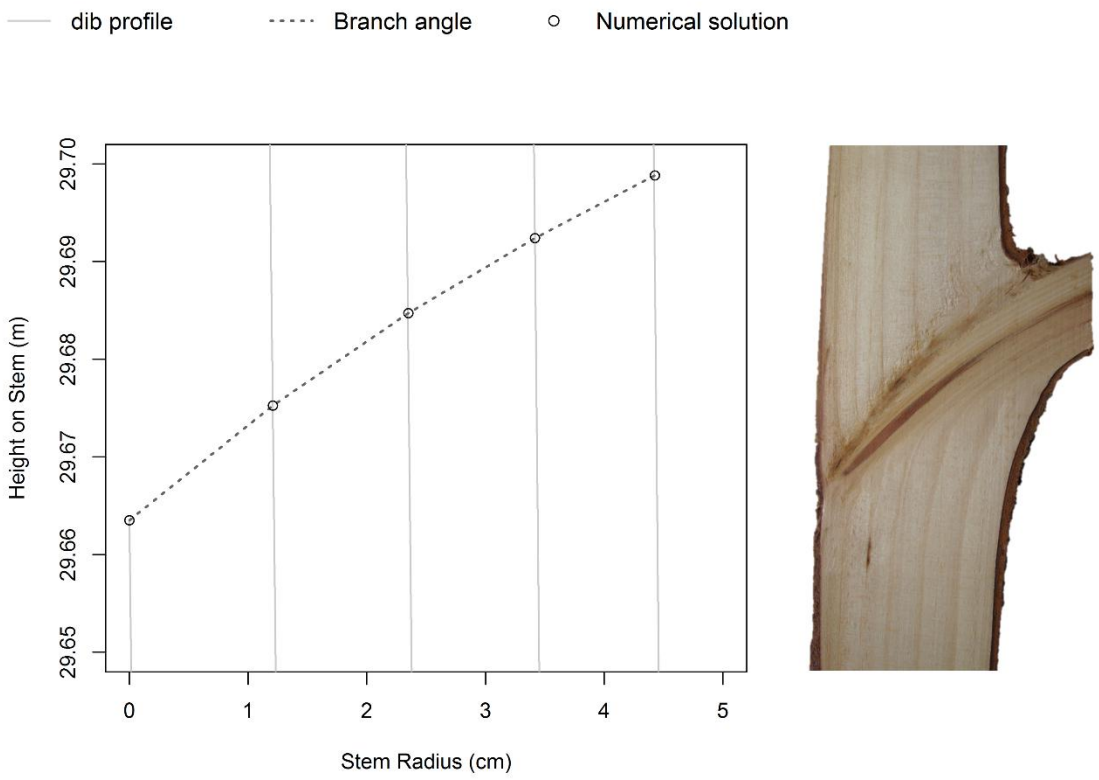

Figure 4.3 Residuals from Equation [1] for describing trend in vertical branch angle plotted against predicted branch angle and relative depth into crown.

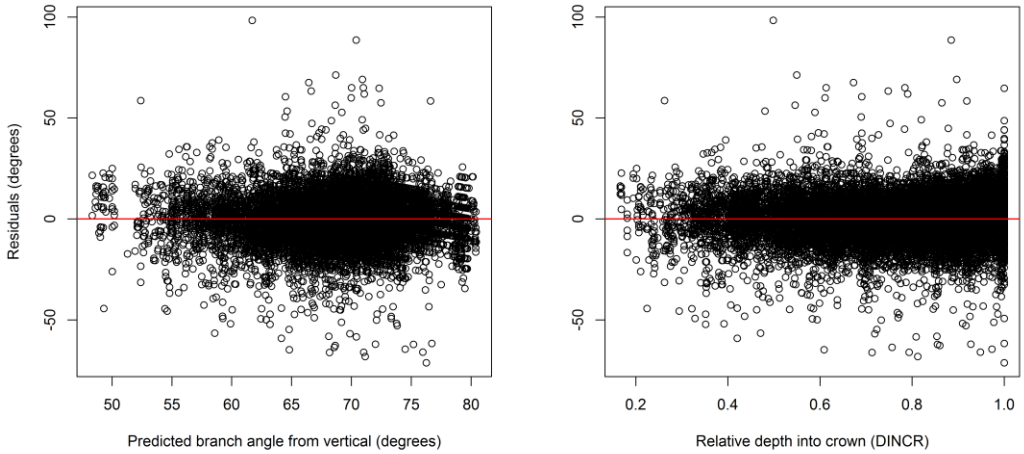

Figure 4.4 Observed branch angle (from vertical) over relative depth into crown by quantile of crown length (m) from the Roeh and Maguire (1997) dataset, with trend in branch angle for the median tree of each quantile predicted using Equation [1].

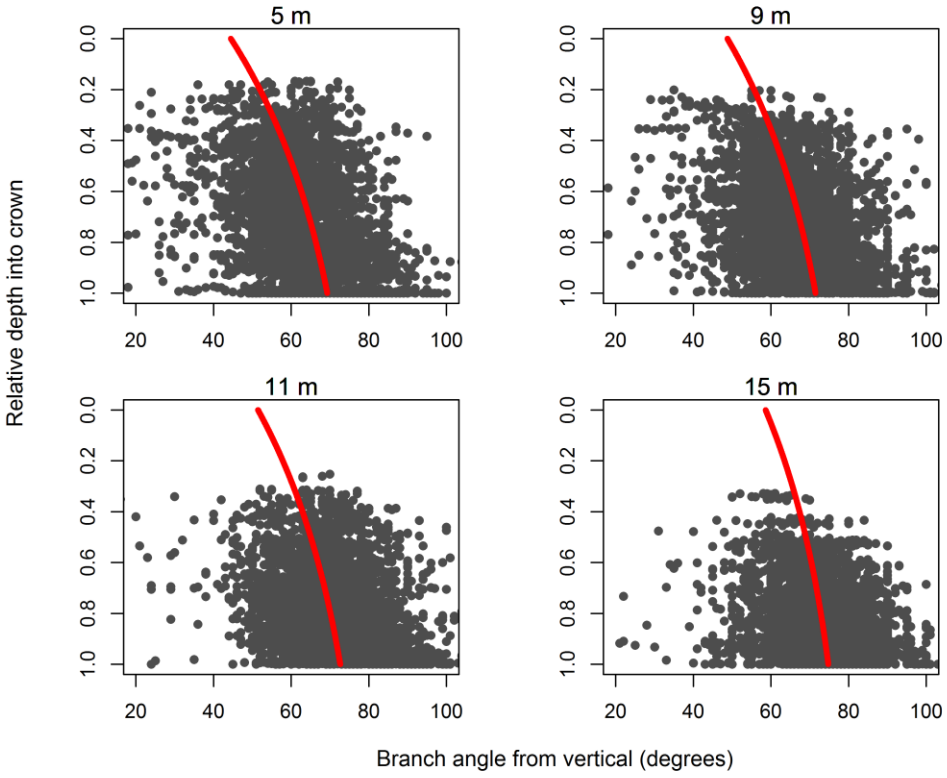

Figure 4.5 Vertical trend in branch angle predicted by Equation [1] and Equation [2] for three trees covering the size range of the Roeh and Maguire (1997) dataset.

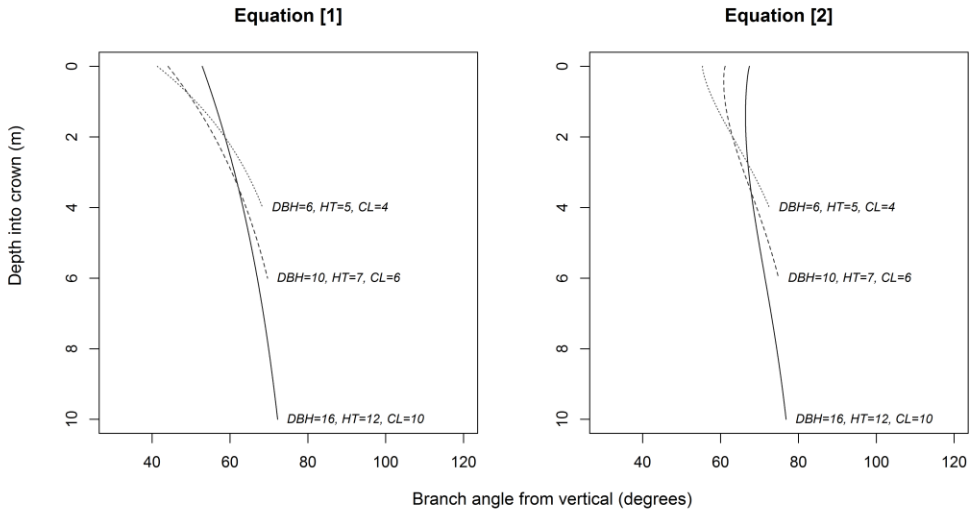

Figure 4.6 Knot pith curvature predicted using Equation [5] for branches at several heights (h1) on a large tree from the Roeh and Maguire (1997) dataset (DBH = 46, HT = 31, CL = 29). The left panel depicts knot curvature on a relative scale in the stem profile and the right pane depicts knot curvature on an absolute scale.

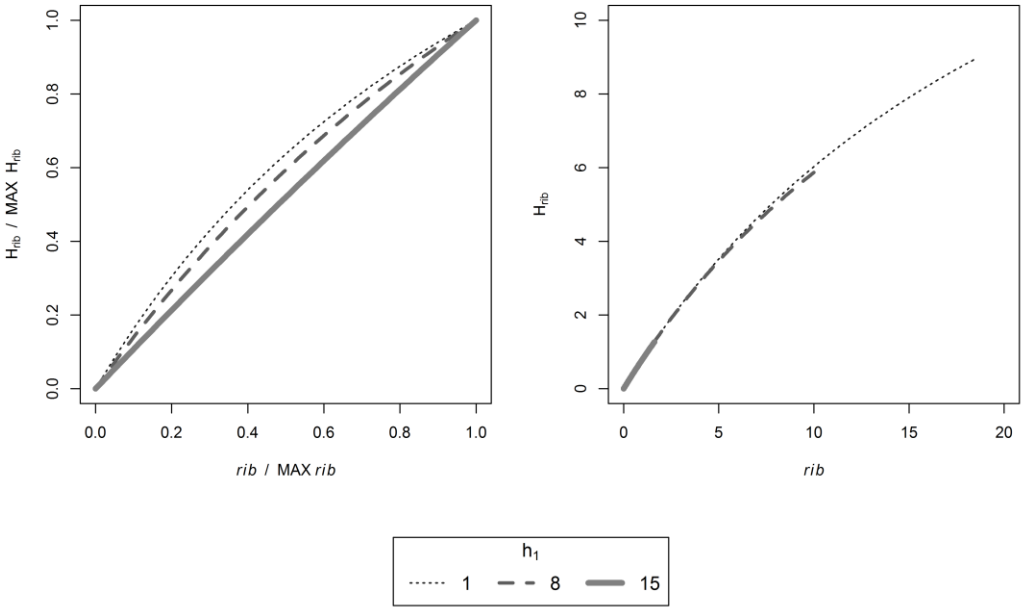

Figure 4.7 Knot geometry for a typical tree in the Roeh and Maguire (1997) dataset (DBH = 26, HT = 16, CL = 14), predicted using Equation [6], Equation [5] and a branch diameter model (Weiskittel et al. 2007a) at several heights along the stem (h1): (A) 4 m, (B) 10 m, (C) 12 m and (D) 14 m.

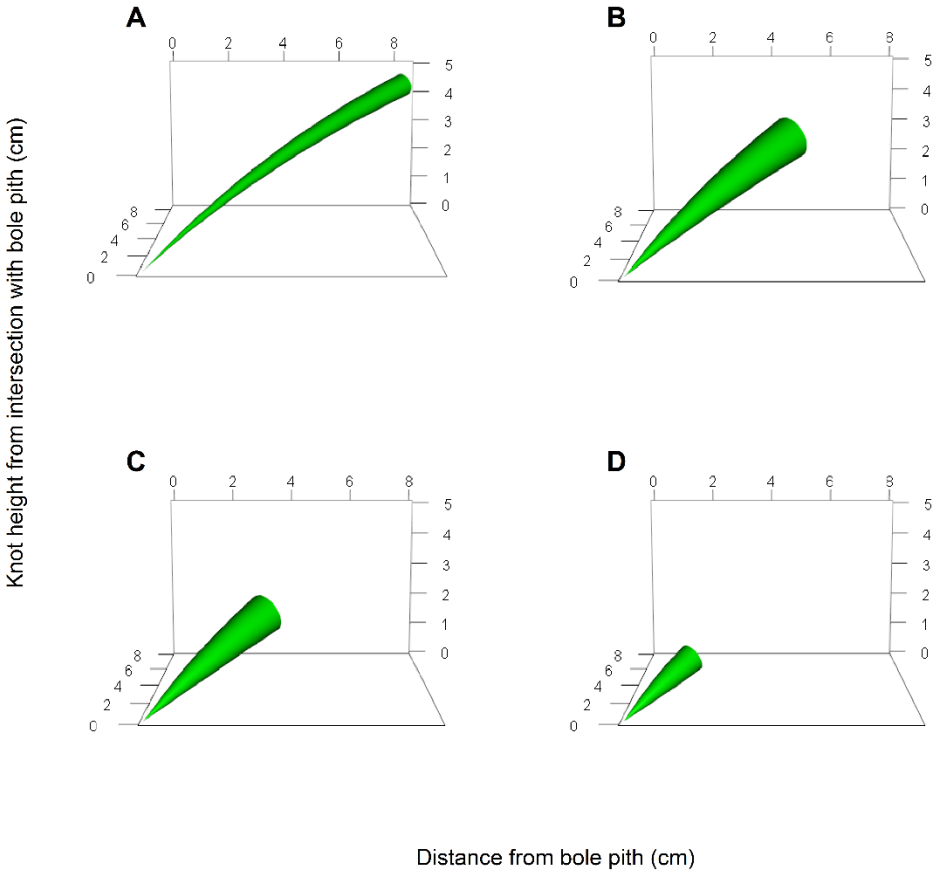

Chapter 5: Estimating the density of coast Douglas-fir (*Pseudotsuga menziesii*) wood samples at different moisture contents using medical X-ray computed tomography

Nathaniel OSBORNE

Olav HØIBØ

Douglas MAGUIRE

Derek GOURLEY

Manuscript in preparation for submittal to:

Computers and Electronics in Agriculture

Abstract

Wood density (ρ) is an important indicator of forest product performance and some aspects of tree ecophysiology. The value of ρ can be predicted within and along a tree stem using basic tree dimensions and information about environmental conditions where the tree is growing. Developing a comprehensive model for predicting ρ in coast Douglas-fir (*Pseudotsuga menziesii*) will require extensive analysis of wood samples across the United States Pacific Northwest. Medical X-ray computed tomography (CT) has been identified as a promising technology for rapidly estimating the density of Douglas-fir wood samples. The density of Douglas-fir wood can be predicted from and has a nearly perfect relationship to X-ray attenuation (R^2: 96%). The moisture content of wood samples has a linear effect on estimating sample density (0.0015 g/cc). Moisture content of a wood sample has a very minor (2.8 E^{-06} g/cc), but significant, interactive relation to X-ray attenuation. While the effect of moisture content explains only a small percentage of residual variance in predicting ρ, it is important to account for to avoid prediction biases. During any CT scan, X-ray scanner settings should be accounted for, as these settings can vary by manufacturer, model and machine. There is a small effect (0.00003 g/cc) of X-ray tube current (*mA*) on estimation of sample density. The filter used to interpolate CT scanning images does not have an observable effect on estimation of sample density (p = 0.084). While it is important to account for scanner settings (mA) and moisture content, more than one-third of the residual variance in predicting sample density can be explained by X-ray attenuation (*H*). Procedural results were identified, which could inform design of future experiments. The volume of wood samples can be estimated several ways, each with potential for systematic bias. Volume of samples at different moisture content can be estimated satisfactorily using volumetric displacement and caliper measurements. The absolute

mean deviance (*AD*) of estimating sample volume from caliper measurement relative to volumetric displacement was 0.45 cc. Many wood samples can also be scanned simultaneously using a balsa wood cassette which expedites CT image analysis. Future research should continue to focus on developing robust automated image processing tools. Even without these tools, CT scanning can be deployed immediately to estimate Douglas-fir wood density at a resolution of 1 mm in support of developing comprehensive models for predicting wood density profiles of trees and logs.

Keywords: Specific gravity; Wood density profile; Wood density gradients.

1. Introduction

Wood density (ρ) in coast Douglas-fir (*Pseudotsuga menziesii*) results from a complex of interacting ecophysiological processes that influence rate of meristematic cell division and the growth in cell diameter, cell length and cell wall thickness (Larson 1969). Wood density integrates the effect of these attributes on important wood properties that in turn affect the performance of most wood products. In the wood of Douglas-fir, ρ largely depends on the dimensions of longitudinal tracheids, which are long, skinny, tubular cells with pinched ends arranged parallel to the stem, branch or root axis (Cahill and Briggs 1992). During the growing season the longitudinal tracheids change in dimension. Earlywood is formed at the onset of growth, and is characterized by relatively short longitudinal tracheid cells with large lumens and thin cell walls. Earlywood transitions to latewood during the latter part of the growing season, apparently driven by one or more environmental factors that also synchronize with the end of terminal growth (Larson 1969). For example, Rapeepan et al. (2010) found latewood production

was correlated with to the onset of soil moisture deficit. The timing of the transition to latewood is probably an adaptation to water and other environmental stresses, so this trait would be expected to exhibit some level of genetic heritability (Rozenberg et al. 2001). Latewood is characterized by relatively long, thick walled longitudinal tracheids with decreased cell diameter and lumen size. Within an annual growth ring, ρ is less in the earlywood than latewood. Formation of longitudinal tracheids also varies spatiotemporally along the longitudinal and radial direction within the tree bole. As the longitudinal distance from the tree tip increases, the transition from earlywood to latewood becomes more abrupt (Emmingham 1977).

The radial profile of ρ at breast height (1.3 m) for managed Douglas-fir trees in the Pacific Northwest United States can be predicted from tree measurements and growing conditions (Filipescu et al. 2014; Rapeepan et al. 2010). Future goals in modeling ρ for managed Douglas-fir trees are to predict spatial variation within the tree bole in the longitudinal and radial directions, to represent response of ρ to thinning and fertilization treatment, and to account for geographic trends and environmental influences on average tree ρ (Osborne et al. 2015). Meeting these goals will require identification and deployment of a mix of technologies to estimate density of wood samples. X-ray densitometry has supported the development of current models for predicting density in Douglas-fir. This high resolution scanning technique (25μ) will continue to support modeling of within or between ring variations in wood density, especially in relation to annual trends of climate. There are many other approaches which could be deployed to estimate the density of Douglas-fir wood, however, each with costs and benefits (Wei et al. 2010). Several authors have demonstrated that medical X-ray computed tomography (CT) can

be used to rapidly estimate the density of unprepared wood samples, when a 1 mm scanning resolution is acceptable (Freyburger et al. 2009; Steffenrem et al. 2014).

Some questions need to be resolved before deploying medical CT scanning to estimate density of Douglas-fir wood samples. The objective of this study was to provide an equation for estimating Douglas-fir wood density (g/cc) as a function of X-ray attenuation (*H*). Within the framework of this equation, the effect of moisture content (percentage), and CT scanner settings were evaluated. Practical methods for scanning unprepared Douglas-fir wood cores and blocks were also explored.

2. Methods and Materials

Developing an equation to estimate Douglas-fir ρ from X-ray attenuation required four analytical steps: (1) collecting wood core and cube samples covering the range of wood density in planted Douglas-fir trees; (2) conditioning samples to three nominal moisture contents; (3) scanning those samples using a combination of CT scanner settings at each nominal moisture content; (4) processing CT scanning imagery into longitudinal data, and using these data for regression.

2.2 *Collecting wood core and block samples*

Thirty 1.27-cm diameter wood cores were drawn from a 30-year old coastal Douglas-fir spacing trial established by the Stand Management Cooperative near Corvallis, Oregon (914 – Lewisburg Saddle; Maguire et al. 1991). These thirty samples were equally drawn from three spacing blocks which were planted at 485 trees ha^{-1}, 190 trees ha^{-1} and 40 trees ha^{-1}. Samples were drawn across a wide range in initial spacing to represent a potentially large range in wood

density, owing to differences in timing of crown closure, degree of stem differentiation, and onset of suppression mortality (Figure 5.1). Within each experimental plot, trees were selected evenly across the diameter distribution, so that all tree social classes within each spacing were represented. For each sample tree, an increment borer was used to extract a single core from breast height (1.37 m) at a random azimuth around the tree bole.

Eighty Douglas-fir wood blocks of approximately the same dimension (2.5 cm x 2.5 cm x 2.5 cm) were also cut from sawn lumber to extend the range of wood density that was scanned for analysis (Figure 5.1). The sawn lumber included several Douglas-fir studs purchased at a local hardware store and planks from a used wood pile. The wood blocks were purposefully selected to represent the widest possible range in Douglas-fir wood density, as implied by the earlywood and latewood cross-sectional areas. Between the 30 wood cores and 80 wood cubes, the average sample ρ values ranged from 0.40 to 0.84 g/cc.

2.3 *Laboratory methods*

Each of the wood cores and cubes were scanned used a TOSHIBA Aquillion medical CT scanner, located at the Oregon State University, College of Veterinary Medicine. Scans were made at one level of X-ray voltage (120 *kVp*), three nominal levels of sample moisture content, and three levels of X-ray tube current (*mA*), and imagery from scanning was processed using two interpolation filters (Table 5.1). For each scanning session, wood samples were oriented to move through the scanner in a radial direction, with the sample cross-section facing up. Wood cores were scanned in a balsa wood cassette, constructed using a method described by Steffenrem et al.

(2014), and wood cubes were oriented in a matrix on a glass plate on the scanner bed (Figure 5.2).

The 0-percent moisture content was achieved by drying samples in an air-circulated oven set to 103^{o} for 24-hours. To maintain a 0-percent moisture content during transportation to the CT scanner, samples were transferred directly from the oven into a glass desiccator lined with silica cobbles. The time between unloading samples from the desiccator and completing the CT scans was around ten minutes. After completing the first scanning session, wood samples were conditioned to a nominal moisture content of 10-percent. The 10-percent moisture content was reached by allowing samples to reach equilibrium in a climate chamber maintained at 65-percent relative humidity and a 20^{o} temperature. To maintain the 10-percent moisture condition, samples were placed in the glass desiccator without silica cobbles for transport from the climate chamber to the CT scanning room. After scanning samples at a 10-percent nominal moisture content, they were allowed to reach an approximate moisture content of 25-percent. To achieve a nominal 25-percent moisture content, wood samples were placed in the glass desiccator with a lining of water about 2 cm deep. The interior of the desiccator was then allowed to maintain a relative humidity of 95-percent and temperature of 20^{o} over four weeks. Significant efforts were made to minimize splashing of water on samples during transportation to the CT scanning room in the desiccator. As before, the time between unloading samples and completing the scans was about ten minutes.

After each scanning session was completed, each wood core and cube was measured for weight (g) and volume (cc). Sample volume was estimated using two approaches. The first approach

was to measure each sample along several dimensions using electronic calipers (VOL_c). Each wood cube was measured in the radial, longitudinal and tangential direction with calipers (nearest 0.1 mm) and volume was estimated assuming a cubic shape. Each wood core was measured for length using a ruler, and diameter at both ends with calipers (nearest 0.1 mm). Using these measurements, and assuming a cylindrical shape, sample volumes were computed. The second approach was to estimate volume through water displacement. Each sample was blotted with a small amount of water, dried with a cloth, submerged under water in a volumetric cylinder and weighed on a scale to estimate displaced volume (VOL_d). Weight (g) and displacement volume (cc) were used to calculate the average density for each sample.

CT images (DICOM) resulting from scanning were analyzed using the ImageJ software (Abràmoff et al. 2004). Each unique combination of experimental levels (Table 5.1) had a stack of flat and pixelated imagery files (Figure 5.2). These files were ordered like slices, starting at the sample top and ending at the sample base. The center slice was consistently used for image analysis (Figure 5.3). During image analysis, a uniformly sized square or rectangle was manually placed on the image of each wood core or cube, carefully arranged to avoid inclusion of airspace or fuzzy borders on a sample. Within the sampling area (square or rectangle) the minimum, maximum and average X-ray attenuation (H: Hounsfield unit) was measured. A database for modeling was constructed by joining estimates of sample density, scanner settings, nominal moisture content, actual sample moisture content, and X-ray attenuation values estimated from image analysis.

2.4 *Equation development regression analysis*

Deviance between sample volumes estimated using the caliper and displacement technique were compared. The purpose of making this assessment was to identify any possible systematic biases between methods, and to cross-validate each approach prior to equation development. The deviance statistics were calculated as follows:

D	=	deviation	=	VOL_c - VOL_d
AD	=	absolute deviation	=	|deviation|
DP	=	deviation percentage	=	$(D / VOL_c) \cdot 100$

A series of models, linear and non-linear, were fit using the functions *lm* and *nls* using the R statistical programming language (R Core Team 2015). A full linear model was specified to test for potential explanatory variables of ρ, interactions between variables, and the importance of each variable as the percentage of explained variance (R^2) following the methods of Grömping (2006):

[1] $\rho = \beta_{10} + \beta_{11}H + \beta_{12}mA + \beta_{13}MC + \beta_{14}Z_1 + \beta_{15}Z_2 + \beta_{16}(H \times MC) + \beta_{17}(H \times mA) + \varepsilon_1$

where ρ is the average wood density (g/cc) of a given sample based on weight and volume estimated through volumetric displacement, β_{10} - β_{17} are parameters to be estimated from the data, *H* is the average Hounsfield unit for a given sample, *mA* is the X-ray tube current, *MC* is the sample moisture content percentage measured for each sample (not the nominal condition), Z_1 is an indicator variable set equal to one if the sample was a wood core and zero otherwise, Z_2 is an indicator variable set equal to one if the lung filter was used and zero otherwise, and ε_1 was the error term with $\varepsilon_1 \sim N(0,\sigma_{\varepsilon 1}^2)$.

Equation [1] was reduced to a more parsimonious model on the basis of parameter significance and interpretation of trends in data. The reduced non-linear model (Equation [2]) tested for the possibility of non-linearity in the moisture content term:

[2] $\rho = \beta_{20} + \beta_{21}H + \beta_{22}mA + \beta_{23}MC^{\beta_{24}} + \beta_{25}(H \times MC) + \varepsilon_2$

where β_{20} - β_{25} are parameters to be estimated from the data, ε_2 was the error term with ε_2 ~N(0,$\sigma_{\varepsilon 2}^2$) and all other terms are defined above.

Equation [2] was reduced to the final linear model for predicting Douglas-fir wood density:

[3] $\rho = \beta_{30} + \beta_{31}H + \beta_{32}mA + \beta_{33}MC + \beta_{34}(H \times MC) + \varepsilon_3$

where $\beta_{30} - \beta_{34}$ are parameters to be estimated from the data, ε_3 was the error term with ε_3 ~N(0,$\sigma_{\varepsilon 3}^2$) and all other terms are defined above.

3. Results

On average there was less than 0.5 cc absolute deviance or -2.6-percent deviance (*DP*) between volumes estimated using calipers and volume estimated from water displacement (Table 5.2). Caliper measurements always estimated less volume than volume estimated using water displacement. Deviance between the two methods of volume estimation was least when the samples were conditioned to zero-percent nominal moisture content. Over half of the total explained variance (R^2) in Equation [1] was attributed to the average X-ray attenuation (*H*) of a

sample. Other significant parameters (p-value < 0.05) explaining variation in sample density were the X-ray tube current, sample moisture content, and the interaction between the X-ray attenuation and sample moisture content. Sample type (cube or core: Z_1) was indicated as significant in Equation [1]. Significance in Z_1 is likely not of practical significance, but instead related to differences in sampling error for average density using either the volumetric displacement or caliper method, as can be observed in the *DP* values of Table 5.2. Equation [1] was reduced to Equation [2] and a test was performed to check for non-linearity in the moisture content term using a floating exponent (β_{24}). There was no evidence of non-linearity in the moisture content term (p-value: 0.466), so Equation [2] was further simplified to a final equation which was a linear function. Equation [3] was well behaved and explained 96.6% percent of the original variation in sample density (Table 5.4). The final equation explained sample density as a function of the average X-ray attenuation, X-ray tube current, actual moisture content and interaction between X-ray attenuation and sample moisture content. Most of the explained variance in Equation [3] is attributable to attenuation (74%) and moisture content (12%) (Figure 5.5). While the X-ray tube current is significant in explaining sample density, this term only accounts for 0.04% of the original variation in ρ, with a minor effect on estimation (Figure 5.6).

4. Discussion

Systematic biases are possible using both the water displacement and caliper measurement approach to volume estimation. When the water displacement method is used, the rate of swelling, air bubbles and other sources of error can produce systematic biases, especially for dry samples (Mantanis et al. 1994). Biases are also possible using the caliper approach to volume estimation. The angle at which calipers are placed on a sample, the force exerted on the caliper

by the experimenter and shape of the sample all affect volume estimation. While both methods have shortcomings and biases, cross-validation provides evidence in support of using sample densities calculated using VOL_d for developing Equation [3]. X-ray tube current was found to have a weak but significant effect of *mA* on density estimation (Table 5.4). This finding corroborates those of Freyburger et al. (2009) who also observed a weak effect of *mA* on estimating sample density. As X-ray tube current increases, the predicted density increases at a rate of 0.00003 g/cc. The modification of attenuation behavior is explained by the interaction of X-ray current (*mA*) and X-ray voltage (*kVp*) and resulting modification of X-ray wavelength (λ) (Flower 2012). To minimize the chance of biases, due to CT scanner settings, it is suggested that experimenters account for the minor effect of X-ray tube current. Moisture content was a significant effect in Equation [3]. As moisture content increases, sample density also increases with an interaction with X-ray attenuation. These findings corroborate those of Hoag (1988), who also found a minor but significant interaction between moisture content of wood and X-ray attenuation. In Equation [3] the actual sample moisture content percentage was used, instead of the nominal moisture content percentage. Using the actual moisture content instead of the nominal moisture content only increased the R^2 value by 0.03% and did not change parameter estimates, at least to the level of precision reported (Table 5.4). If only the nominal moisture content percent is known, this value can be substituted for the actual moisture content value used in Equation [3]. Filter choice in processing the CT scanning images was not found to be significant in predicting sample density. While filters make CT imagery appear different in most image viewing software, this is not because of major differences in pixel values, but rather display thresholds listed in header files due to filter choice. Filter choice could be more important when analyzing the profile of density along a sample. Smoothing of pixel values

between CT scanner slices might slightly alter location of important boundaries, like the delineation between earlywood and latewood.

To minimize the chance of systematic biases in processing CT imagery, automated image analysis software should be used (Steffenrem et al. 2014; Rousseln et al. 2014). Use of this type of software requires that CT imagery be consistently treated or delineated from scan-to-scan. Any change in image coordinates, or position of the samples in the imagery can limit the use of automated image analysis software. This type of software is also insensitive to anomalies in the wood samples. For example, one wood core drawn for this analysis had a staple imbedded, which was only revealed by looking carefully through the stacks of CT imagery (Figure 5.2).

5. Conclusions

Results from this study confirm strong evidence supporting the efficacy of medical X-ray computed tomography for estimating Douglas-fir wood density. This technology has seen minimal applications to biometrics of managed Douglas-fir in the Pacific Northwestern United States. Medical computed tomography, along with high resolution X-ray densitometry, will likely be necessary for developing a comprehensive model of wood density for coast Douglas-fir in the US Pacific Northwest. Researchers should now identify the optimal way to sample trees and utilize both scanning technologies from a statistical and practical perspective.

Acknowledgements

Thanks are extended to Doug Mainwaring (Oregon State University, College of Forestry) and Jason Wiest (Oregon State University, College of Veterinary Medicine). Doug prepared and

supplied many of the wood cubes and aided in their measurement. Jason scanned all of the wood cubes and wood cores using medical computed tomography. This research was made possible by the Veterinary Medicine College at Oregon State University, which allowed use of their diagnostic imagery facility. Funding for this study came from an endowment for a chaired faculty position, the N.B. (Nat) and Jacqueline Giustina Professor of Forest Management.

References

Abràmoff, M. D., Magalhães, P. J., Ram, S. J. 2004. Image processing with ImageJ. Biophotonics International, 11(7): 36-42.

Cahill, B., Briggs, D. 1992. Effects of Fertilization on Wood Quality and Tree Value Proc. Forest Fertilization Pp. 145-161 in H.N. Chappell, G.F. Weetman, and R.E. Miller (eds). Forest Fertilization: Sustaining and improving nutrition and growth of western forests. Institute of Forest Resources, University of Washington, Seattle, WA, USA. Contribution Number 73.

Emmingham, W. 1977. Comparison of selected Douglas-fir seed sources for cambial and leader growth patterns in four western Oregon environments. Canadian Journal of Forest Research. 7(1): 154-164.

Filipescu, C., Lowell, E., Koppenaal, R., Mitchell, A. 2013. Modeling regional and climatic variation of wood density and ring width in intensively managed Douglas-fir. Canadian Journal of Forest Research, 44(3): 220-229.

Flower, M. A. (Ed.). 2012. Webb's physics of medical imaging. CRC Press.

Freyburger, C., Longuetaud, F., Mothe, F., Constant, T., Leban, J. 2009. Measuring wood density by means of X-ray computer tomography. Annals of Forest Science. 66(8): 804.

Grömping, U. 2006. Relative importance for linear regression in R: the package relaimpo. Journal of statistical software, 17(1): 1-27.

Hoag, M. L. 1988. Measurement of within tree density variations in Douglas-fir (Pseudotsuga menziesii (Mirb.) Franco) using direct scanning x-ray techniques.

Larson, P. 1969. Wood formation and the concept of wood quality. Yale Univ. School Forestry, Bull. 74: 9-12.

Maguire, D. A., Bennett, W. S., Kershaw, J. A., Gonyea, R., Chappell, H. N. 1991. Establishment report: Stand Management Cooperative silviculture project field installations. College of Forestry, University of Washington, Seattle, WA, 42.

Mantanis, G. I., Young, R. A., & Rowell, R. M. 1994. Swelling of wood. Wood Science and Technology, 28(2): 119-134.

Osborne, N., Maguire, D., Weiskittel, A. 2015. Simulating forest growth, yield and wood properties of planted Pseudotsuga menziesii in the Pacific Northwest United States: A synthesis. *in preparation*.

Pieper, S., Halle, M., & Kikinis, R. 2004. 3D Slicer. In Biomedical Imaging: Nano to Macro, 2004. IEEE International Symposium Pp. 632-635.
R Development Core Team. 2015. R: A language and environment for statistical computing. R Foundation for Statistical Computing, Vienna, Austria.

Rapeepan, K., Briggs, D. and Turnblom, E. 2010. Modeling effects of soil, climate, and silviculture on growth ring specific gravity of Douglas-fir on a drought-prone site in Western Washington. Forest Ecology and Management. 259(6): 1085-1092.

Roussel, J. R., Mothe, F., Krähenbühl, A., Kerautret, B., Debled-Rennesson, I., Longuetaud, F. 2014. Automatic knot segmentation in CT images of wet softwood logs using a tangential approach. Computers and Electronics in Agriculture, 104:46-56.

Rozenberg, P., Franc, A., Bastien, C., & Cahalan, C. 2001. Improving models of wood density by including genetic effects: a case study in Douglas-fir. Annals of forest science, 58(4): 385-394.

Steffenrem, A., Kvaalen, H., Dalen, K., Høibø, O. 2014. A high-throughput X-ray-based method for measurements of relative wood density from unprepared increment cores from *Picea abies*. Scandinavian Journal of Forest Research. 29(5):506-514.

Wei, Q., Leblon, B., La Rocque, A. 2011. On the use of X-ray computed tomography for determining wood properties: a review. Canadian Journal of Forest Research. 41(11): 2120-2140.

Tables:

Table 5.1 All combinations (n=18) of nominal moisture content, X-ray tube current and image filter used for scanning Douglas-fir wood samples with medical X-ray computed tomography.

X-ray Tube Current

Lung Filter

Nominal Moisture Content	50 mA	80 mA	200 mA
0%	n_1	n_2	n_3
10%	n_4	n_5	n_6
25%	n_7	n_8	n_9

Bone Filter

Nominal Moisture Content	50 mA	80 mA	200 mA
0%	n_{10}	n_{11}	n_{12}
10%	n_{13}	n_{14}	n_{15}
25%	n_{16}	n_{17}	n_{18}

Table 5.2 Deviance between volume (cc) estimated using measurements with calipers (V_c) and volume estimated using water volume displacement (V_d) at three nominal levels of moisture conditioning and averaged over all three levels of moisture conditioning.

Nominal Moisture Content	*D* (cc)		*AD* (cc)		*DP* (%)	
	Cube	*Core*	*Cube*	*Core*	*Cube*	*Core*
0%	-0.28	-026	0.38	0.45	-0.81	-2.44
10%	-0.51	-0.37	0.51	0.40	-3.11	-2.59
25%	-0.45	-0.58	0.45	0.58	-2.61	-4.38
Overall	-0.41		0.45		-2.64	

Table 5.3 Parameter estimates for Equation [1] including parameter estimated p-values, standard errors (SE), and relative importance of parameters (LMG) expressed as a percentage of explained variation in ρ (Grömping 2006).

Parameter	**Term**	**Estimate**	**SE**	**p-value**	**LMG**
β_{10}	-	0.9423378	0.0044181	<0.001	-
β_{11}	H	0.000806	0.0000091	<0.001	55.45
β_{12}	mA	0.0000846	0.000028	0.0025	6.91
β_{13}	MC	0.0016989	0.0002238	<0.001	8.72
β_{14}	Z_1	-0.007343	0.0009575	<0.001	9.79
β_{15}	Z_2	0.0012805	0.0007413	0.0842	0.02
β_{16}	($H \times MC$)	0.0000031	0.0000005	<0.001	5.58
β_{17}	($H \times mA$)	0.0000001	0.0000001	0.0623	10.26

Table 5.4 Model form, parameter estimates, R^2 and root mean square error (RMSE) for equations to estimate basic wood density (ρ) from X-ray attenuation (H).

Equation	Form	R^2	RMSE
[1]	$\hat{\rho} = 0.9423 + 0.0008(H) + 0.00008(mA) + 0.0016(MC) \pm 0.0073(Z_1) + 0.0012(Z_2) + 0.000003(H \times MC) + 0.0000001(H \times mA)$	0.9672	0.015
[2]	$\hat{\rho} = 0.9634 + 0.0008(H) + 0.00003(mA) + 2E^{-07}(MC)^{3.8498} + 1.7E^{-06}(H \times MC)$	0.9697	0.015
[3]	$\hat{\rho} = 0.9564 + 0.0008(H) + 0.00003(mA) + 0.0015(MC) + 2.8E^{-06}(H \times MC)$	0.9660	0.015

Figure Captions:

Figure 5.1 Douglas-fir wood cubes (A) and 1.27-cm diameter cores (B) representative of the range of densities sampled for the modeling dataset.

Figure 5.2 Flat X-ray computed tomography images for (A) wood cores and (B) wood cubes conditioned to a nominal 10% moisture content, using a standard bone filter, with X-ray scanning settings at 120 kVp (X-ray voltage) and 80 mA (X-ray tube current).

Figure 5.3 X-ray flat image drawn from the center of a set of wood cubes, which were reconstructed in three dimensions using the 3D Slicer software (Pieper et al. 2004).

Figure 5.4 Sample density (g/cc) observed and predicted (mA = 80, MC = 12%) using Equation [3] along a gradient of X-ray attenuation (H).

Figure 5.5 Response surface for Equation [3] between sample density (ρ), moisture content percentage (MC) and X-ray attenuation (H).

Figure 5.6 Response surface for Equation [3] between sample density (ρ), X-ray tube current (mA) and X-ray attenuation (H).

Figure 5.1 Douglas-fir wood cubes (A) and 1.27-cm diameter cores (B) representative of the range of densities sampled for the modeling dataset.

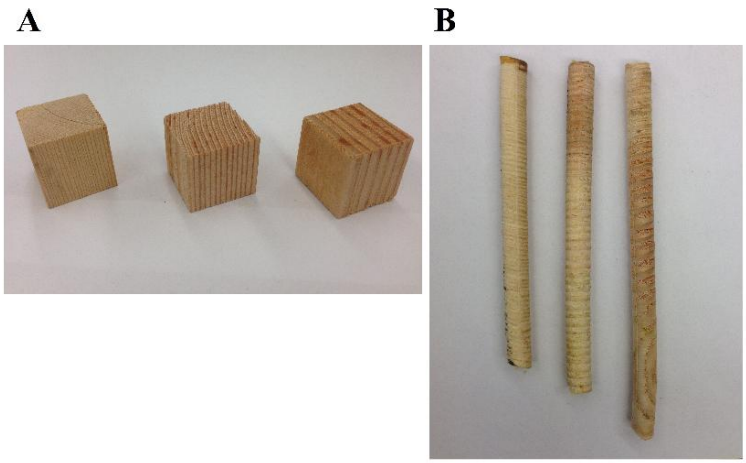

Figure 5.2 Flat X-ray computed tomography images for (A) wood cores and (B) wood cubes conditioned to a nominal 10% moisture content, using a standard bone filter, with X-ray scanning settings at 120 *kVp* (X-ray voltage) and 80 *mA* (X-ray tube current).

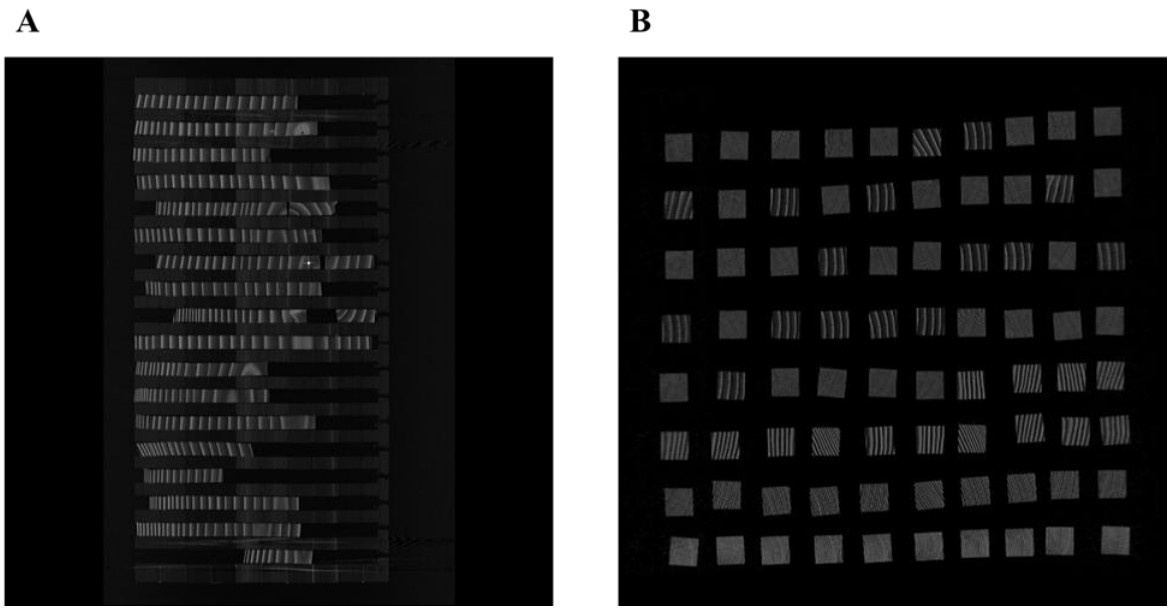

Figure 5.3 X-ray flat image drawn from the center of a set of wood cubes, which were reconstructed in three dimensions using the 3D Slicer software (Pieper et al. 2004).

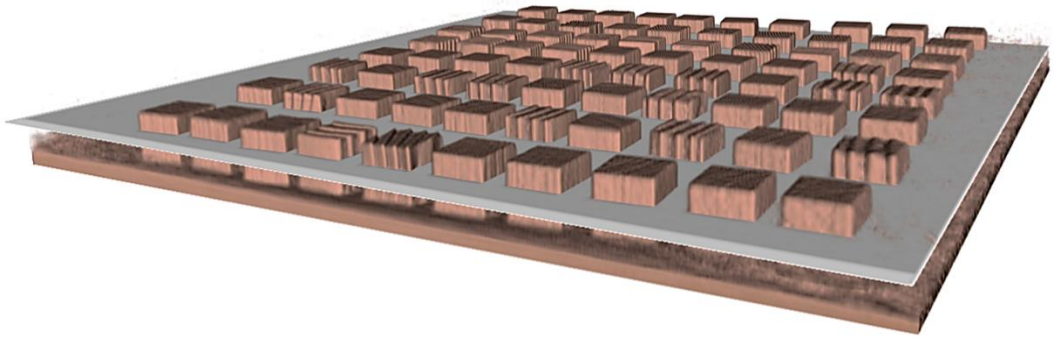

Figure 5.4 Sample density (g/cc) observed and predicted (mA = 80, MC = 12%) using Equation [3] along a gradient of X-ray attenuation (H).

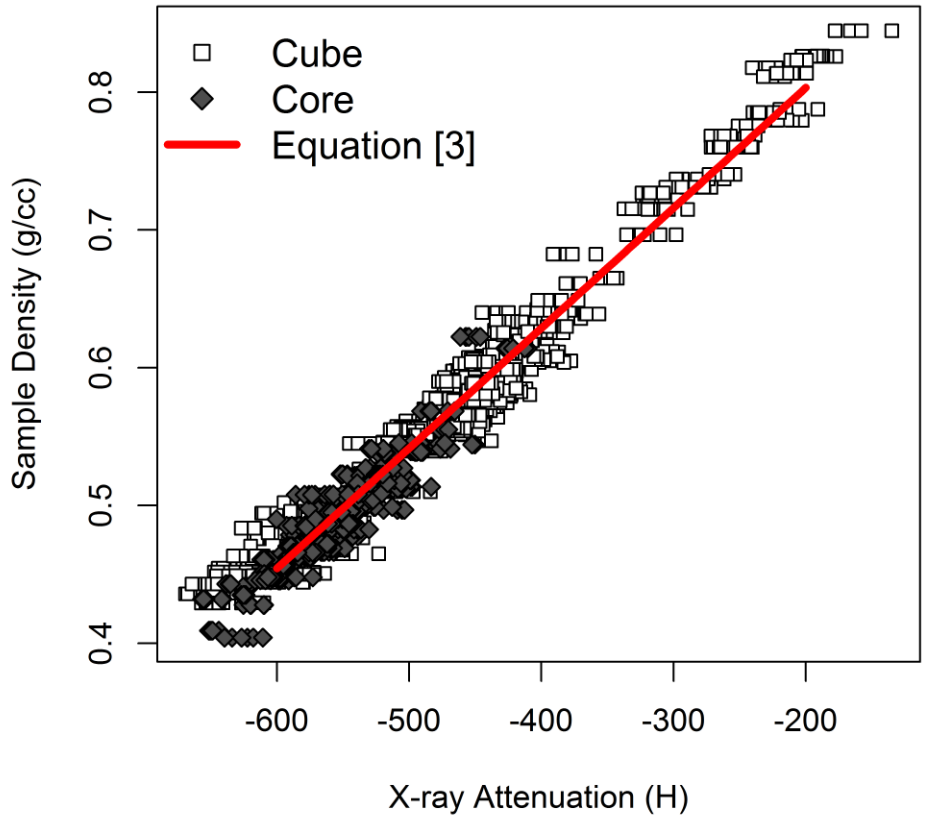

Figure 5.5 Response surface for Equation [3] between sample density (ρ), moisture content percentage (MC) and X-ray attenuation (H).

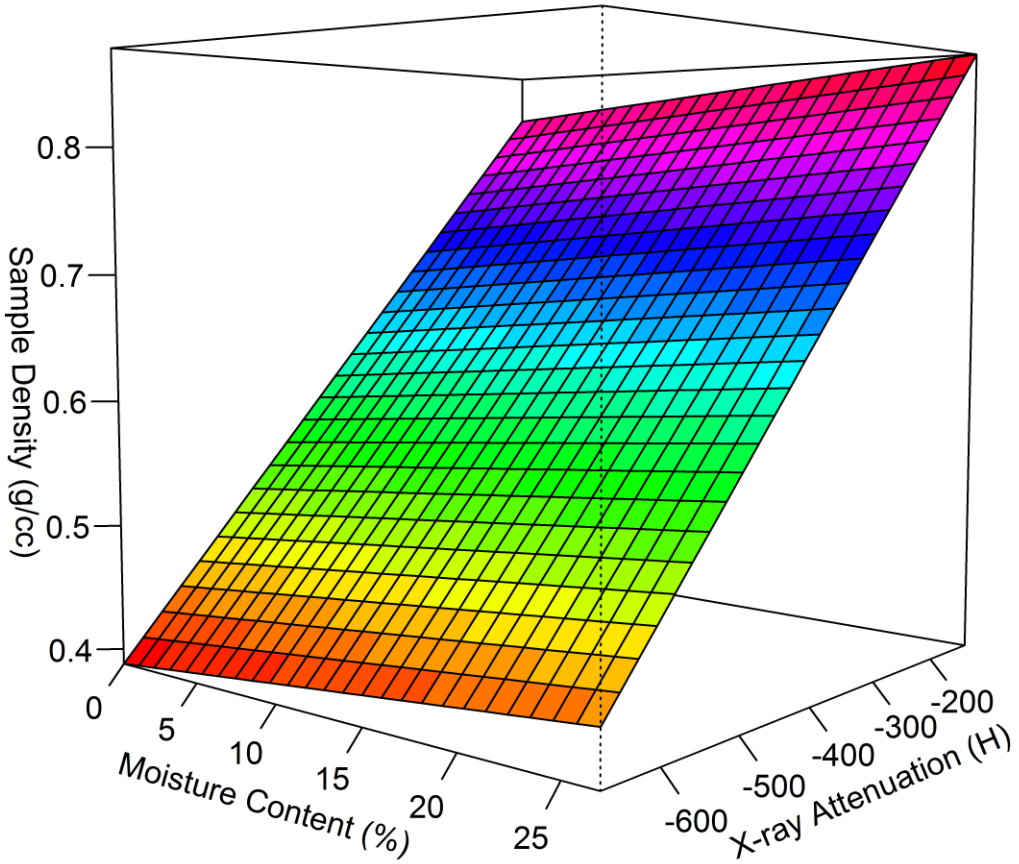

Figure 5.6 Response surface for Equation [3] between sample density (ρ), X-ray tube current (mA) and X-ray attenuation (H).

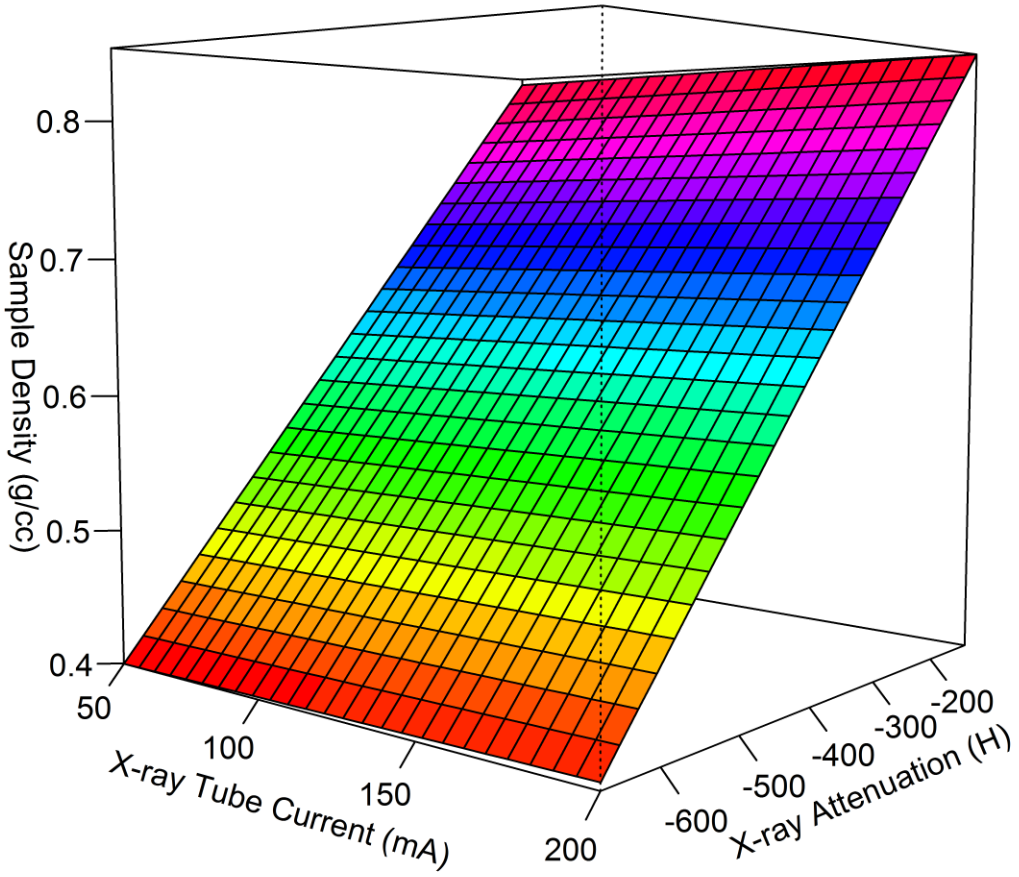

Chapter 6: Development of *cipsr*: a forest growth, yield and wood properties software in the R statistical programming environment.

Nathaniel OSBORNE

Doug MAGUIRE

David HANN

Excerpts from a software vignette:

Osborne, N., Maguire, D., Hann, D. 2015. cipsr: An R interface to the Organon and Cipsanon models. R package version 2.2.3.

Abstract

ORGANON is a forest growth and yield simulator for intensively managed Douglas-fir plantations first developed by Professor David Hann in the early 1980's. Historically, ORGANON has been accessed through a DOS based graphical user interface. *Cipsr* is a new software which has been developed to permit use of ORGANON in the R statistical programming language. In *cipsr* the FORTRAN source code of ORGANON has been compiled into direct link libraries, which are called to simulate the growth and yield of individual trees and forests. Four significant benefits have been achieved through the development of *cipsr*. In *cipsr* many stands can be simulated at once. In the DOS console of ORGANON, only one stand could be simulated at a time. The infrastructure of *cipsr* also promotes future development of ORGANON. The source package of *cipsr* contains the FORTRAN source code, as well as Make files, which compile the dynamic link libraries. This allows developers of *cipsr* to modify the source code, and quickly produce Windows binary files for the *cipsr* software. The third benefit offered by *cipsr* is an enhanced capacity to estimate wood properties for individual trees. Wood properties models have been included in *cipsr* functions which simulate the bucking of trees into lumber by grade, as utility poles and as chip logs. The final benefit is the inclusion of these growth and yield models in a statistical programming environment. Basing the models in R allows for rapid, open-source, software delivery, within a relatively stable programming language. More importantly, any forest simulation made in *cipsr* can be easily post-processed using a wide variety of free statistical and analytical tools provided within the R environment. The development of *cipsr* demonstrates a strong framework for building a forest growth, yield and wood properties simulator in statistical programming language.

Introduction

Forest growth and yield models, and the simulators that provide an interface to them, are critical to decision support in forestry. These models help identify optimal silvicultural regimes and predict the sustainability of landscape-scale forest management. ORGANON is a well-established forest growth and yield model for managed Douglas-fir in the Pacific Northwestern United States (Weiskittel et al. 2011). The following historical account of the development of ORGANON paraphrases and follows that of Hann (2011): ORGANON was first developed by Professor David Hann in the early 1980's as part of the Forestry Intensified Research (FIR) program at Oregon State University. The original intent was to develop ORGANON as a variant of the PROGNOSIS model. That intent was changed with the advent of the IBM PC. To maximize access to ORGANON, Professor Hann designed PC based software to run ORGANON, instead of running the model on a mainframe computer in the tradition of PROGNOSIS. Free from having to conform to the PROGNOSIS model structure, Professor Hann was able to develop ORGANON based upon the most appealing features of many models existing at the time: PROGNOSIS (Wykoff et al. 1982), CRYPTOS (Wensel et al. 1987), CACTOS (Wensel and Biging 1988), SPS (Arney 1988), and STEMS (USDA 1979).

The ORGANON model is a system of many static and dynamic equations that support the prediction of individual tree growth, yield and wood properties. There are three versions of ORGANON, each with their own set of equations. The first version was developed for southwestern Oregon (SWO). Professor Hann developed the southwestern Oregon version with Doug Maguire, John Scrivani, Dave Larsen, Martin Ritchie, Chao-Huan Wang, Abdel Azim Zumrawi, Dave Walters and Merlise Clyde. The work initially involved developing equations for

predicting: total stem volume; merchantable stem volume; tree bole taper; stump diameter; bark thickness; branch diameter up the stem; and height growth rate for six major conifer species in the region. In addition, equations for height to diameter ratio; maximum crown width; largest crown width; height to crown base; diameter growth rate; and mortality rate were developed for 18 tree species. A methods for estimating maximum size-density trajectories was also developed for stands in the region. The Northwest Oregon (NWO) version of ORGANON was developed with a similar set of equations around the same time, based on data from the Oregon State University College of Forestry properties. Professor Hann developed this version with Martin Ritchie, Chao-Huan Wang and Abdel Azim Zumrawi. The third version of ORGANON was developed for the Stand Management Cooperative (SMC) using a system of permanent research plots in southwestern British Columbia, western Washington and western Oregon. Access to these permanent plots allowed development of treatment response modifiers for thinning and fertilization. These were done in a manner that could then be applied to the SWO and NWO versions of ORGANON. Professor Hann completed the SMC version of ORGANON with David Marshall and Mark Hanus.

Each version of ORGANON has been continually refined over the past thirty years. The southwestern Oregon version was expanded substantially so it could be applied to older conifer and hardwood stands during the early 1990's. This work involved sampling mixed coniferous and hardwood stands with tree ages in excess of 350 years and stands that consisted almost exclusively of hardwood trees. Professor Hann completed this extensive sampling effort and model development with Mark Hanus. The SMC version continues to be enhanced by new data collected across SMC installations. Using data from progeny tests managed by the Northwest

Tree Improvement Cooperative, Peter Gould, David Marshall, Randy Johnson, and Greg Johnson developed genetic gain multipliers for height growth rate and diameter growth rate of Douglas-fir. Likewise, Connie Harrington and Peter Gould developed height to diameter ratio, height to crown base, diameter growth rate, and mortality equations for Oregon white oak from an independent dataset.

Finally, a version of ORGANON referred to as RAP was developed for red alder plantations by David Hann, Andrew Bluhm, David Hibbs, Aaron Weiskittel, and Tzeng-Yih Lam. The equations developed for red alder included top height, height to diameter ratio, maximum crown width, live crown width, crown profile, height to crown base, diameter increment, height increment, crown recession rate, mortality rate, size-density trajectory, and thinning multipliers.

The Center for Intensive Planted-forest Silviculture (CIPS) was established at Oregon State University in 2007, and has been directed by Professor Doug Maguire. As part of the CIPS mission, a number of ORGANON equations have been enhanced by David Hann, Doug Maguire, Junhui Zhao and Doug Mainwaring. CIPSANON is a model currently under development by the CIPS staff as a spin-off from ORGANON.

A forest growth, yield and wood properties simulator in R

The *cipsr* software is the latest contribution to the development of ORGANON (Osborne et al. 2015). This software provides an interface to the ORGANON and CIPSANON models in the R statistical programming environment (R Core Team 2015). CIPSANON is an experimental spin-off of the ORGANON model. The CIPSANON model includes unique features not found in

ORGANON: annualized predictions of forest growth and yield; and the ability to condition tree growth based upon soil water holding capacity percent (WHC) and precipitation over the growing season (PPTDD). The values for WHC and PPTDD can be supplied by the model user or estimated from a raster file (Figure 6.1). The raster file for WHC was created using the NRCS SSURGO database (Soil Survey Staff 2014). PPTDD is calculated as the inches of precipitation for days with average daily temperatures greater than or equal to 41^{o}. ClimateWNA was used to estimate the variables necessary to calculate PPTDD for Washington and Oregon (Wang et al. 2012). Both raster files for WHC and PPTDD were computed using the ArcGIS software (ESRI 2011). The raster files for WHC and PPTDD are loaded and called in R using the *raster* (Hijmans 2014), *rgdal* (Bivand et al. 2014) and *sp* (Pebesma and Bivand 2005) packages, which are *cipsr* dependencies.

Simulating individual tree growth and yield

ORGANON and CIPSANON are accessed using the *grow* function of *cipsr*, by calling sets of FORTRAN source code that were compiled as direct link libraries (DLL) (Figure 6.2). The first library called is an editing DLL, which prepares tree lists and stand data as input for simulation. The inputs to the editing DLL consist of three elements: usual forest inventory data (e.g. tree diameter, tree species etc.), instructions for the growth and yield simulator, and instructions for any silvicultural activities to be imposed. These three elements can imported to the R environment using an Excel template provided by the software or created in R directly. The forest inventory data are lists of tree attributes (Table 6.1). Instructions for the growth and yield simulation are included in the second element and are wide ranging (Table 6.2). Silvicultural activities like thinning and fertilization can be indicated in the third element (Table 6.3). The set

of three elements are usually loaded into the R environment using a *cipsr* function called *load.data*. Loading of data from Excel is made possible by Windows ODBC language, made simple by the *XLConnect* package (Mirai Solutions 2014) which is a dependency of *cipsr*.

After the inputs are prepared, they are passed to a growth DLL which is called repeatedly (i.e. all of this happens automatically in the *grow* function without user intervention). Any silvicultural treatments like thinning or fertilization imposed by the user are carried out during this growth process. Outputs from the growth DLL are formatted in the same manner as the inputs (e.g. tree height, diameter, expansion factor, etc.). Outputs from repeated calls to the growth DLL are passed to a yield DLL. Using the yield DLL, the cubic foot and Scribner volume for each tree is estimated, conditional on constraints imposed by the user. The last step in the *grow* function is to estimate select wood properties for each tree. These select wood properties are estimated using a procedure developed by Doug Maguire in the late 1990's. Wood properties estimated from the wood quality DLL include branch diameter (Maguire et al. 1999), juvenile wood core delineation (Maguire et al. 1991), and taper of the tree bole inside bark (Walters and Hann 1986). The estimated wood properties are given at the height of every fifth whorl in correspondence to the five-year growth prediction resolution.

Simulated bucking of virtual trees

Additional wood properties models have been incorporated into *cipsr* to predict the diameter of the heartwood core, width of the sapwood rind, and distribution and geometry of knots. A call to the *grow* function of *cipsr* produces a list which includes estimates of tree size over time. This tree list can be passed to the *process* function in *cipsr*. The *process* function simulates the

bucking of individual trees into lumber by grade (Fahey et al. 1991), into utility poles by class (Landgren et al. 1983), and into chips if not suitable for sawlogs or poles. This simulated bucking procedure relies on several wood properties models. The outputs from calls to the *process* function are easily passed to post-processing analysis, for example, identification of an economically optimal forest management regime or estimation of financial returns from silvicultural regimes. Several examples using the *process* function and the other functions mentioned above can be found in the *cipsr* user-manual (Osborne et al. 2015).

Recommendations for future development of the *cipsr* software

The *cipsr* software is a powerful analytical tool, ready for deployment to decision support in forest management and to silvicultural analysis in research. There are still critical gaps in *cipsr* and the underlying forest growth and wood properties models. Opportunities for continued software development also exist. Some of the most critical areas for software improvement are as follows: improve raster files for climate and soil variables used to condition forest growth and wood properties models; develop and incorporate models to predict Douglas-fir surface defects; identify an open-source sawing simulator which can be compiled and included in the *cipsr* software; aggregate existing wood properties models of *cipsr* into glass logs, which can be passed to the sawing simulator; develop regionally comprehensive models for wood density and microfibril angle and incorporate these models into glass logs, to predict strength features like modulus of elasticity (MOE) and modulus of rupture (MOR) (Lachenbruch et al. 2010); continue to modify and recompile FORTRAN source code included in *cipsr* to reflect ongoing research on tree genetic gain, and multipliers for thinning and fertilization. This dissertation provides a framework for modeling forest growth, yield and wood properties in the R statistical

programming environment. However, the full potential of this effort has not been realized and more research and attention is needed.

Literature Cited

Arney, J. D. 1988. SPS guide for the Stand Projection System (SPS), vers. 2.0. Applied Biometrics, Issaquah, WA.

Bivand, R., Keitt, T., Rowlingson, B. 2014. rgdal: Bindings for the Geospatial Data Abstraction Library. R package version 0.9-1.

ESRI. 2011. ArcGIS Desktop: Release 10. Redlands, CA: Environmental Systems Research Institute.

Pebesma, E.J., Bivand, R.S. 2005. Classes and methods for spatial data in R. R News 5:(2)

Roeh, R. L., and Maguire, D. A. 1997. Crown profile models based on branch attributes in coastal Douglas-fir. Forest Ecology and Management 96(1): 77–100.

Hann, D. 2011. "History of the Development of ORGANON", a short text from the ORGANON homepage: http://www.cof.orst.edu/cof/fr/research/organon. Accessed in September, 2015.

Hijmans, R.J. 2014. raster: raster: Geographic data analysis and modeling. R package version 2.3-12.

Lachenbruch, B., Johnson, G.R., Downes, G. M., Evans, R. 2010. Relationships of density, microfibril angle, and sound velocity with stiffness and strength in mature wood of Douglas-fir. Canadian journal of forest research, 40(1): 55-64.

Landgren, C. G., Bondi, M. C., & Emmingham, W. H. 1983. Growing and harvesting Douglas-fir poles. Corvallis, Oregon: Extension Service, Oregon State University.

Maguire, D. A., Kershaw, J. A., Hann, D. W. 1991. Predicting the effects of silvicultural regime on branch size and crown wood core in Douglas-fir. Forest Science, 37(5):1409-1428.

Mirai Solutions GmbH (2014). XLConnect: Excel Connector for R. R package version 0.2-9.

Osborne, N., Maguire, D., Hann, D. 2015. cipsr: An R interface to the ORGANON and CIPSANON models. R package version 2.2.2.

USDA, F.S., 1979. A generalized forest growth projection system applied to the Lake States region. General Technical Report NC-49. St. Paul, MN: U.S. Dept. of Agriculture, Forest Service, North Central Forest Experiment Station

R Development Core Team. 2015. R: A language and environment for statistical computing. R Foundation for Statistical Computing, Vienna, Austria. ISBN 3-900051-07-0.

Roeh, R. L., and Maguire, D. A. 1997. Crown profile models based on branch attributes in coastal Douglas-fir. Forest Ecology and Management 96(1): 77–100.

Soil Survey Staff. 2014. Soil Survey Geographic (SSURGO) Database. Natural Resources Conservation Service, United States Department of Agriculture

Wang, T., Hamann, A., Spittlehouse, D., Murdock, T. 2012. ClimateWNA - High-Resolution Spatial Climate Data for Western North America J. Appl. Meteor. Climatol., Vol. 51(1):16-29

Walters, D. K., Hann, D. W. 1986. Taper equations for six conifer species in southwest Oregon. Oregon State University, School of Forestry, Forest Research Laboratory.

Weiskittel, A.R., Hann, D.W., Kershaw, J.A., Vanclay, J.K. 2011. Forest Growth and Yield Modeling. John Wiley & Sons, Hoboken, NJ. 340p.

Wensel, L. C., Krumland, B. E., Meerschaert, W. J. 1987. Cryptos User's Guide: Cooperative Redwood Yield Project Timber Output Simulator. Division of Agriculture and Natural Resources. University of California.

Wensel, L. C., Biging, G. S. 1988. The cactos system individual-tree growth simulation in the mixed conifer forests of California. USDA Forest Service general technical report NC-North Central Forest Experiment Station (USA).

Wykoff, W. R., Crookston, N. L., Stage, A. R. 1982. User's guide to the stand prognosis model.

Tables:

Table 6.1 Variables in the sample list of a database used for forest growth and yield simulations in the grow function of the cipsr software.

Variable	Variable Description
unit	Identifier for a forest management unit
sample	Identifier for a sample of tree measurements within a given forest unit
tree	Identifier for a tree within a sample
expan	Tree expansion factor (trees/acre)
user	User code for thinning treatments
species	Tree species code
dbh	Diameter at breast height (in)
tht	Total tree height (ft)
cr	Crown length divided by tree height
radgro	Five year radial growth (in)

Table 6.2 Variables in the units list of a database used for forest growth and yield simulation in the grow function of the cipsr software

Variable	Variable Description
unit	Identifier for a forest management unit
latitude	Approximate latitude of the unit (decimal degrees)
longitude	Approximate longitude of the unit (decimal degrees)
pptdd	Average precipitation for degree ≥ 41 degrees (in)
whc	Average water holding capacity percent in the top 20-inches of soil
wantplot	Indicator to make descriptive growth and yield plots
wanttable	Indicator to print growth and yield output to a folder on the computer
woodqual	Indicator to call the ORGWQ.dll
model	Indicator for model to use for simulating forest growth
variant	Variant of the model to use for simulating forest growth
driver	Indicator to condition growth on climatic or soil variables
groyrs	Years to grow the unit
iseven	Indicator for if the stand is even-age
partcut	Indicator for if the stand has been partially cut
pastfert	Indicator for if the stand has been fertilized
stage	Age of the stand
bhage	Breast height age of the stand
dfsi	Douglas-fir site index (ft)
otsi	Other species site index (ft)
dhcal	Indicator to calibrate on diameter height ratio
ccal	Indicator to calibrate on crown ratio
dgrocal	Indicator to calibrate on diameter growth
triple	Indicator to use tripling
maxsdi	Indicator to enforce a maximum size density
dfsdi	Douglas-fir maximum size density
wgsdi	White or grand fir maximum size density
phsdi	Ponderosa and Western hemlock maximum size density
gdval	Genetic worth value for diameter growth
ghval	Genetic worth value for height growth
dfret	Douglas-fir needle retention
genes	Indicator to use genetic worth values
snc	Indicator if the stand has been infected with Swiss needle cast
core	Indicator to use a crown wood, or juvenile wood core definition
cftd	Top diameter used to estimate tree cubic foot volume (in)
cfsh	Stump height used to estimate tree cubic foot volume (ft)
logll	Maximum log length used to estimate tree Scribner volume (ft)
logml	Minimum log length used to estimate tree Scribner volume (ft)
logtd	Top diameter used to estimate tree Scribner volume (in)
logsh	Stump height used to estimate tree Scribner volume (ft)
logta	Trim allowance used to estimate tree Scribner volume (in)

Table 6.3 Variables in the activities list of a database used for forest growth and yield simulation in the grow function of the cipsr software

Variable	Variable Description
unit	Identifier for a forest management unit
trigger	Unit statistic used to trigger a silvicultural activity; e.x. year, basal area per acre (ft^2/acre), trees per acre, quadratic mean diameter (in)
when	Level of the specified trigger to reach before imposing a silvicultural treatment; e.x. 200 ft^2/acre of basal area, 55% relative density
what	Indicator to impose thinning or fertilization if triggered
how	How to apply the treatment; e.x. thinning from below or proportionally
metric	Metric used to define the desired residual unit condition after treatment; e.x. number of trees per acre or basal area per acre
target	The desired residual condition of the unit after treatment

Figure captions:

Figure 6.1. Raster files called in *cipsr* for water holding capacity percentage in the top 20-inches of soil and growing day precipitation for Oregon and Washington.

Figure 6.2. Simplified example of calling a set of ORGANON DLL's to simulate forest growth and yield in the R statistical programming environment.

Figure 6.1 Raster files called in cipsr for water holding capacity percentage in the top 20-inches of soil and growing day precipitation for Oregon and Washington.

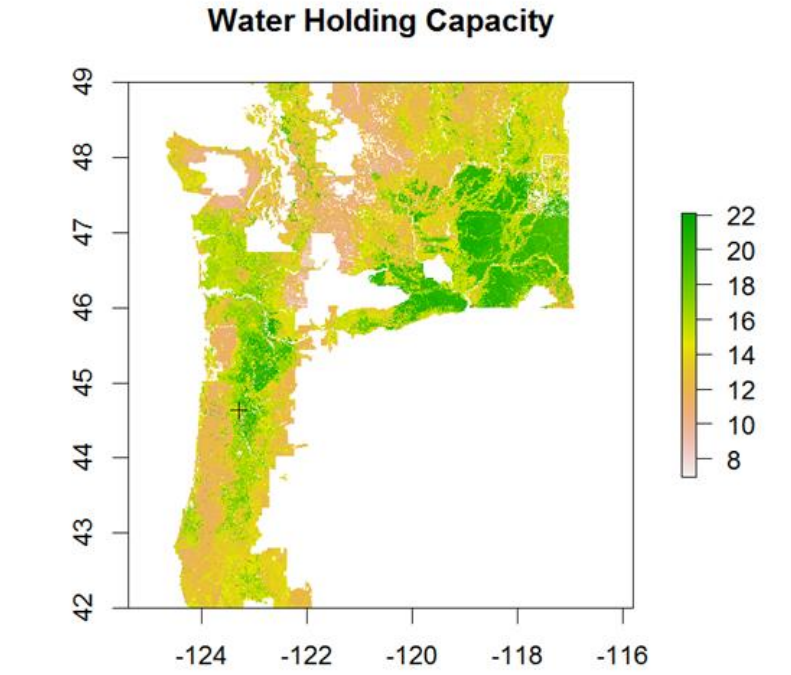

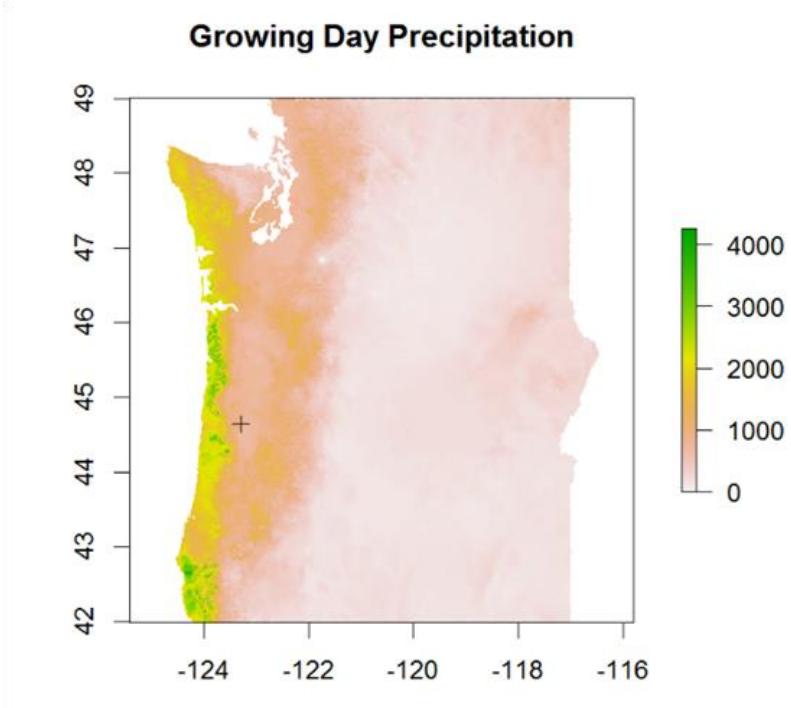

Figure 6.2 Simplified example of calling a set of ORGANON DLL's to simulate forest growth and yield in the R statistical programming environment.

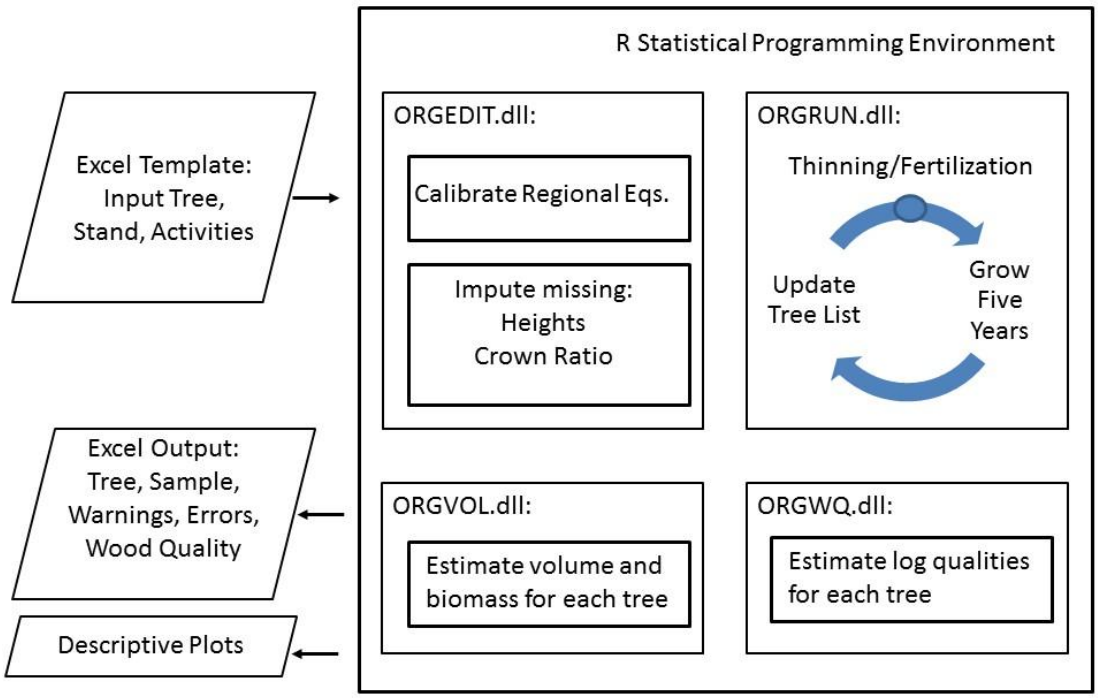

Chapter 7: Conclusions - Integrating simulation of wood properties into forest growth and yield models for planted *Pseudotsuga menziesii* in the Pacific Northwest United States: A synthesis

Nathaniel OSBORNE

Douglas MAGUIRE

Aaron WEISKITTEL

Manuscript in preparation for submittal to:

Annals of Forest Science

Key message

Models for static and dynamic wood properties models can be integrated with individual tree growth and yield models. The coupled modeling system can be implemented in forestry decision support software, enhancing forest planning and evaluation of economic performance. Further research and development is necessary to realize significant benefits from the coupled modeling system.

Abstract

Context: In globally competitive forest products markets, it is necessary to produce not only wood volume but also wood with desirable properties. Coupled tree growth, yield and wood property (GYWP) modeling systems are critical to planning future forests for global wood demand. These modeling systems are readily incorporated in decision support software, lending managerial insight into the economic performance of alternative silvicultural regimes. Several technical and scientific advances are necessary to link components of GYWP systems and associated software. Aims: This review synthesizes the current state of knowledge for modeling growth, yield, and wood properties in Douglas-fir (*Pseudotsuga menziesii* var. *menziesii* (Mirb.) Franco). Recommendations for future research, technological and scientific, are outlined. Results: Three steps are recommended to advance GYWP development: (1) incorporate dynamic environmental conditions and ecophysiological processes in new and existing wood properties equations at micro- and macro-anatomical scales; (2) facilitate parallel processing at different time and spatial scales to allocate anatomical properties within and between initially undifferentiated growth layers using empirically determined correlative relationships; and (3) enhancing post-processing output from growth, yield and wood properties simulation.

Conclusions: Despite extensive research, our current understanding of Douglas-fir wood formation is fragmented and controls are not well understood, or easily transferred to GYWP systems. Targeted research and technical developments can synthesize and augment knowledge required for GYWP system implementation in forest planning.

Additional Keywords: Ecophysiology; Wood anatomy; Growth layers; Environmental controls.

Introduction

The source of industrial wood in the Pacific Northwest United States is dominated by coastal Douglas-fir (*Pseudotsuga menziesii* var. *menziesii* (Mirb.) Franco) plantations, which have historically grown products of superior quality for construction. Douglas-fir yields wood properties that are desirable for structural applications, under almost any management regime, but the role of active management in improving the yield of wood with the most desirable properties has been known for a long time (McArdle and Meyer 1930). To maintain the global competitiveness of planted second-growth Douglas-fir, relative to emerging centers of timber production, it is necessary to produce stands with optimal volume and trees of optimal wood properties (Kennedy 1995). Designing silvicultural regimes for optimal future forests can be enhanced through use of coupled individual tree growth, yield and wood properties modeling systems (GYWP). These GYWP systems can be integrated into decision support software to optimize the economic performance of working forest landscapes.

The terms wood properties and wood quality have wide ranging and consistently vague definitions. In most cases, wood properties are a selection of tree anatomical features and

various parameters derived from them. Some macroscopic anatomical properties include: knots (occluded branches), sapwood, heartwood, juvenile wood, shape and condition of the xylem, and defects along the wood surface and within the xylem (Figure 7.1). The definition of each of these features is elaborated upon later. Microscopic wood properties include cell length and width, microfibril angle, and earlywood:latewood ratios (Figure 7.2). A composite of microscopic and macroscopic features influences wood properties like modulus of elasticity (breaking point) or modulus of rupture (deformation point) (Lachenbruch et al. 2010). Ultimately, wood quality is determined by the combination of wood properties and wood end use. Wood with poor qualities for one application can be superior for another use (Larson 1969), which makes the term wood quality vague and inconsistently defined. GYWP modeling systems therefore offer the advantage of simulating response of micro- and macro-anatomical properties to silvicultural treaments and site conditions, and maintaining the flexibility to allow evaluation of their implications for a wide range in potential wood products.

Development of a GYWP system requires understanding and modeling complex wood formation processes and their functional interactions or correlative relationships. The objectives of the GYWP will determine the resolution that these relationships are represented. Modeling wood properties at a coarse scale may be perfectly suitable for one application, and insufficient for another. While connecting wood properties models to growth and yield models are described here across many scales (macroscopic to microscopic), it should be noted that modeling can usually be done at any scale using surrogate parameters. In some cases the use of surrogates for wood properties parameters would be preferred, due to difficulty in measuring the actual parameters, or representing their variation to a degree that could be scaled well to other

parameters of the system or final system outputs. Wood formation is a dynamic ecophysiological and anatomical response to the growing environment. Wood properties ultimately depend on the process of wood cell formation in the main stem and branches, and the integrative effect of relative locations of wood cells possessing specific attributes within a manufactured product. Previous reviews of GYWP provided useful broad assessments of the state of our knowledge across multiple species (Mäkelä et al. 2010; Burkhart and Tome 2012; Weiskittel 2013). In general, GYWP are either static (wood properties predicted from the outcome of growth projections) or dynamic (wood properties simulated dynamically and simultaneously with growth), although most examples in the literature adopt the former approach, despite the latter having several theoretical advantages. In this review we recommend directions for future research from the viewpoint of primarily the second approach.

Given the importance of Douglas-fir in the United States, Europe, New Zealand and to some extent South America, along with the long history of research on the species (e.g. Lowell et al. 2014), this review focused on Douglas-fir as a case study. The objective of the analysis was to synthesize the current knowledge of ecophysiological and environmental controls on wood properties variation in Douglas-fir in the Pacific Northwest region (PNW) of the United States and adjacent areas of Canada. Critical knowledge gaps are identified, and recommendations for resolving them are given. Finally, a combined mechanistic and statistical framework for modeling Douglas-fir tree growth, yield and wood properties is given, with discussion on how to extract product value from modeling system outputs.

Discussion

1. Mechanisms controlling variation in wood properties

Wood formation processes result in forest growth and yield, but also control the properties of wood contributing to growth and yield. Xylem formation, which is always initially sapwood, begins with anticlinal and periclinal division of fusiform initials in the vascular cambium. The cambial zone is situated between tree xylem and phloem tissues (Figure 7.1). The geometry and cell type produced from fusiform initial cells depends largely on plant growth hormone concentration (Little and Savidge 1987), and the availability of photosynthate and moisture (Edmonds 1982). Plant growth hormones like indole-3-acetic acid (IAA) are distributed from apical controls at leaf buds and the apical meristem through phloem, stimulating cellular growth starting from the tree tip to the stem base (Grotta et al. 2005). Consequently, tree growth and yield has a strong feedback relationship with wood formation, including micro- and macro-anatomical properties. The location of the tree crown determines plant hormone concentration along the tree bole, thereby controlling wood formation. At the same time, wood formation controls tree growth and yield, the space occupied by a tree, and eventually the size of tree crown. Environmental factors influencing tree growth, like soil moisture availability, temperature, and radiation (Drever and Lertzman 2001) are relatively well established for Douglas-fir (e.g., Waring et al. 2008). Because the total amount, transpiration rate, and net photosynthesis of foliage form a feedback loop to wood properties such as tracheid length, width, and lumen, it is not surprising that environmental controls and ecophysiological processes are correlated with wood anatomy, although the causal mechanisms are not completely known. In short, wood micro-anatomical properties respond to carbohydrates and plant growth regulators generated in the crown, and to water and nutrient availability in the transpirational stream.

The goal of a GYWP system is to simulate wood formation processes and/or associated correlative relationships simultaneously with simulation of traditional tree dimensions such as total height, stem profile, and crown size that are addressed by individual-tree growth models. There are several current gaps in modeling wood properties (Table 7.1), and already modeled wood properties have been represented with different levels of sophistication and scope. The following sections describe the current state of knowledge of mechanisms controlling wood properties in Douglas-fir and in some cases, models that represent specific mechanisms.

Control of the sapwood rind and heartwood core

All cells forming the tree xylem are initially alive and contained within the outer edge of the sapwood zone. Over time, most of the cells in the sapwood zone die as their cell wall lignifies, thicken and cells lose nuclei and protoplasm (Esau 1965). Some of the sapwood cells are kept alive, like ray parenchyma which store and translocate starches and water across the longitudinal conductive cells (Bamber 1961). The living ray cells are critical to wood formation and ensuring successful division of fusiform initials (Zimmerman and Brown 1971). Sapwood is always comprised of non-living cells. In many of cases, only two-percent of sapwood cells are living (Franklin et al. 1987). When all sapwood cells die, there is a transition to heartwood, although the specific mechanisms of transition are not well known (Taylor et al. 2002). Heartwood does not serve a physiological function in the tree, but does provide decay resistance and mechanical support functions (Long et al. 1981).

There is strong evidence that the transition from sapwood to heartwood is correlated to features of the living crown. There is a functional relationship between the distribution of Douglas-fir foliage and cross-sectional area of sapwood (Hazenburg and Yang 1991) as well as the amount of foliage that is serviced by this conductive tissue (Büsgen and Münch 1929; Shinozaki et al. 1964; Kershaw and Maguire 1995). As sapwood area increases, so does tree conductive capacity. As tree conductivity increases, the possible crown size also increases, completing the feedback loop ensuring a dynamic equilibrium between sapwood area necessary for foliage support (Waring et al. 1980; Maguire and Hann 1989). The implications of sapwood area on crown size and tree growth potential and responsiveness to silvicultural treatment motivated the first models for Douglas-fir sapwood area at the crown base (Maguire and Hann 1987). Later modeling allowed prediction of sapwood area as a continuous function of height on the tree bole (Maguire and Batista 1996). Models for sapwood area in Douglas-fir have evident value in predicting tree growth and yield in a mechanistic-statistical modeling framework (Figure 7.3). Models for sapwood area are also important from a wood properties perspective. The area of sapwood informs the type of silvicultural regime necessary to produce certain wood products, like high value utility poles that require a minimum sapwood width for penetration of preservatives (Landgren et al. 1994; Islam et al. 2009).

Controls on branch size and knot geometry

The angle, length and diameter of branches allow estimation of crown size (Roeh and Maguire 1997; Maguire et al. 1999; Maguire et al. 1994; Weiskittel et al. 2007; Hann and Hanus 2004; Wykoff 1990) and are required for characterization of foliage distribution. These tree physiological characteristics are important predictors in the mechanistic framework of a GYWP

system (Figure 7.3) but are also important for determining macroscopic (e.g., knot size) and microscopic (e.g., wood density) properties of stemwood (Lowell et al. 2014). While branches occupy space outside the xylem, their development over time and gradual encasement within the stem allows direct prediction of knot size and geometry (Osborne and Maguire 2015; Figure 7.4). The importance of knots (branches) in planted Douglas-fir forests has been recognized since the first second-growth forests were established in the Pacific Northwest (Paul 1947; Fleischer 1949). Silvicultural field experiments identified that the principle control of knot and branch size is achieved by stand density management (Grah 1961; Maguire et al. 1991; Briggs et al. 2007). Lesser known are the controls for knot geometry and branch angle. There is some evidence that some variation in branch angle is controlled through genetics (Birot and Christophe 1983) but environmental controls could be more important (St. Clair 1994). Uncovering the sources of variation in branch angle, and covariance within and between whorls, could provide useful insights into simulation of internal knot structure in stems and forest products, which can today only be attributed to random variation (Colin and Houllier 1992). Identifying controls on knot geometry is important from the wood products perspective because the number, size, and distribution of branches or knots influence product recovery (Fahey et al. 1991; Osborne and Maguire 2014) and ultimately financial returns from a silvicultural regime (Lowell et al. 2014).

Controls on the juvenile wood core

Juvenile wood is inner core in the xylem limited to about 5 – 20 rings from the bole pith, depending on the wood attributes used to define it, on the relative growth rate of the tree, and perhaps on the rate of crown recession past a given height of wood formation (Abdel-Gadir et al. 1993; Figure 7.1). While the juvenile wood zone is delineated discretely, this zone represents

several continuously changing wood properties (Larson et al. 2001). As cambial age increases so does the density of wood, longitudinal tracheid length, modulus of elasticity, modulus of rupture, cell wall thickness, transverse shrinkage, and percentage latewood. Other features decreasing with cambial age are fibril angle, longitudinal shrinkage, and incidence of spiral grain (Cahill and Briggs 1992). The concepts described in this review suggest that the living tree crown has an important role in formation of juvenile wood properties. However, the controls for juvenile wood properties not well understood or at least continue to be debated. Gartner et al. (2002) found there was no significant relationship between crown position and a composite of wood properties defining the juvenile wood core. It is likely that crown distribution may just one of several important controls on the constituent wood properties of the juvenile wood core. For example, Rozenberg et al. (2001) found genetic effects could explain variations in wood density, supporting the concept that crown mass could be an important predictor of the juvenile wood core after accounting for other genetically controlled ecophysiological parameters. There are no static models for predicting delineation of the juvenile wood core, but a dynamic simulation procedure was demonstrated by Maguire et al. (1991), terminating juvenile wood formation by either cambial age or crown recession.

2. Recommendations for future research

To fully realize the benefit of a GYWP system for Douglas-fir, a number of scientific and technical research advancements are necessary. These include: (1) Incorporating dynamic influence of environmental conditions and ecophysiological processes not only on diameter, height and volume growth, but simultaneously on anatomical properties of the wood formed during a growth cycle; (2) Facilitating parallel processing to accommodate a range in temporal

and spatial scales of growth processes; and (3) Enhancing post-processing output from growth, yield and wood properties simulation. Approaches to achieving these recommended enhancements are described in more detail below.

Incorporating dynamic conditions and ecophysiological processes into models

Most current wood properties models are static, based on empirical relationships, and do not incorporate the influence of environmental factors on growth or wood properties. Although Deckmyn et al. (2006) presented a mechanistic model for wood development that was parameterized for Scots pine (Pinus sylvestris L.) and European oak (Quercus robur L.), a similar model does not currently exist for Douglas-fir. Weiskittel et al. (2010) developed a hybrid growth model for intensively managed Douglas-fir plantations in the Pacific Northwest, but except for a detailed representation of branch development, wood anatomy was beyond the scope of that effort. Meeting this objective would likely require consideration of the effects of environmental conditions and ecophysiological processes on traditional wood volume and biomass increment and their simultaneous effects on micro-anatomical and macro-anatomical attributes of the predicted growth layer. This simultaneous estimation of wood volume increment and embedded anatomical properties will require development of new models for wood properties within a combined mechanistic-statistical framework (Figure 7.3). Key environmental conditions to consider should be the soil water holding capacity (WHC), growing season (GS) weather (i.e. particularly vapor pressure deficits, and the net effects on internal water potentials, and secondarily nutrient availability and effects of potential nutrient deficiencies on wood properties). Candidate models inevitably will be based on environmental variables that are directly measured on intensive research sites as well interpolated from regional models. Several

databases are accessible in the Pacific Northwest for estimating soil properties (e.x. NRCS SSURGO) and spatially interpolated climate and weather variables (Wang et al. 2012).

If alternative models are developed using either actual weather and soil properties measured onsite or regional estimates from interpolation algorithms, they will provide greater flexibility for GYWP users who may or may not have direct measurements of weather or soil features available. Effects of environmental conditions inherent to the site are influenced by silvicultural intervention. Although the effects of silvicultural treatments on wood attributes have been studied, few models incorporate the effect of thinning, fertilization, early vegetation control or genetic stock on wood properties. These type of silvicultural interventions are critical aspects of silvicultural regimes in planted Douglas-fir stands, and should be accounted for in any GYWP system through a synthesis of the many documented studies. The possibility to include important physiological parameters in wood properties equations, like the spatial and temporal distribution of growth regulators, photosynthate, water, and nutrients through the tree bole should be explored. Including detailed physiological parameters in a GYWP system may be difficult, but substituting surrogates like crown density and foliage distribution could prove effective for simulating some wood properties.

The information for covering essential components of a GYWP system for Douglas-fir are not complete or at least not publically available (Table 7.1). These knowledge gaps must be filled to develop a complete and reliable GYWP system. Osborne and Maguire (2015) modeled the geometry of knots in Douglas-fir, but did not distinguish between a live and dead knot zone. However, this delineation can be implied by dynamic simulators like ORGANON, which

provide estimates of stem dib and maximum branch diameter at time of whorl mortality (Maguire et al. 1991). In fact, under the option of defining juvenile wood as crown wood, the juvenile wood core is equivalent to the live or red knot zone. Knot type is an important determinant of lumber and veneer grade recovery, so this dynamic simulation approach or a post-processing static approach could be applied to distinguish between the red/live knot and black/dead knot zones in simulated trees. The latter approach would require a model that estimated the average live/red knot core for a tree with a given combination of DBH, total height, and crown size. Data for developing such a model could collected by X-ray scanning (Krähenbühl et al. 2014) Douglas-fir whorls across a wide range of tree growth conditions, silvicultural regimes and heights on the tree bole. Automated tools for knot detection from computed tomography (CT) imagery, like the "Gourmands" application developed at the Institut national de la recherche agronomique (INRA), could prove useful in developing a knot type modeling database (Tong et al. 2015). However, trees from thinned or fertilized stands may contain more abrupt changes in the diameter of the red/live knot zone corresponding to years of silvicultural intervention.

To the authors' knowledge, there are no published models to predict Douglas-fir micro-fibril angle in the S_2 wall of longitudinal tracheids in Douglas-fir. This lack of capacity presents a problem because to predict derivative parameters like the modulus of elasticity (MOE) or modulus of rupture (MOR), both the density of wood and fibril angle should be known (Lachenbruch et al. 2010). Predicting fibril angle also allows a better accounting of longitudinal and transverse swelling in wood (Rafsanjani et al. 2014), which varies with cambial age. Predicting gradients or zones of attributes like density, fibril angle, and possibly other aspects of

cell geometry, could be more useful than delineating the juvenile wood core based on coarser criteria like cambial age (Figure 7.1). Models for the density of wood in Douglas-fir (Filipescu et al. 2013; Kantavichai et al. 2010) have provided valuable insights to wood formation at the microscopic scale (Figure 7.2). However, these models cannot yet be applied to a GYWP system because the radial trend in wood density has only been modeled at breast height (1.37 m). Important considerations for modeling wood density in Douglas-fir include the following: 1) additional predictors within the statistical-mechanistic framework (Figure 7.3); 2) profile models for percentage latewood, providing direct link between environmental controls and coarser resolution wood density; 3) density within the earlywood and latewood of a given tree ring to increase precision of wood density estimates; and 4) links between density profiles of the entire tree bole and foliage amount and distribution. Accounting for within ring variation in wood density will likely rely on X-ray densitometry (Kantavichai et al. 2010). The use of medical CT scanning to rapidly estimate wood density has been demonstrated for Douglas-fir and several other tree species (Osborne et al. 2015; Freyburger et al. 2009). The main drawback of medical CT scanning in density estimation is the resolution of estimates. Medical CT scanning typically estimates density of objects at a true resolution of 1 mm, while X-ray densitometry can estimate density at resolutions of 25µ. Developing a large database for modeling wood density will likely rely on a combination of high resolution X-ray densitometry data and lower resolution data from CT scanning.

Estimating the distribution of common wood surface and xylem defects is important to avoid biasing wood product recovery and estimating unrealistically optimistic grade distributions. Assigning stem surface and xylem defects should be an important area of research in Douglas-

fir. The simplest way to estimate defect incidence may be to assess and estimate variance of incidence across a large set of Douglas-fir growing conditions and silvicultural treatments. With an estimated variance, defect incidence could be assigned stochastically to trees by drawing randomly from a normal distribution with a predicted or regional average: $N \sim (\mu, \sigma_{defect}^2)$. A more robust approach could be to model the same defects along the tree bole using logistic regression, accounting for macro- and micro-site variables that explain defect incidence.

Facilitating parallel processing at varied temporal and spatial scales

A second step in developing a GYWP system for Douglas-fir will be to facilitate parallel processing at different time and spatial scales to allocate anatomical properties within and between initially undifferentiated growth layers using correlative and mechanistic relationships. Most statistical growth and yield (GY) systems for Douglas-fir operate on a five or ten year time horizon (Table 7.2). Finer temporal resolutions are possible from Douglas-fir GY systems using hybrid (e.g., Weiskittel et al. 2010) or pure process (ecophysiological) modeling approaches. However, the Center for Intensive Planted-forest Silviculture (CIPS) at Oregon State University is working primarily with both mechanistic and empirical components of an annualized version of ORGANON that is more amenable to simulating responses to intensive silviculture of shorter-rotation Douglas-fir plantations. The best temporal scale for simulating wood properties is yet to be demonstrated, but may be any level from daily up to annual. In a GYWP system the output from each component model must be scaled to the largest time step in the system. The assumption driving an architecture with processes occurring in parallel but at differing time steps is that biological realism is gained by matching a process more closely to our understanding of the key mechanism, and then integrating up to the time scale of model output and reporting. If a

growth model predicts stem growth (xylem expansion) over five-years, it is necessary to simulate wood attribute responses and assign wood properties estimated from a daily, monthly or annual scale across that undifferentiated xylem growth. Assigning wood properties across undifferentiated growth requires establishing correlative or mechanistic relationships among each modeling component in a GYWP system. These correlative and mechanistic relationships must be established in such a way that the entire modeling system produces results representative of known growth and yield principles (Leary 1992), as well as any principles of wood formation. The value of physiological growth predictors, like sapwood area at crown base, leaf area index (LAI), soil water status, growing season precipitation, evaporative demand, and resulting internal gradients in water potential, has already been demonstrated in statistical-mechanistic frameworks for GY systems, so transfer to GYWP systems logically follows.

Enhancing post-processing output from growth, yield and wood properties simulation

Development of GYWP systems provide significant scientific benefit for exploring wood formation and tree development under varied environmental conditions and silvicultural interventions without any significant post-processing of the system outputs. Outputs from a GYWP system can be used to assess the possible effects of changing climate on carbon storage (wood density), harvesting regime on nutrient cycling (partitioning of tree mass), and many other important and salient forest management issues. With only an estimated maximum branch diameter (LLAD) and ideally the juvenile wood core percentage (JPC) along a virtual log, lumber and veneer grade distribution can be estimated with product recovery equations (Fahey et al. 1991). The value and feasibility of linking relatively coarse wood property outputs (maximum branch size and juvenile wood core percentage) to product recovery equations is well

demonstrated (Weiskittel et al. 2006; Osborne and Maguire 2014). Converting the outputs from GYWP systems to estimates of product recovery promote feedback to fine-tune of silvicultural regimes in a way that should maximize financial returns under the assumed value differentials, with consideration of wood properties. Existing product recovery equations are reliant upon mill configuration and the products produced by the mill where the recovery study was conducted, so a compelling case can be made for advancing to milling simulation.

The versatility of simulated sawing of virtual logs (Mäkelä et al. 2010) has been well demonstrated for many tree species, but there can be substantial differences between simulated and observed lumber yields (e.g Todoroki et al. 2005). Developing and improving the capacity for simulated sawing of virtual Douglas-fir logs using GYWP system outputs should be a high priority. In most cases simulated sawing is applied to images of logs scanned "in-line" at the sawmill using industrial X-ray computed tomography (Andreu and Rinnhofer 2003). A list of currently available sawing simulators includes: SAWSIM (Halco 1970), BOF (Lewis 1985), AutoSaw (Todoroki 1990), RadSawSim (Ištvanić et al. 2010), Grasp (Occeña and Schmoldt 1995), LogCast (Occeña et al. 2000), TopSaw (Yun et al. 2008), Optitek (FPInnovations 2014), WoodCim (Usenius 2000) and Cutlog (Turcan 2005). Most of these listed models are proprietary, or at least not open-source, which limits usefulness and portability. Achieving the goal of sawing simulation in an open-source GYWP system requires that two technical goals are achieved. First an open-source sawing simulator should be developed and incorporated into a GYWP system. An important consideration should be to maintain model or software portability, through development of callable direct link libraries (DLL), in both the sawing simulator and components of the GYWP system (Robinson and Monserud 2003). The second technical goal

requires converting the continuous type of output from GYWP systems to voxel or pixel formatted images which are typically supplied to sawing simulators (Figure 7.4). The resolution at which discrete objects like knots in trees are condensed to pixelated flat files will largely depend on computer processing time and the sensitivity of this conversion on analysis results.

Simulation validation and reporting uncertainty

For the outputs of GYWP system to be useful, they must be both accurate and valid. Validation of wood properties models for Douglas-fir is scant at best, and the majority of validations have not been completed using truly independent datasets. Ensuring the validity of estimates in GYWP systems should be taken at both the model component and modeling system resolutions. Individual models, like models for knot geometry (Osborne and Maguire 2015), should be validated using independent databases collected specifically for purposes of validation. It is possible for individual components of a GYWP system to be valid, but for the outputs of the modeling system as a whole to lack those characteristics (Leary 1997), as well as vice versa. The modeling system outputs should be evaluated on the basis of meeting biologic expectations; providing estimates within the range of extreme and average values which have been observed; and minimizing prediction error in the most important outputs.

The majority of GY systems for Douglas-fir (Table 7.2) do not provide measures of uncertainty with their outputs, but tracking GY system error is possible (Weiskittel et al. 2011). Tracking and reporting the cumulative uncertainty resulting from model components in a GY or GYWP system is critical to any managerial application. Without a measure of uncertainty, it is not possible to distinguish between silvicultural regimes, which on average could be different, but in

fact are not significantly different (i.e. the error bounds overlap). There are two challenges that need to be overcome to report the cumulative error around estimates in both GY and GYWP systems. The first challenge is to account for the propagation of errors through the modeling system, which requires a careful accounting in model chains. The second challenge is to elegantly convey these measures of uncertainty with GYWP system outputs. There is not a standard procedure for addressing these challenges, and the work of reporting uncertainty in GYWP systems will likely require individualized solutions.

Conclusions

Significant research and technical developments are necessary to produce a useful, reliable and robust mechanistic/statistical GYWP system for planted Douglas-fir in the Pacific Northwest. These research and technical developments will require a concerted effort and significant collaboration among research cooperatives in the Pacific Northwest. These cooperatives have sufficient incentive to collaborate given their pursuit of common goals, albeit from different perspectives. Their efforts should include targeted research on the influence of genetics, silviculture, and ecophysiology on wood formation, with clear application to forest models. In addition, the work of software developers should be better incorporated into the process of wood properties model development. Their collaboration should produce more robust software and expedite the successful completion of complex coding required to accommodate any sawing simulation applications. The goal of producing a mechanistic GYWP system is a long-term goal, so early demonstrations of research and development will be critical to ensuring success. Assembling the necessary growth, yield and wood properties datasets and revealing the key mechanisms is a major challenge, but is arguably essential to planning planted Douglas-fir

forests in the Pacific Northwest. Publically available software that allows for the optimization of wood volume characterized by specific properties is necessary to keep the region globally competitive in support of larger social and environmental goals.

References

Abdel-Gadir, A.Y., Krahmer, R.L. 1993. Estimating the age of demarcation of juvenile and mature wood in Douglas-fir. Wood and Fiber Science 25(3): 242-249.

Andreu J.P., Rinnhofer, A. 2003. Modeling knot geometry in Norway spruce from industrial CT Images, in: SCIA 2003: 786-791.

Bamber, R.K. 1961. Sapwood and heartwood. Forestry Commission of New South Wales, Technical Pub No. 2.

Birot, Y., Christophe, C. 1983. Genetic structures and expected genetic gains from multitrait selection in wild populations of Douglas-fir and Sitka spruce. Silvae Genetica 32(5/6): 141-151.

Briggs, D., Ingaramo, L., Turnblom, E. 2007. Number and diameter of breast-height region branches in a Douglas-fir spacing trial and linkage to log quality. Forest Products Journal 57(9): 28.

Burkhart, H.E., Tomé, M. 2012. Modelling forest trees and stands. Springer. Netherlands. pp. 405-427.

Büsgen, M, Münch, E. 1929. The Structure and Life of Forest Trees. (English translation) John Wiley & Sons, New York.

Cahill, B.C., Briggs, D.G. 1992. Effects of fertilization on wood quality and tree value. In: Proceedings of Forest Fertilization: Sustaining and improving nutrition and growth of western forest. 12–14 February 1991, Seattle, Washington. University of Washington, College of Forest Resources. Pp. 145-160.

Colin, F., Houllier, F. 1992. Branchiness of Norway spruce in northeastern France: predicting the main crown characteristics from usual tree measurements. Annals of Forest Science 49(5): 511-538.

Colin, F., Laborie, M.P., Fortin, M. 2015. Wood properties: future needs, measurement and modelling. Annals of Forest Science 72(6): 665-670.

Deckmyn G, Evans SP, Randle TJ (2006) Refined pipe model theory for mechanistic modeling of wood development. Tree Physiology 26: 703-717.

Drever, C.R., Lertzman, K.P. 2001. Light-growth responses of coastal Douglas-fir and western redcedar saplings under different regimes of soil moisture and nutrients. Canadian Journal of Forest Research 31(12): 2124-2133.

Edmonds, R.L. 1982. Analysis of coniferous forest ecosystems in the Western United States, Hutchinson Ross Pub. Co.

Esau, K. 1965. Plant Anatomy, 2nd edition. New York: John Wiley and Sons. Pp. 249-250.

Fahey, T.D., Cahill, J.M., Snellgrove, T.A., Heath, L. 1991. Lumber and veneer recovery from intensively managed young-growth Douglas-fir. Res. Pap. PNW-RP-437. Portland, OR: U.S. Department of Agriculture, Forest Service, Pacific Northwest Research Station. 25 p.

Fleischer, H.O. 1949. The suitability of second-growth Douglas-fir logs for veneer. Journal of Forestry 47(7): 533-537.

FPInnovations 2014. Optitek 10: user's manual. FPInnovations, Quebec, Canada.

Franklin, J.F., Shugart, H.H., Harmon, M.E. 1987. Tree death as an ecological process. BioScience 37(8): 550-556.

Freyburger, C., Longuetaud, F., Mothe, F., Constant, T., Leban, J.M. 2009. Measuring wood density by means of X-ray computer tomography. Annals of Forest Science 66(8): 804.

Gartner, B.L., North, E.M., Johnson, G.R., Singleton, R. 2002. Effects of live crown on vertical patterns of wood density and growth in Douglas-fir. Canadian Journal of Forest Research 32: 439-447.

Grah, R.F. 1961. Relationship between tree spacing, knot size, and log quality in young Douglas-fir stands. Journal of Forestry 59(4): 270-272.

Grotta, A.T., Gartner, B.L., Radosevich, S.R., Huso, M. 2005. Influence of red alder competition on cambial phenology and latewood formation in Douglas-fir. IAWA Journal 26(3): 309-324.

Halco Inc. 1970. SAWSIM: Sawmill Simulation Program, Carroll-Hatch, Vancouver, Canada.

Hann, D.W., Hanus, M.L. 2004. Evaluation of nonspatial approaches and equations forms used to predict tree crown recession. Canadian Journal of Forest Research 34: 1993-2003.

Hazenberg, G., Yang, K.C. 1991. Sapwood/heartwood width relationships with tree age in balsam fir. IAWA Journal 12(1): 95-99.

Islam, M.N., Ando, K., Yamauchi, H., Hattori, N. 2009. Preservative treatment of Douglas-fir lumber by the passive impregnation method with copper azole. European Journal of Wood and Wood Products 67(1): 77-81.

Ištvanić, J., Piljak, K., Antonović, A., Luˇić, R.B., Jambreković, V., Pervan, S. 2010. The theory and mathematical model underlying the radial sawing simulator—RadSawSim. Forest Products Journal 60(1): 48–56.

Kantavichai, R., Briggs, D., Turnblom, E. 2010. Modeling effects of soil, climate, and silviculture on growth ring specific gravity of Douglas-fir on a drought-prone site in Western Washington. Forest Ecology and Management 259(6):1085-1092.

Kennedy, R.W. 1995. Coniferous wood quality in the future: concerns and strategies. Wood Science and Technology, 29(5): 321-338.

Kershaw, J.A., Maguire, D.A. 1995. Crown structure in western hemlock, Douglas-fir, and grand fir in western Washington: trends in branch-level mass and leaf area. Canadian Journal of Forest Research 25(12): 1897-1912.

Krähenbühl, A., Kerautret, B., Debled-Rennesson, I., Mothe, F., Longuetaud, F. 2014. Knot segmentation in 3D CT images of wet wood. Pattern Recognition 47(12): 3852-3869.

Lachenbruch, B., Johnson, G.R., Downes, G.M., Evans, R. 2010. Relationships of density, microfibril angle, and sound velocity with stiffness and strength in mature wood of Douglas-fir. Canadian Journal of Forest Research 40(1): 55-64.

Landgren, C.G., Bondi, M.C., Emmingham, W.H. 1983. Growing and harvesting Douglas-fir poles. Corvallis, Oregon: Extension Service, Oregon State University EC 1134, Pp. 7.

Larson, P.R. 1969. Wood formation and the concept of wood quality. Yale Univ. School Forestry Bul 74: 1-54.

Larson, P.R., Kretschmann, D.E., Clark, A., Isebrands, J.G. 2001. Formation and properties of juvenile wood in southern pines: a synopsis. Gen. Tech. Rep. FPL-GTR-129. Madison, WI: U.S. Department of Agriculture, Forest Service, Forest Products Laboratory. 42 p.

Leary, R.A. 1997. Testing models of unthinned red pine plantation dynamics using a modified Bakuzis matrix of stand properties. Ecological Modelling, 98(1): 35-46.

Lewis, D. 1985. Sawmill simulation and the best opening face system: a user's guide. USDA Forest Service, Forest Products Laboratory FPL-48. Madison, WI. 29 p.

Long, J.N., Smith, F.W., Scott, D.R. 1981. The role of Douglas-fir stem sapwood and heartwood in the mechanical and physiological support of crowns and development of stem form. Canadian Journal of Forest Research 11(3): 459-464.

Lowell, E.C., Maguire, D.A., Briggs, D.G., Turnblom, E.C., Jayawickrama, K.J.S., Bryce, J. 2014. Effects of silviculture and genetics on branch/knot attributes of coastal Pacific Northwest Douglas-fir and implications for wood quality – A synthesis. Forests 5(7): 1717-1736.

Maguire, D.A., Hann, D.W. 1987. Equations for predicting sapwood area at crown base in southwestern Oregon Douglas-fir. Canadian Journal of Forest Research 17(3): 236-241.

Maguire, D.A., Hann, D.W. 1989. The relationship between gross crown dimensions and sapwood area at crown base in Douglas-fir. Canadian Journal of Forest Research 19(5):557-565.

Maguire, D.A., Kershaw, J.A., Hann, D.W. 1991. Predicting the effects of silvicultural regime on branch size and crown wood core in Douglas-fir. Forest Science 37(5):1409-1428.

Maguire, D.A., Moeur, M., Bennett, W.S. 1994. Models for describing basal diameter and vertical distribution of primary branches in young Douglas-fir. Forest Ecology and Management 63(1): 23-55.

Maguire, D.A., Batista, J.L. 1996. Sapwood taper models and implied sapwood volume and foliage profiles for coastal Douglas-fir. Canadian Journal of Forest Research 26(5): 849-863.

Maguire, D.A., Johnston, S.R., Cahill, J. 1999. Predicting branch diameters on second-growth Douglas-fir from tree-level descriptors. Canadian Journal of Forest Research 29(12): 1829-1840.

Mäkelä, A., Grace, J., Deckmyn, G., Kint, A.K.V. 2010. Simulating wood quality in forest management models. Forest Systems 19(S1): 48-68.

McCardle, R.E., Meyer, W.H. 1930. The yield of Douglas-fir in the Pacific Northwest. US Dept. Agr. Tech. Bul 201.

Occeña, L.G., Schmoldt, D.L. 1995. GRASP - A Prototype Interactive GRAphical Sawing Program. MU-IE Technical Report, Pp. 1–17.

Occeña, L.G., Santitrakul, E., Schmoldt, D.L. 2000. Hardwood sawyer trainer. Pp. 43-47 in Proc. 28th Annual Hardwood Symposium – West Virginia Now – The Future for the Hardwood Industry, Davis, WV. National Hardwood Lumber Assoc., Memphis, TN.

Osborne, N.L., Maguire, D.A., Hann, D.W. 2014. Simulating Douglas-fir tree and stand development under varying initial spacings with ORGANON: Knot size and juvenile wood core effects on grade recovery of lumber. Center for Intensive Planted-forest Silviculture Annual Report 2013: 22-28.

Osborne, N.L., Maguire, D.A. 2015. Modeling knot geometry from branch angles in Douglas-fir (*Pseudotsuga menziesii*), Canadian Journal of Forest Research, *under review*.

Osborne, N., Høibø, O., Maguire, D., Gourley, D. 2015. Estimating the density of coast Douglas-fir wood samples at different moisture contents using medical X-ray computed tomography. Computers and Electronics in Agriculture. *in preparation*.

Paul, B.H. 1947. Knots in second-growth Douglas-fir. US Department of Agriculture Forest Service, Forest Products Laboratory, Madison Wisconsin. No. R1690.

Rafsanjani, A., Stiefel, M., Jefimovs, K., Mokso, R., Derome, D., Carmeliet, J. 2014. Hygroscopic swelling and shrinkage of latewood cell wall micropillars reveal ultrastructural anisotropy. Journal of The Royal Society Interface 11: 20140126.

Robinson, A.P., Monserud, R.A. 2003. Criteria for comparing the adaptability of forest growth models. Forest Ecology and Management, 172(1): 53-67.

Roeh, R.L., Maguire, D.A. 1997. Crown profile models based on branch attributes in coastal Douglas-fir. Forest Ecology and Management 96(1): 77-100.

Rozenberg, P., Franc, A., Bastien, C., Cahalan, C. 2001. Improving models of wood density by including genetic effects: a case study in Douglas-fir. Annals of Forest Science 58(4): 385-394.

St. Clair, J.B. 1994. Genetic variation in tree structure and its relation to size in Douglas-fir. II. Crown form, branch characteristics, and foliage characters. Canadian Journal of Forest Research 24(6): 1236-1247.

Shinozaki, K, Yoda, K, Hozumi, K, Kira, T. 1964. A quantitative analysis of plant form. The pipe model theory. I. Basic analyses. Japanese Journal of Ecology 14: 97-105.

Soil Survey Staff, Natural Resources Conservation Service, United States Department of Agriculture. Soil Survey Geographic (SSURGO) Database.

Taylor, A., Gartner, B., Morrell, J. 2002. Heartwood formation and natural durability: A review. Wood and Fiber Sci. 34(4): 587-611.

Todoroki, C.L. 1990. AUTOSAW system for sawing simulation. New Zealand Journal of Forestry Science 20(3): 332-348.

Todoroki, C.L., Monserud, R.A., Parry, D.L. 2005. Predicting internal lumber grade from log surface knots: Actual and simulated results. Forest Products Journal 55(6): 38-47.

Tong, Q., Duchesne, I., Belley, D., Beaudoin, M., Swift, E. 2013. Characterization of knots in plantation white spruce. Wood Fiber Sci. 45: 84-97.

Turcan, P. 2005. CutLog: Optimum sawing solution software, Tekl STUDIO. Detva, Slovakia.

Usenius, A. 2000. WoodCim – Integrated planning and optimizing system for sawmilling industry. VTTs Building Technology. Internal Report. 8 p.

Wang, T., Hamann, A., Spittlehouse, D.L., Murdock, T.Q. 2012. ClimateWNA-high-resolution spatial climate data for western North America. Journal of Applied Meteorology and Climatology 51(1): 16-29.

Waring, R.H., Thies, W.G., Muscato, D. 1980. Stem growth per unit of leaf area: a measure of tree vigor. Forest Science 26(1): 112-117.

Weiskittel, A.R., Maguire, D.A., Monserud, R.A., Rose, R., Turnblom, E.C. 2006. Intensive management influence on Douglas fir stem form, branch characteristics, and simulated product recovery. New Zealand Journal of Forestry Science 36(2/3): 293.

Weiskittel, A.R., Maguire, D.A., Monserud, R.A. 2007. Modeling crown structural responses to competing vegetation control, thinning, fertilization, and Swiss needle cast in coastal Douglas-fir of the Pacific Northwest, USA. Forest Ecology and Management 245(1): 96-109.

Weiskittel, A.R., Maguire, D.A., Monserud, R.A., Johnson, G.P. 2010. A hybrid model for intensively managed Douglas-fir plantations in the Pacific Northwest, USA. European Journal of Forest Research 129(3): 325-338.

Weiskittel, A.R., Hann, D.W., Kershaw, J.A., Vanclay, J.K. 2011. Forest growth and yield modeling. John Wiley & Sons.

Weiskittel, A. 2013. Forest growth and wood quality modeling: past, present and future. https://colloque6.inra.fr/memowood/ MeMoWood-presentations. Accessed 3 August 2015

Wykoff, W.R. 1990. A basal area increment model for individual conifers in the northern Rocky Mountains. Forest Science 36: 1077-1104.

Yun, Z., Chang, S., Lei, Z., Gabrielle, A., Ashwin, B. 2008. Grid-enabled Sawing Optimization: from scanning images to cutting solution. Proceedings of the 15th ACM Mardi Gras Conference, Baton Rouge, LA. Pp. 1-8.

Zimmerman, M.H., Brown, C.L. 1971. Trees: Structure and Function. New York: Spinger-Verlag.

Tables:

Table 7.1 Predictive models for essential wood anatomical properties determining Douglas-fir wood quality in the Pacific Northwest, which are readily incorporated into growth yield and wood properties simulation software.

Tree attribute	Select reference
MACRO-ANATOMY	
Distribution of growth rings and log shape	
2D taper	Walters and Hann (1986)
3D taper	Garcia (2015)
Primary branches	
Diameter	Maguire et al. (1999);
Angle	Roeh and Maguire (1997); Weiskittel et al. (2007)
Distribution	Maguire et al. (1994); Weiskittel et al. (2007)
Primary knots	
Pith curvature	Osborne and Maguire (2015)
Diameter	
Classification	*No reference*
Xylem delineation	
Heartwood and Sapwood	Maguire and Batista (1996) Maguire (2015)
Juvenile wood core	Maguire et al. (1991)
Lumber properties	
Wood strength	
Wood shrinkage or twisting	*No reference*
Defect incidence	
MICRO-ANATOMY	
Annual ring or within ring	
Fibril angle	*No reference*
Specific gravity	Filipescu et al. (2013)

Table 7.2 Temporal resolution of select Douglas-fir model types from the Pacific Northwest

Model Name	Model Type	Spatial Resolution	Temporal Resolution	Wood Property Considerations
FVS	Statistical	Tree	5-10 year	No
ORGANON	Statistical	Tree	5 year	*Yes*
TASS	Hybrid	Tree	Annual	*Yes*
3PG	Hybrid	Mean Tree	Monthly	No
Forest-BGC	Mechanistic	Stand	Daily	No
SORTIE	Gap	Tree	Annual	No

Captions of figures:

Figure 7.1 Schematic illustration of selected stem zones relevant to wood properties in Douglas-fir and other conifer trees.

Figure 7.2 Three examples of scale for estimating and measuring wood properties: (left) cellular scale; (center) growth ring scale; (right) tree bole scale.

Figure 7.3 Simplified conceptual framework for statistically modeling individual growth, yield and wood properties conditional on environmental conditions and ecophysiological mechanisms.

Figure 7.4 Two types of wood properties output types amendable to Douglas-fir forest growth and yield simulation: discrete three-dimensional knot (Osborne and Maguire 2015) and continuous voxels for a wood cube (Osborne et al. 2015).

Figures:

Figure 7.1 Schematic illustration of selected stem zones relevant to wood properties in Douglas-fir and other conifer trees.

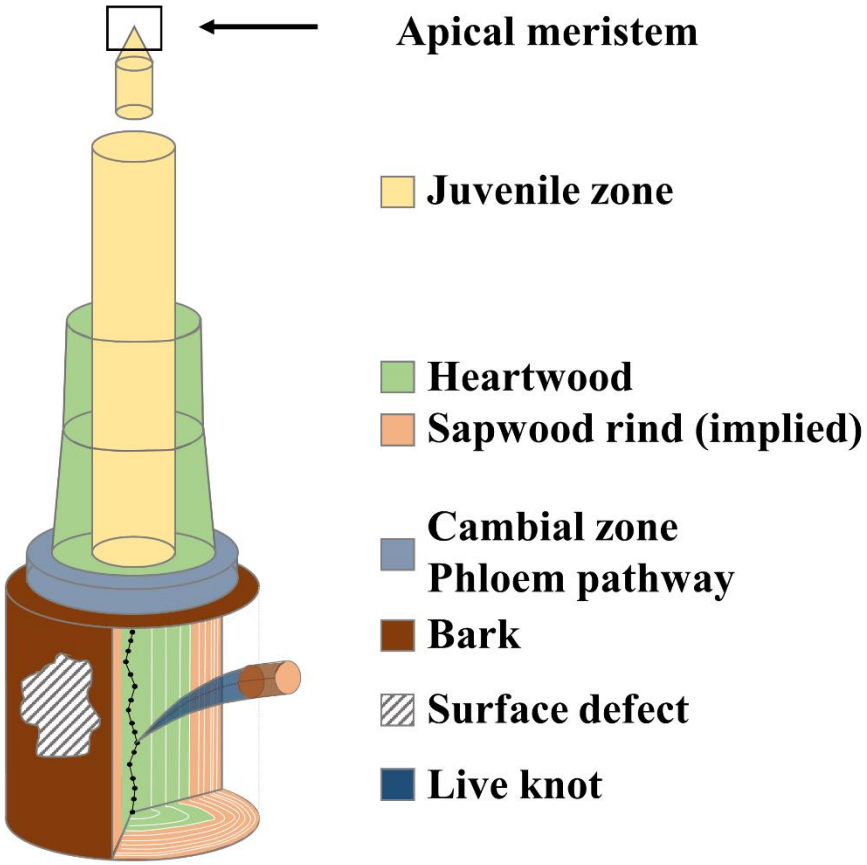

Figure 7.2 Three examples of scale for estimating and measuring wood properties: (left) cellular scale; (center) growth ring scale; (right) tree bole scale.

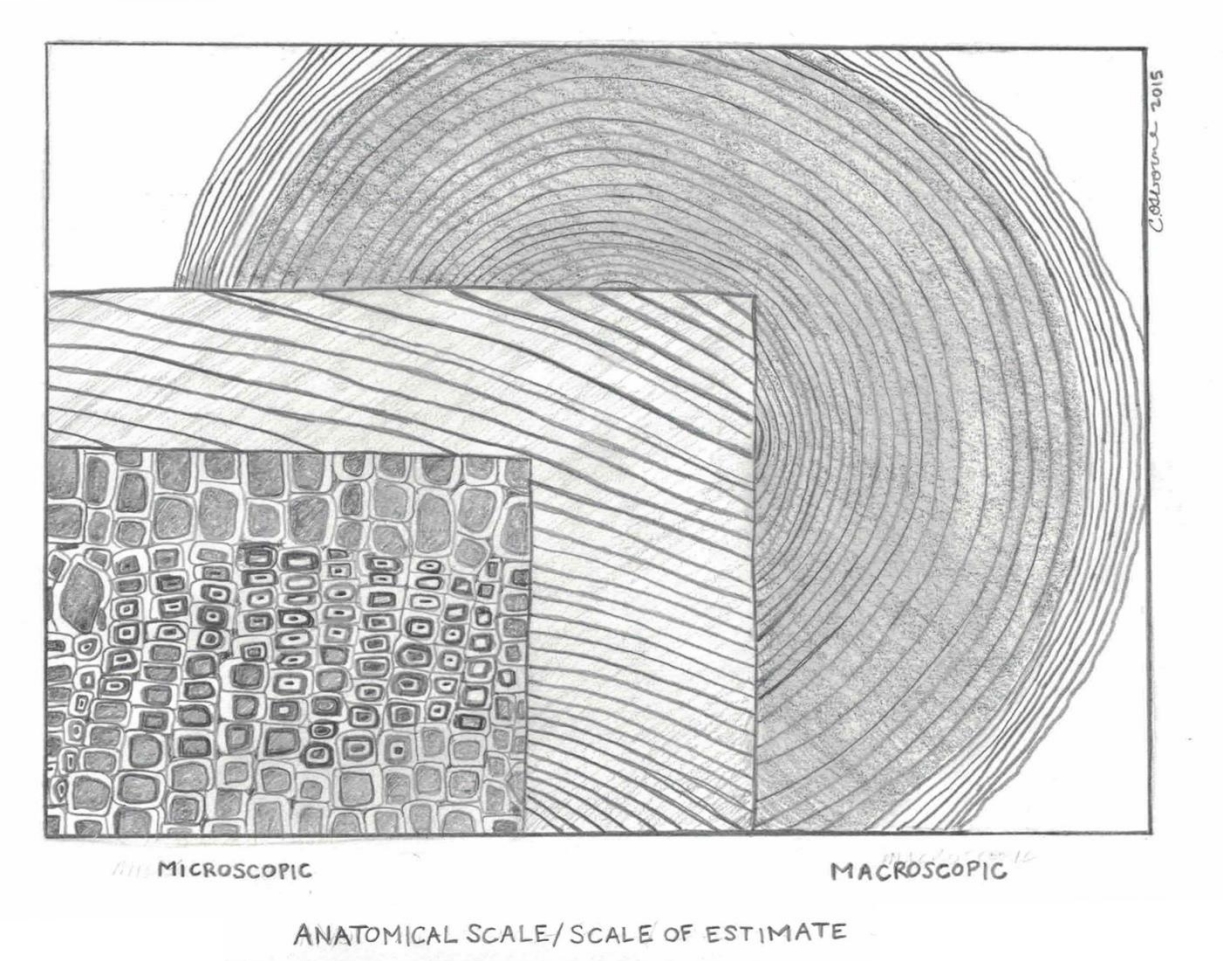

Figure 7.3 Simplified conceptual framework for statistically modeling individual growth, yield and wood properties conditional on environmental conditions and ecophysiological mechanisms.

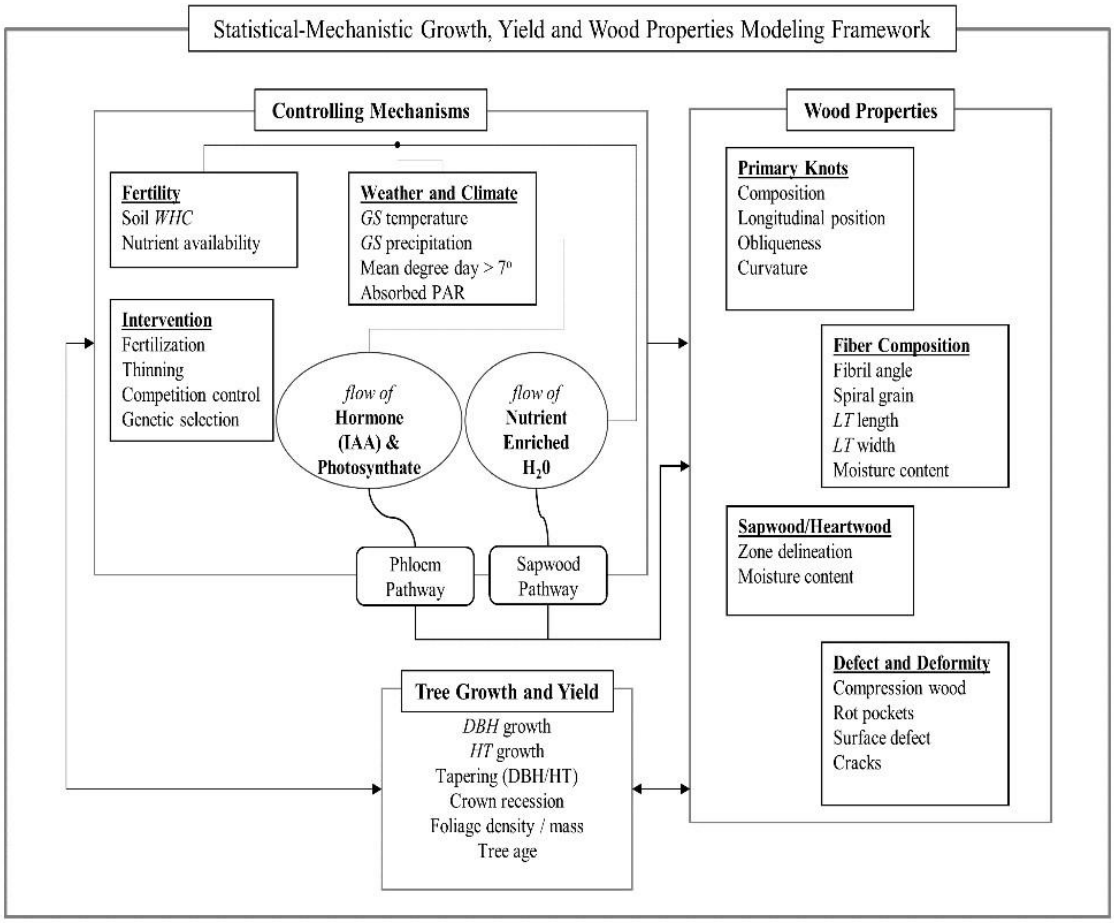

Figure 7.4 Two types of wood properties output types amendable to Douglas-fir forest growth and yield simulation: discrete three-dimensional knot (Osborne and Maguire 2015) and continuous voxels for a wood cube (Osborne et al. 2015).

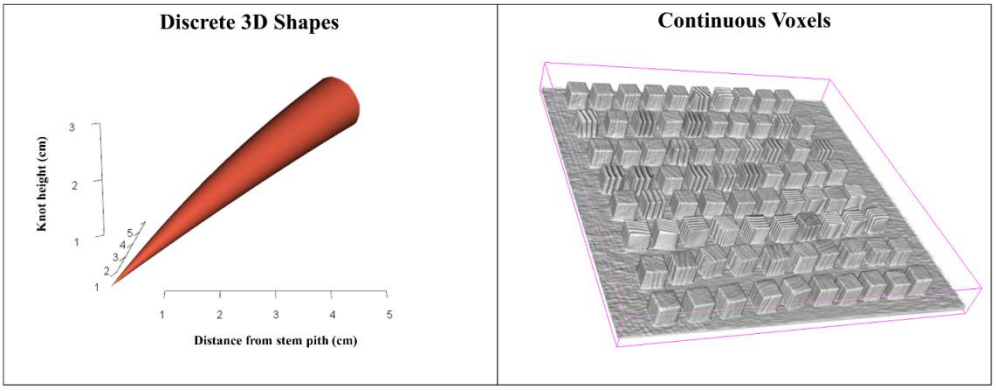

BIBLIOGRAPHY

Abdel-Gadir, A.Y., Krahmer, R.L. 1993. Estimating the age of demarcation of juvenile and mature wood in Douglas-fir. Wood and Fiber Science 25(3): 242-249.

Abràmoff, M. D., Magalhães, P. J., Ram, S. J. 2004. Image processing with ImageJ. Biophotonics International, 11(7): 36-42.

Andreu J.P., Rinnhofer, A. 2003. Modeling knot geometry in Norway spruce from industrial CT Images, in: SCIA 2003: 786-791.

Aussenac, G., Granier, A. 1988. Effects of thinning on water stress and growth in Douglas-fir. Canadian Journal of Forest Research, 18(1):100-105.

Ares, A., Terry, T., Harrington, C., Devine, W. 2007. Biomass removal, soil compaction, and vegetation control effects on five-year growth of Douglas-fir in coastal Washington. Forest Science. 53(5): 600–611.

Arney, J. D. 1988. SPS guide for the Stand Projection System (SPS), vers. 2.0. Applied Biometrics, Issaquah, WA.

Assman, E. 1970. The principles of forest yield study. Pergamon, Oxford, New York. 506 p.

Bamber, R.K. 1961. Sapwood and heartwood. Forestry Commission of New South Wales, Technical Pub No. 2.

Bamber, R. K. 1976. Heartwood, its function and formation. Wood Science and Technology, 10(1):1-8.

Barbour, R. J., Johnston, S., Hayes, J. P., Tucker, G. F. 1997. Simulated stand characteristics and wood product yields from Douglas-fir plantations managed for ecosystem objectives. Forest Ecology and Management, 91(2):205-219.

Barbour, R.J., Parry, D.L. 2001. Log and lumber grades as indicators of wood quality in 20- to 100-year old Douglas-fir trees from thinned and unthinned stands. USDA Forest Service Pacific Northwest Research Station, Portland, Oregon. Gen. Tech. Rep. PNW-GTR-510. 22 p.

Barbour, R. J., Marshall, D.D., Lowell, E.C. 2003. Managing for wood quality. In Compatible forest management. Springer Netherlands. Pp. 299-336.

Beedlow, P.A., Tingey, D. T., Lee, E. H., Phillips, D. L., Andersen, C. P., Waschmann, R. S., Johnson, M. G. 2007. Sapwood moisture in Douglas-fir boles and seasonal changes in soil water. Canadian Journal of Forest Research, 37(7):1263–1271.

Birot, Y., Christophe, C. 1983. Genetic structures and expected genetic gains from multitrait selection in wild populations of Douglas-fir and Sitka spruce. Silvae Genetica 32(5/6): 141-151.

Bivand, R., Keitt, T., Rowlingson, B. 2014. rgdal: Bindings for the Geospatial Data Abstraction Library. R package version 0.9-1.

Briggs, D.G., Fight, R.D. 1992. Assessing the effects of silvicultural practices on product quality and value of coast Douglas-fir trees. Forest Products Journal 42(1): 40-46.

Briggs, D., Ingaramo, L., Turnblom, E. 2007. Number and diameter of breast-height region branches in a Douglas-fir spacing trial and linkage to log quality. Forest Products Journal 57(9): 28.

Brix, H. 1972. Nitrogen fertilization and water effects on photosynthesis and earlywood-latewood production in Douglas-fir. Canadian Journal of Forest Research, 2(4): 467-478.

Brix, H. 1981. Effects of thinning and nitrogen fertilization on branch and foliage production in Douglas-fir. Canadian Journal of Forest Research, 11(3):502-511.

Brix, H., Mitchell, A. K. 1983. Thinning and nitrogen fertilization effects on sapwood development and relationships of foliage quantity to sapwood area and basal area in Douglas-fir. Canadian Journal of Forest Research, 13(3):384-389.

Brix, H., Mitchell, A. K. 1985. Effects of disrupting stem sapwood water conduction on the water status in Douglas-fir crowns. Canadian Journal of Forest Research, 15(5):982-985.

Bruce, D. 1981. Consistent height-growth and growth-rate estimates for remeasured plots. Forest Science, 27(4):711-725.

Burkhart, H.E., Tomé, M. 2012. Modelling forest trees and stands. Springer. Netherlands. pp. 405-427.

Buksnowitz, C., Hackspiel, C., Hofstetter, K., Müller, U., Gindl, W., Teischinger, A., Konnerth, J. 2010. Knots in trees: strain distribution in a naturally optimised structure. Wood science and technology, 44(3): 389-398.

Cahill, B.C., Briggs, D.G. 1992. Effects of fertilization on wood quality and tree value. In: Proceedings of Forest Fertilization: Sustaining and improving nutrition and growth of western forest. 12–14 February 1991, Seattle, Washington. University of Washington, College of Forest Resources. Pp. 145-160.

Chmura, D.J., Rahman, M.S., Tjoelker, M.G. 2007. Crown structure and biomass allocation patterns modulate aboveground productivity in young loblolly pine and slash pine. Forest Ecology and Management 243(2): 219-230.

Cochrane, L., Ford, E.D. 1978. Growth of a Sitka spruce plantation: analysis and stochastic description of the development of branching structure. Journal of Applied Ecology 15: 227-244.
Colin, F., Houllier, F. 1992. Branchiness of Norway spruce in northeastern France: predicting the main crown characteristics from usual tree measurements. Annals of Forest Science 49(5): 511-538.

Colin, F., Laborie, M.P., Fortin, M. 2015. Wood properties: future needs, measurement and modelling. Annals of Forest Science 72(6): 665-670.

Cown, D. J. 1992. Corewood (juvenile wood) in Pinus radiata–should we be concerned. New Zealand Journal of Forestry Science, 22(1):87-95.

Curtis, Robert O. 1970. Stand density measures: an interpretation. Forest Science. 16(4):403-414.

Curtis, R. O. 1982. A simple index of stand density for Douglas-fir. Forest Science, 28(1):92-94.

Curtis, R., Marshall, D., Bell, J. 1997. LOGS: a pioneering example of silvicultural research in coast Douglas-fir. Journal of Forestry (USA) 95(7): 19–25.

Deckmyn, G., Evans, S.P., Randle, T.J. 2006. Refined pipe model theory for mechanistic modeling of wood development. Tree Physiology 26: 703-717.

Di Lucca, C.M. 1989. Juvenile - Mature Wood Transition. Pp. 23-38 in R.M. Kellog (ed). Second growth Douglas-fir: Its management and conversion for value. Forintek Canada, Vancouver, BC, Canada. Spec. Publ. No. SP-32.

Doruska, P.F., Burkhart, H.E. 1994. Modeling the diameter and locational distribution of branches within the crowns of loblolly pine trees in unthinned plantations. Canadian Journal of Forest Research 24: 2362-2376.

Duchateau, E., Longuetaud, F., Mothe, F., Ung, C., Auty, D., Achim, A. 2013. Modelling knot morphology as a function of external tree and branch attributes. Canadian Journal of Forest Research, 43(3): 266-277.

Duchateau, E., Auty, D., Mothe, F., Longuetaud, F., Ung, C.H., Achim, A. 2015. Models of knot and stem development in black spruce trees indicate a shift in allocation priority to branches when growth is limited. PeerJ, 3:e873.

Drever, C.R., Lertzman, K.P. 2001. Light-growth responses of coastal Douglas-fir and western redcedar saplings under different regimes of soil moisture and nutrients. Canadian Journal of Forest Research 31(12): 2124-2133.

Drew, T.J., J.W. Flewelling. 1977. Some recent Japanese theories of yield-density relationships and their application to Monterey pine plantation. Forest Science 23:517-534.

Edmonds, R.L. 1982. Analysis of coniferous forest ecosystems in the Western United States, Hutchinson Ross Pub. Co.

Emmingham, W. 1977. Comparison of selected Douglas-fir seed sources for cambial and leader growth patterns in four western Oregon environments. Canadian Journal of Forest Research. 7(1): 154-164.

ESRI. 2011. ArcGIS Desktop: Release 10. Redlands, CA: Environmental Systems Research Institute.

Esau, K. 1965. Plant Anatomy, 2nd edition. New York: John Wiley and Sons. Pp. 249-250.

Evans, R., Ilic, J. 2001. Rapid prediction of wood stiffness from microfibril angle and density. Forest products journal, 51(3): 53.

Fahey, T.D., Cahill, J.M., Snellgrove, T.A., Heath, L. 1991. Lumber and veneer recovery from intensively managed young-growth Douglas-fir. Res. Pap. PNW-RP-437. Portland, OR: U.S. Department of Agriculture, Forest Service, Pacific Northwest Research Station. 25 p.

Filipescu, C., Lowell, E., Koppenaal, R., Mitchell, A. 2013. Modeling regional and climatic variation of wood density and ring width in intensively managed Douglas-fir. Canadian Journal of Forest Research, 44(3): 220-229.

Fleischer, H.O. 1949. The suitability of second-growth Douglas-fir logs for veneer. Journal of Forestry 47(7): 533-537.

Flower, M. A. (Ed.). 2012. Webb's physics of medical imaging. CRC Press.

FPInnovations 2014. Optitek 10: user's manual. FPInnovations, Quebec, Canada.

Franklin, J.F., Shugart, H.H., Harmon, M.E. 1987. Tree death as an ecological process. BioScience 37(8): 550-556.

Freyburger, C., Longuetaud, F., Mothe, F., Constant, T., Leban, J.M. 2009. Measuring wood density by means of X-ray computer tomography. Annals of Forest Science 66(8): 804.

Gartner, B.L., North, E.M., Johnson, G.R., Singleton, R. 2002. Effects of live crown on vertical patterns of wood density and growth in Douglas-fir. Canadian Journal of Forest Research 32: 439-447.

Gartner, B.L. 2005. Assessing wood characteristics and wood quality in intensively managed plantations. Journal of Forestry 103(2): 75–77.

Grah, R.F. 1961. Relationship between tree spacing, knot size, and log quality in young Douglas-fir stands. Journal of Forestry 59(4): 270-272.

Grömping, U. 2006. Relative importance for linear regression in R: the package relaimpo. Journal of statistical software, 17(1): 1-27.

Grotta, A.T., Gartner, B.L., Radosevich, S.R., Huso, M. 2005. Influence of red alder competition on cambial phenology and latewood formation in Douglas-fir. IAWA Journal 26(3): 309-324.

Halco Inc. 1970. SAWSIM: Sawmill Simulation Program, Carroll-Hatch, Vancouver, Canada.

Hann, D.W., Hanus, M.L. 2004. Evaluation of nonspatial approaches and equations forms used to predict tree crown recession. Canadian Journal of Forest Research 34: 1993-2003.

Hann, D.W. 2011. ORGANON User's Manual, Edition 9.1. College of Forestry, Oregon State University, Corvallis, OR, USA.

Hazenberg, G., Yang, K.C. 1991. Sapwood/heartwood width relationships with tree age in balsam fir. IAWA Journal 12(1): 95-99.

Hein, S., Mäkinen, H., Yue, C., Kohnle, U. 2007. Modelling branch characteristics of Norway spruce from wide spacings in Germany. Forest Ecology and Management 242(2): 155–164.

Hijmans, R.J. 2014. raster: raster: Geographic data analysis and modeling. R package version 2.3-12.

Hoag, M. L. 1988. Measurement of within tree density variations in Douglas-fir (Pseudotsuga menziesii (Mirb.) Franco) using direct scanning x-ray techniques.

Høibø, O., Vestøl, G.I. 2010. Modelling the variation in modulus of elasticity and modulus of rupture of Scots pine round timber. Canadian Journal of Forest Research 40(4): 668–678.

Houllier, F., Leban, J., Colin, F. 1995. Linking growth modelling to timber quality assessment for Norway spruce. Forest Ecology and Management 74(1): 91–102.

Howe, G.T., Jayawickrama, K.M., Cherry, Johnson, G. R., Wheeler, N. C. 2006. Breeding Douglas-fir. Plant Breeding Review 27: 245-353.

Islam, M.N., Ando, K., Yamauchi, H., Hattori, N. 2009. Preservative treatment of Douglas-fir lumber by the passive impregnation method with copper azole. European Journal of Wood and Wood Products 67(1): 77-81.

Ištvanić, J., Piljak, K., Antonović, A., Luˇić, R.B., Jambreković, V., Pervan, S. 2010. The theory and mathematical model underlying the radial sawing simulator—RadSawSim. Forest Products Journal 60(1): 48–56.

Islam, M. N., Ando, K., Yamauchi, H., Kobayashi, Y., Hattori, N. 2008. Comparative study between full cell and passive impregnation method of wood preservation for laser incised Douglas fir lumber. Wood Science and Technology. 42(4):343-350.

Jensen, E.C., Long, J.N. 1983. Crown structure of a co-dominant Douglas-fir. Canadian Journal of Forest Research 13:264-269.

Josza L.A., Richards J., Johnson S.G. 1989. Relative density. Pp. 5-19 in R.M. Kellogg (ed). Second growth Douglas-fir: Its management and conversion for value. Forintek Canada, Vancouver, BC, Canada. Spec. Publ. No. SP-32.

Jozsa, L.A., Brix, H. 1989. The effects of fertilization and thinning on wood quality of a 24-year-old Douglas-fir stand. Canadian journal of forest research, 19(9): 1137-1145.

Kantavichai, R., Briggs, D., Turnblom, E. 2010. Modeling effects of soil, climate, and silviculture on growth ring specific gravity of Douglas-fir on a drought-prone site in Western Washington. Forest Ecology and Management 259(6):1085-1092.

Kennedy, R.W. 1995. Coniferous wood quality in the future: concerns and strategies. Wood Science and Technology, 29(5): 321-338.

Kershaw, J.A., Maguire, D.A. 1995. Crown structure in western hemlock, Douglas-fir, and grand fir in western Washington: trends in branch-level mass and leaf area. Canadian Journal of Forest Research 25(12): 1897-1912.

King, J.E. 1966. Site index curves for Douglas-fir in the Pacific Northwest. Weyerhaeuser For. Pap. 8. Weyerhaeuser Research Technology Center, Federal Way, WA. 49 p.

King, J.N., Yeh, F.C., Heaman, J.C., Dancik, B.P. 1992. Selection of crown form traits in controlled crosses of coastal Douglas-fir. Silvae Genetica 41: 362-370.

Knowe, S. A., Radosevich, S. R., & Shula, R. G. 2005. Basal area and diameter distribution prediction equations for young Douglas-fir plantations with hardwood competition: Coast Ranges. Western Journal of Applied Forestry, 20(2):77-93.

Kollmann, F.F., Côte Jr, W.A. 1968. Principles of Wood Science and Technology: in Chapter 2 "Chemical Composition of Wood". Springer-Verlag.

Krähenbühl, A., Kerautret, B., Debled-Rennesson, I., Mothe, F., Longuetaud, F. 2014. Knot segmentation in 3D CT images of wet wood. Pattern Recognition 47(12): 3852-3869.

Kramer, P.J., Kozlowski, T.T. 1979. Physiology of woody plants. Academic press. New York.

Lachenbruch, B., Johnson, G.R., Downes, G.M., Evans, R. 2010. Relationships of density, microfibril angle, and sound velocity with stiffness and strength in mature wood of Douglas-fir. Canadian Journal of Forest Research 40(1): 55-64.

Landgren, C.G., Bondi, M.C., Emmingham, W.H. 1983. Growing and harvesting Douglas-fir poles. Corvallis, Oregon: Extension Service, Oregon State University EC 1134, Pp. 7.

Larson, P.R. 1969. Wood formation and the concept of wood quality. Yale Univ. School Forestry Bul 74: 1-54.

Larson, P.R., Kretschmann, D.E., Clark, A., Isebrands, J.G. 2001. Formation and properties of juvenile wood in southern pines: a synopsis. Gen. Tech. Rep. FPL-GTR-129. Madison, WI: U.S. Department of Agriculture, Forest Service, Forest Products Laboratory. 42 p.

Leary, R.A. 1997. Testing models of unthinned red pine plantation dynamics using a modified Bakuzis matrix of stand properties. Ecological Modelling, 98(1): 35-46.

Lewis, D. 1985. Sawmill simulation and the best opening face system: a user's guide. USDA Forest Service, Forest Products Laboratory FPL-48. Madison, WI. 29 p.

Lemieux, H., Samson, M., Usenius, A. 1997. Shape and distribution of knots in a sample of *Picea abies* logs. Scandinavian Journal of Forest Research 12(1): 50-56.

Leonardon, M., Altaner, C.M., Vihermaa, L., Jarvis, M.C. 2010. Wood shrinkage: influence of anatomy, cell wall architecture, chemical composition and cambial age. European Journal of Wood and Wood Products, 68(1): 87-94.

Li, Y., Xue, J., Clinton, P.W., Dungey, H.S. 2015. Genetic parameters and clone by environment interactions for growth and foliar nutrient concentrations in radiata pine on 14 widely diverse New Zealand sites. Tree Genetics and Genomes 10(11): 1-16.

Long, J.N., Smith, F.W., Scott, D.R. 1981. The role of Douglas-fir stem sapwood and heartwood in the mechanical and physiological support of crowns and development of stem form. Canadian Journal of Forest Research 11(3): 459-464.

Lowell, E.C., Maguire, D.A., Briggs, D.G., Turnblom, E.C., Jayawickrama, K.J.S., Bryce, J. 2014. Effects of silviculture and genetics on branch/knot attributes of coastal Pacific Northwest Douglas-fir and implications for wood quality – A synthesis. Forests 5(7): 1717-1736.

Lumley T. 2009. leaps: Regression Subset Selection. R package version 2.9.

Maguire, D.A., Hann, D.W. 1987. Equations for predicting sapwood area at crown base in southwestern Oregon Douglas-fir. Canadian Journal of Forest Research 17(3): 236-241.

Maguire, D.A., Hann, D.W. 1989. The relationship between gross crown dimensions and sapwood area at crown base in Douglas-fir. Canadian Journal of Forest Research 19(5):557-565.

Maguire, D.A., Kershaw, J.A., Hann, D.W. 1991. Predicting the effects of silvicultural regime on branch size and crown wood core in Douglas-fir. Forest Science 37(5):1409-1428.

Maguire, D., Bennett, W.S., Kershaw, J. 1991. Establishment report: Stand Management Cooperative silviculture project field installations. College of Forest Resources, University of Washington, Seattle WA. 42 p.

Maguire, D.A., Moeur, M., Bennett, W.S. 1994. Models for describing basal diameter and vertical distribution of primary branches in young Douglas-fir. Forest Ecology and Management 63(1): 23-55.

Maguire, D.A., Batista, J.L. 1996. Sapwood taper models and implied sapwood volume and foliage profiles for coastal Douglas-fir. Canadian Journal of Forest Research 26(5): 849-863.

Maguire, D.A., Johnston, S.R., Cahill, J. 1999. Predicting branch diameters on second-growth Douglas-fir from tree-level descriptors. Canadian Journal of Forest Research 29(12): 1829-1840.

Maguire, D.A., Mainwaring, D.B., Rose, R., Garber, S.M., Dinger, E.J. 2009. Response of coastal Douglas-fir and competing vegetation to repeated and delayed weed control treatments during early plantation development. Canadian Journal of Forest Research 39: 1208-1219.

Maguire, D. A., Kanaskie, A. 2002. The ratio of live crown length to sapwood area as a measure of crown sparseness. Forest science, 48(1):93-100.

Maguire, D. Models for the height and shape of the heartwood core in Douglas-fir. 2014. Pp. 37-41 in D.A. Maguire and D.B. Mainwaring (eds). CIPS 2013 Annual Report. Center for Intensive Planted-forest Silviculture, College of Forestry, Oregon State University, Corvallis, OR, USA.

Mäkelä, A., Grace, J., Deckmyn, G., Kint, A.K.V. 2010. Simulating wood quality in forest management models. Forest Systems 19(S1): 48-68.

Mäkinen, H., Colin, F. 1998. Predicting branch angle and branch diameter of Scots pine from usual tree measurements and stand structural information. Canadian Journal of Forest Research 28(11): 1686–1696.

Mantanis, G. I., Young, R. A., & Rowell, R. M. 1994. Swelling of wood. Wood Science and Technology, 28(2): 119-134.

Max, T.A., Burkhart, H.E. 1976. Segmented polynomial regression applied to taper equations. Forest Sci. 22:283-289.

Mirai Solutions GmbH (2014). XLConnect: Excel Connector for R. R package version 0.2-9.

Moberg, L. 2001. Models of internal knot properties for *Picea abies*. Forest Ecology and Management 147(2): 123–138.

Moberg, L. 2006. Predicting knot properties of *Picea abies* and *Pinus sylvestris* from generic tree descriptors. Scandinavian Journal of Forest Research 21(S7): 49–62.

Monleon, V.J., Azuma, D., Gedney, D. 2004. Equations for predicting uncompacted crown ratio based on compacted crown ratio and tree attributes. Western Journal of Applied Forestry 19(4): 260-267

McArdle, R.E., Meyer, W.H. 1930. The yield of Douglas-fir in the Pacific Northwest. US Dept. Agr. Tech. Bul 201.

Occeña, L.G., Schmoldt, D.L. 1995. GRASP - A Prototype Interactive GRAphical Sawing Program. MU-IE Technical Report, Pp. 1–17.

Occeña, L.G., Santitrakul, E., Schmoldt, D.L. 2000. Hardwood sawyer trainer. Pp. 43-47 in Proc. 28th Annual Hardwood Symposium – West Virginia Now – The Future for the Hardwood Industry, Davis, WV. National Hardwood Lumber Assoc., Memphis, TN.

Ormarsson, S., Dahlblom, O., Petersson, H. 2000. A numerical study of the shape stability of sawn timber subjected to moisture variation. Wood Science and Technology, 34(3): 207-219.

Osborne, N.L., Maguire, D.A., Hann, D.W. 2014. Simulating Douglas-fir tree and stand development under varying initial spacings with ORGANON: Knot size and juvenile wood core effects on grade recovery of lumber. Center for Intensive Planted-forest Silviculture Annual Report 2013: 22-28.

Osborne, N.L., Maguire, D.A. 2015. Modeling knot geometry from branch angles in Douglas-fir (*Pseudotsuga menziesii*), Canadian Journal of Forest Research, *under review*.

Osborne, N., Høibø, O., Maguire, D., Gourley, D. 2015. Estimating the density of coast Douglas-fir wood samples at different moisture contents using medical X-ray computed tomography. Computers and Electronics in Agriculture. *in preparation*.

Osborne, N., Maguire, D., Weiskittel, A. 2015. Simulating forest growth, yield and wood properties of planted Pseudotsuga menziesii in the Pacific Northwest United States: A synthesis. *in preparation.*

Osborne, N., Maguire, D., Hann, D. 2015. cipsr: An R interface to the ORGANON and CIPSANON models. R package version 2.2.2.

Oja, J. 2000. Evaluation of knot parameters measured automatically in CT-images of Norway spruce (Picea abies (L.) Karst.). European Journal of Wood and Wood Products, 58(5): 375-379.

Paul, B.H. 1947. Knots in second-growth Douglas-fir. US Department of Agriculture Forest Service, Forest Products Laboratory, Madison Wisconsin. No. R1690.

Pebesma, E.J., Bivand, R.S. 2005. Classes and methods for spatial data in R. R News 5:(2)

Petzoldt, T., Maechler, M. 2013. akima: Interpolation of irregularly spaced data. Package version 0.5.11.

Pieper, S., Halle, M., & Kikinis, R. 2004. 3D Slicer. In Biomedical Imaging: Nano to Macro, 2004. IEEE International Symposium Pp. 632-635.

R Development Core Team. 2013. R: A language and environment for statistical computing. R Foundation for Statistical Computing, Vienna, Austria.

R Development Core Team. 2015. R: A language and environment for statistical computing. R Foundation for Statistical Computing, Vienna, Austria.

Rafsanjani, A., Stiefel, M., Jefimovs, K., Mokso, R., Derome, D., Carmeliet, J. 2014. Hygroscopic swelling and shrinkage of latewood cell wall micropillars reveal ultrastructural anisotropy. Journal of The Royal Society Interface 11: 20140126.

Rapeepan, K., Briggs, D. and Turnblom, E. 2010. Modeling effects of soil, climate, and silviculture on growth ring specific gravity of Douglas-fir on a drought-prone site in Western Washington. Forest Ecology and Management. 259(6): 1085-1092.

Robinson, A.P., Monserud, R.A. 2003. Criteria for comparing the adaptability of forest growth models. Forest Ecology and Management, 172(1): 53-67.

Roeh, R.L., Maguire, D.A. 1997. Crown profile models based on branch attributes in coastal Douglas-fir. Forest Ecology and Management 96(1): 77-100.

Roussel, J. R., Mothe, F., Krähenbühl, A., Kerautret, B., Debled-Rennesson, I., Longuetaud, F. 2014. Automatic knot segmentation in CT images of wet softwood logs using a tangential approach. Computers and Electronics in Agriculture, 104:46-56.

Rozenberg, P., Franc, A., Bastien, C., Cahalan, C. 2001. Improving models of wood density by including genetic effects: a case study in Douglas-fir. Annals of Forest Science 58(4): 385-394.

Samson, M. 1993. Modeling of Knots in Logs. Wood Science and Technology 27(6): 429–437.

Shinozaki, K., K. Yoda, K. Hozumi, and T. Kira. 1964. A quantitative analysis of plant form – the pipe model theory. I. Basic analyses. Japanese Journal of Ecology 14:97-105.

Sucre, E.B., Harrison, R.B., Turnblom, E.C., Briggs, D.B. 2008. The use of various soil and site variables for estimating growth response of Douglas-fir to multiple applications of urea and determining potential long-term effects on soil properties. Canadian Journal of Forest Research 38: 1458-1469.

Sung-Mo, K., Morrell, J. 2000. Fungal colonization of Douglas-fir sapwood lumber. Mycologia. 609-615.

St. Clair, J.B. 1994. Genetic variation in tree structure and its relation to size in Douglas-fir. II. Crown form, branch characteristics, and foliage characters. Canadian Journal of Forest Research 24(6): 1236-1247.

St. Clair, J.B., Mandel, N.L., Jayawickrama, K.J.S. 2004. Early realized genetic gains for coastal Douglas-fir in the northern Oregon Cascades. Western Journal of Applied Forestry 19(3): 195-201.

Steffenrem, A., Kvaalen, H., Dalen, K., Høibø, O. 2014. A high-throughput X-ray-based method for measurements of relative wood density from unprepared increment cores from *Picea abies*. Scandinavian Journal of Forest Research. 29(5):506-514.

Soil Survey Staff, Natural Resources Conservation Service, United States Department of Agriculture. Soil Survey Geographic (SSURGO) Database.

Spicer, R., Gartner, B.L. 2001. The effects of cambial age and position within the stem on specific conductivity in Douglas-fir (Pseudotsuga menziesii) sapwood. Trees, 15(4): 222-229.

Taylor, A., Gartner, B., Morrell, J. 2002. Heartwood formation and natural durability: A review. Wood and Fiber Sci. 34(4): 587-611.

Todoroki, C.L. 1990. AUTOSAW system for sawing simulation. New Zealand Journal of Forestry Science 20(3): 332-348.

Todoroki, C.L., Monserud, R.A., Parry, D.L. 2005. Predicting internal lumber grade from log surface knots: Actual and simulated results. Forest Products Journal 55(6): 38-47.

Tong, Q., Duchesne, I., Belley, D., Beaudoin, M., Swift, E. 2013. Characterization of knots in plantation white spruce. Wood Fiber Sci. 45: 84-97.

Trincado, G., Burkhart, H. 2008. A model of knot shape and volume in loblolly pine trees. Wood and Fiber Science 40(4): 634-646.

Turcan, P. 2005. CutLog: Optimum sawing solution software, Tekl STUDIO. Detva, Slovakia.

USDA, F.S., 1979. A generalized forest growth projection system applied to the Lake States region. General Technical Report NC-49. St. Paul, MN: U.S. Dept. of Agriculture, Forest Service, North Central Forest Experiment Station

Usenius, A. 2000. WoodCim – Integrated planning and optimizing system for sawmilling industry. VTTs Building Technology. Internal Report. 8 p.

Vestøl, G.I., Colin, F., Loubère, M. 1999. Influence of progeny and initial stand density on the relationship between diameter at breast height and knot diameter of *Picea abies*. Scandinavian Journal of Forest Research 14(5): 470–480.

Vikram, V., Cherry, M. L., Briggs, D., Cress, D. W., Evans, R., Howe, G. T. 2011. Stiffness of Douglas-fir lumber: effects of wood properties and genetics. Canadian Journal of Forest Research. 41(6):1160-1173.

Walters, D., Hann, D. 1986. Taper equations for six conifer species in southwest Oregon. Forest Research Lab, Oregon State University, Corvallis, OR. Research Bulletin 56.

Wang, T., Hamann, A., Spittlehouse, D.L., Murdock, T.Q. 2012. ClimateWNA-high-resolution spatial climate data for western North America. Journal of Applied Meteorology and Climatology 51(1): 16-29.

Waring, R.H., Thies, W.G., Muscato, D. 1980. Stem growth per unit of leaf area: a measure of tree vigor. Forest Science 26(1): 112-117.

Wei, Q., Leblon, B., La Rocque, A. 2011. On the use of X-ray computed tomography for determining wood properties: a review. Canadian Journal of Forest Research. 41(11): 2120-2140.

Weiskittel, A.R., Maguire, D.A., Monserud, R.A., Rose, R., Turnblom, E.C. 2006. Intensive management influence on Douglas fir stem form, branch characteristics, and simulated product recovery. New Zealand Journal of Forestry Science 36(2/3): 293.

Weiskittel, A.R., Maguire, D.A., Monserud, R.A. 2007. Modeling crown structural responses to competing vegetation control, thinning, fertilization, and Swiss needle cast in coastal Douglas-fir of the Pacific Northwest, USA. Forest Ecology and Management 245(1): 96-109.

Weiskittel, A.R., Maguire, D.A., Monserud, R.A., Johnson, G.P. 2010. A hybrid model for intensively managed Douglas-fir plantations in the Pacific Northwest, USA. European Journal of Forest Research 129(3): 325-338.

Weiskittel, A.R., Hann, D.W., Kershaw, J.A., Vanclay, J.K. 2011. Forest growth and yield modeling. John Wiley & Sons.

Weiskittel, A. 2013. Forest growth and wood quality modeling: past, present and future. https://colloque6.inra.fr/memowood/ MeMoWood-presentations. Accessed 3 August 2015

Wensel, L. C., Krumland, B. E., Meerschaert, W. J. 1987. Cryptos User's Guide: Cooperative Redwood Yield Project Timber Output Simulator. Division of Agriculture and Natural Resources. University of California.

Wensel, L. C., Biging, G. S. 1988. The cactos system individual-tree growth simulation in the mixed conifer forests of California. USDA Forest Service general technical report NC-North Central Forest Experiment Station (USA).

Wykoff, W. R., Crookston, N. L., Stage, A. R. 1982. User's guide to the stand prognosis model.

Wykoff, W.R. 1990. A basal area increment model for individual conifers in the northern Rocky Mountains. Forest Science 36: 1077-1104.

Yun, Z., Chang, S., Lei, Z., Gabrielle, A., Ashwin, B. 2008. Grid-enabled Sawing Optimization: from scanning images to cutting solution. Proceedings of the 15th ACM Mardi Gras Conference, Baton Rouge, LA. Pp. 1-8.

Zimmerman, M.H., Brown, C.L. 1971. Trees: Structure and Function. New York: Spinger-Verlag.